The Influence of Organic Coatings on the Toxicity of Titanium Dioxide Nanoparticles to Developing Zebrafish (*Danio rerio*)

By

Sarah P. Yang

A dissertation submitted in partial fulfillment of

the requirements for the degree of

Doctor of Philosophy

Molecular and Environmental Toxicology

at the

UNIVERSITY OF WISCONSIN-MADISON

2013

Date of final oral examination: 3/4/13

The dissertation is approved by the following members of the Final Oral Committee:

Joel A. Pedersen, Professor, Soil Science
Richard E. Peterson, Professor, School of Pharmacy
Warren Heideman, Professor, School of Pharmacy
Ralph M. Albrecht, Professor, Animal Science
Robert J. Hamers, Professor, Chemistry

Abstract

Titanium dioxide (TiO_2) nanoparticles (NPs) are currently used in applications ranging from personal care products to paints to photovoltaics. With the production of TiO_2 NPs increasing, the likelihood that these materials will enter the environment also increases.

As a wide band gap semiconductor, absorption of energy equal to or greater than the band gap energy causes the excitation of an electron from the valence band of TiO_2 to the conduction band. For TiO_2 NPs, this band gap lies within the UV to violet region. Upon excitation, a hole is created in the valence band and a free electron exists in the conduction band. The free electron and hole can also interact in other manners, but in environmental matrices the electron and hole can react with nearby molecules to form reactive oxygen species (ROS).

By altering electrostatic and steric interactions between individual nanoparticles, surface chemistry can impact aggregation. Alterations in aggregation can affect whether nanoparticles remain in the water column or sediment out affecting transport in aquatic matrices and exposure to free-swimming and benthic organisms. During synthesis, nanoparticles are functionalized to control size, suspension stability, product incorporation, and reactivity. In the environment, nanoparticles can acquire a coating of natural organic matter (NOM). Such coatings can reduce nanoparticle aggregation.

To date, no studies have examined the influence of organic coating (e.g., functionalization, natural organic ligands) on the toxicity of TiO_2 NP to aquatic vertebrates.

A handful of studies have examined the influence of functionalization on the toxicity of quantum dot, gold, and lead sulfide nanoparticles to aquatic vertebrates warranting further research on how functionalization can alter NP toxicity in aquatic species.

To date, all studies examining TiO_2 NP toxicity in aquatic vertebrates have employed uncoated particles. While studies conducted using standard laboratory lighting found very low levels of toxicity, studies that have utilized lighting that mimics the natural environment found significantly increased levels of toxicity. Such studies concluded that the increased toxicity was caused by increased oxidative stress which occurred as a result of photo-enhanced ROS production by TiO_2 NPs. These studies indicate the need to examine the toxicity of TiO_2 NPs further and the importance of conducting studies under environmentally relevant conditions.

This thesis is a compilation of studies that examined the influence of organic ligands (intentional and those acquired in the environment) on the inherent and photo-enhanced toxicity of TiO_2 NPs to developing zebrafish. In chapter 2, the overall objective was to determine the extent that adsorption of DOM alters the inherent and photo-enhanced toxicity of TiO_2 NPs toward developing zebrafish. To accomplish this, we exposed embryo/larval zebrafish were exposed to unfunctionalized TiO_2 NPs in the absence and presence Suwannee River humic acid, fulvic acid and natural organic matter isolate. Fish were exposed in both the presence and absence of illumination with simulated sunlight to determine the influence on inherent and photo-enhanced toxicity, respectively. We found that adsorption of HA decreased TiO_2 NP exposure in both the presence and absence of

simulated sunlight illumination. Furthermore, small but significant increases in lethality were observed in fish exposed to TiO_2 NPs in the presence of HA. These increases in toxicity corresponded with increases in oxidative stress in both the presence and absence of simulated sunlight illumination. These results suggest that the presence of HA increases TiO_2 NP-induced oxidative stress resulting in increased toxicity. Similar effects were not observed with FA and NOM suggesting that the composition of DOM affects TiO_2 NP induced toxicity.

In chapter 3, the overall objective was to examine the influence of intentional functionalization on inherent and photo-enhanced toxicity of TiO_2 NPs towards developing zebrafish. To accomplish this, we exposed embryo/larval zebrafish to bare, citrate, ascorbate, and 3,4-dihydroxybenzaldehyde (DHBA) functionalized TiO_2 NPs in the presence and absence of simulated sunlight illumination. We found that functionalization altered the toxicity of TiO_2 NPs. Functionalization also increased TiO_2 NP suspension stability and altered TiO_2 NP association levels. While exposure to TiO_2 NPs increased oxidative DNA damage and differences in damage were apparent between bare and functionalized TiO_2 NPs, illumination did not increase oxidative DNA damage for any of the TiO_2 NP preparations.

These studies highlighted the importance of thoroughly investigating the impact of organic coating on TiO_2 NP suspension stability and uptake. Although differences in suspension stability may result in differences in uptake, these changes did not necessarily

correspond with differences in toxicity. Both studies found evidence that the organic coatings increased toxicity by increasing oxidative stress. However, further studies need to be preformed in order to ascertain the mechanism behind this increase.

Acknowledgements

I would first like to thank my PhD advisor, Dr. Joel Pedersen. Joel has taught an immense about science, research, writing, and myself. He taught me how to express myself on a number of levels. I will always be grateful for all that he has done for me.

I would also like to thank my committee members, Dr. Dick Peterson, Dr. Warren Heideman, Dr. Ralph Albrecht, and Dr. Bob Hamers, for their invaluable advice and support over the years. I am also grateful for the support and advice provided by the Molecular and Environmental Toxicology Center especially Mark Marohl and Dr. Chris Bradfield.

There are a number of people throughout campus that have helped me get through grad school. Dorothy Nesbit in the zebrafish room has been both an invaluable asset to my research and great friend. I am eternally appreciative for all the assistance by Jackie Bastyr-Cooper in the School of Engineering; she has run hundreds of ICP samples for me without protest.

I have made a number of lifelong friends in the Pedersen lab. First and foremost, Dr. Paige Wiecinski taught me the ropes of grad school. Without her, I doubt I would have made it! Dr. Kurt Jacobson has also been a great colleague and friend. He is always willing to help out and seems to know everything about everything in the Pedersen lab. Mercedes Ruiz has been a wonderful officemate and friend. I owe her a ton of hot chocolate for all the help she provided with experiments and lab errands. Clarissa Shaffer is always willing to grab a coffee and commiserate on the struggles of grad school. I will miss all of you!

I would also like to thank the furry/feathery members of my family especially Princess, Anemone, and Peanut who are no longer with us. Together with Yingie and Confucius, they helped me make it through every day-always waiting for me to get home and always glad to see me. I love you all!

The support that my family has provided has made everything possible. Without the encouragement from my mom and dad, I would have never even made it to grad school much gotten a PhD. It is hard to put into words how much my mom means to me. Throughout my entire life, she has always been willing to listen. Her hugs have gotten me through the hardest parts of grad school. I love you so much, Mom! My dad is always eager

to talk science. He has encouraged me throughout my journey on becoming a scientist always mentioning how proud he is of me. I love you Dad!

It has been incredible to watch my sister grow throughout my time in grad school. She is now only a few years younger than I was when I started. I love being able to talk to her about science. She is one of my dearest friends. I love you Amy. My brother has been a great help when I need distractions from science. He is always willing to talk about almost anything. I am sure the Wisconsin beer that I bring him doesn't hurt. I love you Scott!

This last year, I was blessed with the most amazing and beautiful baby girl. Hailey Irene was born just three weeks after I defended my thesis. She has changed my whole life and made everything that I have worked hard for worth it. I want nothing more that to be able to love her and provide her with the best life possible. I love you more than anything Hailey!

There is no way that I could have gotten a PhD without my husband, Ted. Ted has spent hours upon hours with me throughout this entire process. He helped me study, do experiments, revise papers… When I was buried beneath a seemingly never-ending heap of research, he did all of the housework and took care of Hailey. He deserves a PhD in being an

awesome, supporting husband and father. There are not enough words to express how much I LOVE YOU TED!

Table of Contents

Chapter 1: Introduction

1.1 Applications of Titanium Dioxide (TiO_2) Nanoparticles (NPs)

Titanium dioxide (TiO_2) nanoparticles (NPs) are currently used in applications ranging from cosmetics and personal care products to paints to photovoltaics. Many of the applications of TiO_2 NPs arise from the ability for TiO_2 to absorb ultraviolet (UV; 100–400 nm) light. Depending on particle size, TiO_2 NPs are able to absorb and reflect UV-A (315–400 nm) and UV-B (280–315 nm) light making them desirable for use in sunscreens and UV-resistant coatings.[1]

Because TiO_2 is a wide band gap semiconductor and TiO_2 NPs absorb UV light, TiO_2 NPs are of interest in photovoltaic and photocatalytic applications. For TiO_2, absorption of energy equal to or greater than the band gap energy causes the excitation of an electron from the valence band to the conduction band. For TiO_2 NPs, this band gap lies within the UV to violet region (e.g., 3.0-5.0 eV; 250-415 nm) with this range reflecting differences in particle size and crystal phase.[2] Upon excitation, a hole is created in the valence band and a free electron exists in the conduction band (Equation 1).

$$TiO_2 + h\upsilon \rightarrow h^+_{vb} + e^-_{cb} \quad (1)$$

In photovoltaic applications, the free electron can conduct electricity. The wavelength range for such interactions can be extended by sensitization with organic dyes or other semicoductors to allow for the absorption of visible light as well.[3]

The free electron and hole can also interact in other manners. For instance, in environmental matrices, the electron and hole can react with nearby molecules to form reactive oxygen species (ROS). For instance, the hole can oxidize water yielding hydroxyl

radicals (OH·) while the free electron can reduce molecular oxygen producing superoxide anions (O_2·$^-$) (Equations 2 and 3, respectively).[3-4]

$$H_2O + h^+_{vb} \rightarrow OH\cdot + H^+ \quad (2)$$

$$O_2 + e^-_{cb} \rightarrow O_2^-\cdot \quad (3)$$

These reactive oxygen species can then degrade organic molecules in the surrounding environment. For instance, hydroxyl radicals can directly oxidize organic species ultimately degrading them into carbon dioxide and water (Equation 4).[3-4]

$$OH\cdot + \text{organic} \rightarrow\rightarrow CO_2 + H_2O \quad (4)$$

On the other hand, depending on pH, superoxide can be protonated into more reactive species (e.g., hydroperoxidal radicals, hydrogen peroxide) which can then oxidize organic species into carbon dioxide and water (Equation 5).[3-4]

$$\begin{aligned} &O_2^-\cdot + H^+ \rightarrow HO_2\cdot \\ &2HO_2\cdot + 2H^+ \rightarrow H_2O_2 + O_2 \\ &H_2O_2 + \text{organic} \rightarrow\rightarrow CO_2 + H_2O \end{aligned} \quad (5)$$

Furthermore, the hole can directly oxidize organic molecules ultimately degrading them into carbon dioxide and water (Equation 6).[3-4]

$$h^+_{vb} + \text{organic}_{ads} \rightarrow \text{organic}^+ \quad (6)$$

TiO_2 NPs can photocatalytically degrade aldehydes, carboxylic acids, anilines, phenols, dyes, ethers, fungicides, herbicides, ketones, pharmaceuticals, and polymers.[5] The photocatalytic

degradation of organics by ROS and/or the hole is the basis for many photocatalytic applications of TiO_2 NPs such as wastewater treatment and self-cleaning windows.

1.2 Lifecycle of TiO_2 NPs

As the number of applications of TiO_2 NPs increase, production volumes also increase. A study by Robichaud *et al.* examined TiO_2 NP production levels in the United States. They estimated that 10% of the TiO_2 produced in the US (> 260,000 metric tons) would be nano-sized by 2015.[6] With the production of TiO_2 NPs increasing, the likelihood that these materials will enter the environment also increases.

Recently, Gottschalk *et al.* employed a probabilistic material flow analysis to investigate the life-cycle of TiO_2 NPs.[7] They determined that plastics, cosmetics, coatings and cleaning agents, and filter aggregates make up 90% of the applications of TiO_2 NPs.[7] Although these materials can be released into environmental matrices (i.e., atmosphere, soil, surface water, groundwater, sediments) directly through production, manufacturing, and consumption, they projected that the majority of particles will enter landfills or sewage treatment plants.[7] For instance, they estimated that 80% of the TiO_2 NPs released from plastics will enter landfills while 90% of the TiO_2 NPs released from cosmetics and coatings will enter sewage treatment plants.[7]

As this model assumed that landfills were sealed such that practically nothing leached into the soil or surrounding water, the majority of TiO_2 NPs released into the environment were predicted to come from sewage treatment plants.[7] TiO_2 NPs can enter the soil from application of sewage treatment plant sludge (~50%) or they can also be released into surface waters from treated and untreated effluent (~25%).[7] Once in surface

waters, this model assumed that the majority of TiO_2 NPs will be deposited in sediments (99%) while a small percentage (< 1%) may be transported to the groundwater.[7]

Although this study gives a general overview of the types of matrices in which TiO_2 NPs may be deposited upon entering the environment, this study did not investigate how physicochemical properties of the nanomaterial and solution conditions may affect the life-cycle of the material.

1.3 Influence of Surface Chemistry on Nanoparticle Fate

Physicochemical properties of the nanomaterial and solution conditions can affect the environmental fate of engineered nanomaterials through a variety of processes. For instance, alterations in surface chemistry, solution pH, and/or ionic strength and composition can affect aggregation.[8] Nanoparticle properties and solution conditions that increase aggregation often produce aggregates that sediment out of the water column resulting in decreased transport in aquatic matrices and increased exposure to benthic organisms.[9-11] On the other hand, properties/conditions that reduce aggregation produce stable nanoparticle suspensions resulting in increased transport in the water column and increased bioavailability to free-swimming organisms.[9-11]

By altering electrostatic and steric interactions between individual nanoparticles, surface chemistry can impact aggregation. In general, as electrostatic and/or steric interactions increase, the propensity for aggregation decreases.[8] This has been demonstrated for a variety of nanomaterials.[12-15] For instance, a study by Mudunkotuwa *et al.* found that the presence of citric acid made the ζ-potential more negative and reduced the hydrodynamic diameter of TiO_2 NP aggregates thereby reducing sedimentation.[15]

Particles can acquire such coatings either intentionally via functionalization during synthesis or unintentionally through adsorption of natural organic ligands in the environment.

During synthesis, nanoparticles are functionalized to control size, suspension stability, product incorporation, and reactivity. For metal oxides, multi-dentate organic ligands (e.g., carboxylic acids, catechols, phosphonates, silanes) are the most effective as the multiple ligand-metal oxide binding sites makes ligand removal less likely and, thus, reduce the likelihood of aggregation.[16]

In the environment, natural organic matter (NOM) is one of the most abundant sources of organic ligands. NOM is a result of microbial transformation of plant residues and is found in practically all environmental matrices including soil, sediment, and natural waters.[17] In natural waters, NOM exists as dissolved organic matter (DOM) where concentrations range from 1 to 30 mg carbon L^{-1}.[18] The composition of DOM is extremely complex consisting of a heterogeneous mixture of organic molecules bearing carboxylate, phenol, amine, quinone, and other functional groups.[17] Adsorption of DOM can reduce nanoparticle aggregation.[19-26] For example, Domingos *et al.* found that the presence of fulvic acid, a polarity fraction of DOM, significantly reduced the hydrodynamic diameter of unfunctionalized TiO_2 NP aggregates.[26]

Nanoparticle stability studies such as those by Mudunkotuwa *et al.* and Domingos *et al*. indicate that adsorption of organic ligands, either intentionally during synthesis or unintentionally in the environment, alters nanoparticle aggregation state and surface

charge and, thus, suspension stability. Consequently, such ligands have the ability to impact nanoparticle fate and are expected to influence their bioavailability and toxicity.

1.4 Influence of Organic Ligands on Nanoparticle Toxicity

Although functionalization is commonly used in industry to stabilize NPs and nanomaterials are likely to encounter a wide array of organic ligands in the environment, no studies have examined the influence of organic coating (e.g., functionalization, natural organic ligands) on the toxicity of TiO_2 NP to aquatic vertebrates.

A handful of studies have examined the influence of functionalization on the toxicity of quantum dot, gold, and lead sulfide nanoparticles to aquatic vertebrates.[27-29] These studies have found that functionalization does indeed impact toxicity. Different functionalizations were hypothesized to illicit differences in nanoparticle bioavailability, tissue distribution, and/or stability resulting in differences in toxicity. For instance, King-Heiden *et al.* found that quantum dots (CdSe:ZnS core:shell) functionalized with methoxy-terminated poly(ethylene) glycol (PEG) caused decreased incidence/severity of morphological malformations (i.e., tail malformation, yolk malformation, opaque head and body tissue/necrosis) than QDs functionalized with carboxy- and amine-terminated PEG.[27] The authors hypothesized that the reduction in toxicity was caused by differences in tissue distributions as difference in Cd body burdens were not observed between the three functionalizations.[27] These studies indicate that functionalization can alter NP toxicity in aquatic species and suggests that further research is this area is warranted.

1.5 Toxicity of Uncoated TiO_2 NPs to Aquatic Vertebrates

To date, all studies examining TiO_2 NP toxicity in aquatic vertebrates have employed uncoated particles. Studies conducted using standard laboratory lighting found very low levels of toxicity regardless of fish species and age and exposure duration and route.[30-34]

On the other hand, studies that have utilized lighting that mimics the natural environment (i.e., solar simulator, simulated sunlight lamp) found significantly increased levels of toxicity.[35-37] For instance, Bar-Ilan *et al*. found that developing zebrafish (*Danio rerio*) exposed to a commercially available TiO_2 NP preparation under simulated sunlight illumination had a dose-dependent decrease in survival and increase in incidence of morphological endpoints (e.g., edema, failed yolk sac absorption, malformed head and tail, stunted growth) compared with those exposed to NPs under standard laboratory lighting.[35] These increases in toxicity corresponded with increased levels of *in vivo* superoxide, antioxidant response element (ARE) activation, and increased oxidative DNA damage.[35] This study, and other similar studies, concluded that the increased toxicity was caused by increased oxidative stress which occurred as a result of photo-enhanced ROS production by TiO_2 NPs.[35-37] These studies indicate the need to examine the toxicity of TiO_2 NPs further and the importance of conducting studies under environmentally relevant conditions.

1.6 Statement of Objectives

This thesis is a compilation of studies that examined the influence of organic ligands (intentional and those acquired in the environment) on the inherent and photo-enhanced toxicity of TiO_2 NPs to developing zebrafish. In chapter 2, the overall objective was to determine the extent that adsorption of DOM alters the inherent and photo-enhanced

toxicity of TiO_2 NPs toward developing zebrafish. To accomplish this, we exposed embryo/larval zebrafish (4-6h post-fertilization to 5d post fertilization) to uncoated TiO_2 NPs in the absence and presence of two DOM fractions (Suwannee River humic acid and fulvic acid) and an unfractionated DOM isolate (Suwannee River natural organic matter). Fish were exposed in the dark to determine the influence of DOM on inherent toxicity and under simulated sunlight illumination to determine the influence on photo-enhanced toxicity. The influence of DOM on TiO_2 NP suspension stability and uptake was also examined. In chapter 3, the overall objective was to examine the influence of intentional functionalization on inherent and photo-enhanced toxicity of TiO_2 NPs towards developing zebrafish. To accomplish this, we exposed embryo/larval zebrafish to bare, citrate, ascorbate, and 3,4-dihydroxybenzaldehyde (DHBA)-functionalized TiO_2 NPs in the presence and absence of simulated sunlight illumination. The influence of functionalization on TiO_2 NP suspension stability, uptake, and oxidative DNA damage was also examined.

For this work, the zebrafish was employed as a model organism. Zebrafish are an ideal *in vivo* model for investigating the effects of uptake and toxicity of engineered NPs. The entire genome is sequenced allowing for comparisons between other aquatic fish species as well as humans, and the rapid, well-studied development of zebrafish embryos makes them suitable for both acute and chronic studies.[38] Furthermore, the zebrafish species has a high fecundity and small size allowing two to three hundred fertilized eggs to be obtained weekly and sample volumes to be as low as 100 μL. For these reasons, the zebrafish has been used by numerous groups to examine the toxicity of carbon-based,[39-43] metal,[31, 44-48] and metal oxide[32, 49-51] NPs.

References

1. Popov, A. P.; Zvyagin, A. V.; Lademann, J.; Roberts, M. S.; Sanchez, W.; Priezzhev, A. V.; Myllyla, R. Designing inorganic light-Protective skin nanotechnology products. *J. Biomed. Nanotechnol.* **2010**, *6*, 432-451.
2. Guisbiers, G.; Van Overschelde, O.; Wautelet, M. Theoretical investigation of size and shape effects on the melting temperature and energy bandgap of TiO_2 nanostructures. *Appl. Phys. Lett.* **2008**, *92*, 103121-103123.
3. Hoffmann, M. R.; Martin, S. T.; Choi, W. Y.; Bahnemann, D. W. Environmental applications of semiconductor photocatalysis. *Chem. Rev.* **1995**, *95*, 69-96.
4. Kwon, S.; Fan, M.; Cooper, A. T.; Yang, H. Q. Photocatalytic applications of micro- and nano-TiO_2 in environmental engineering. *Crit. Rev. Environ. Sci. Technol.* **2008**, *38*, 197-226.
5. Gaya, U. I.; Abdullah, A. H. Heterogeneous photocatalytic degradation of organic contaminants over titanium dioxide: A review of fundamentals, progress and problems. *J. Photochem. Photobio. C*, **2008**, *9*, 1-12.
6. Robichaud, C. O.; Uyar, A. E.; Darby, M. R.; Zucker, L. G.; Wiesner, M. R. Estimates of upper bounds and trends in nano-TiO_2 production as a basis for exposure assessment. *Environ. Sci. Technol.* **2009**, *43*, 4227-4233.
7. Gottschalk, F.; Sonderer, T.; Scholz, R. W.; Nowack, B. Modeled environmental concentrations of engineered nanomaterials (TiO_2, ZnO, Ag, CNT, Fullerenes) for different regions. *Environ. Sci. Technol.* **2009**, *43*, 9216-9222.
8. Elimelech, M.; Jia, X.; Gregory, J.; Williams, R. *Particle Deposition & Aggregation: Measurement, Modelling and Simulation*. 1; Butterworth-Heinemann: Oxford, England, 1998.
9. Klaine, S. J.; Alvarez, P. J. J.; Batley, G. E.; Fernandes, T. F.; Handy, R. D.; Lyon, D. Y.; Mahendra, S.; McLaughlin, M. J.; Lead, J. R. Nanomaterials in the environment: Behavior, fate, bioavailability, and effects. *Environ. Toxicol. Chem.* **2008**, *27*, 1825-1851.
10. Farre, M.; Gajda-Schrantz, K.; Kantiani, L.; Barcelo, D. Ecotoxicity and analysis of nanomaterials in the aquatic environment. *Anal. Bioanal. Chem.* **2009**, *393*, 81-95.
11. Mudunkotuwa, I. A.; Grassian, V. H. The devil is in the details (or the surface): Impact of surface structure and surface energetics on understanding the behavior of nanomaterials in the environment. *J. Environ. Monitor.* **2011**, *13*, 1135-1144.
12. Liufu, S. C.; Mao, H. N.; Li, Y. P. Adsorption of poly(acrylic acid) onto the surface of titanium dioxide and the colloidal stability of aqueous suspension. *J. Colloid Interf. Sci.* **2005**, *281*, 155-163.
13. Phenrat, T.; Saleh, N.; Sirk, K.; Kim, H. J.; Tilton, R. D.; Lowry, G. V. Stabilization of aqueous nanoscale zerovalent iron dispersions by anionic polyelectrolytes: Adsorbed anionic polyelectrolyte layer properties and their effect aggregation and sedimentation. *J. Nanopart. Res.* **2008**, *10*, 795-814.
14. Jiang, J. K.; Oberdorster, G.; Biswas, P. Characterization of size, surface charge, and agglomeration state of nanoparticle dispersions for toxicological studies. *J. Nanopart. Res.* **2009**, *11*, 77-89.
15. Mudunkotuwa, I. A.; Grassian, V. H. Citric acid adsorption on TiO_2 nanoparticles in aqueous suspensions at acidic and circumneutral pH: Surface coverage, surface

speciation, and its impact on nanoparticle-nanoparticle interactions. *JACS* **2010**, *132*, 14986-14994.
16. Schubert, U.; Neouze, M. A. Surface modification and functionalization of metal and metal oxide nanoparticles by organic ligands. *Monatsh. Chem.* **2008**, *139*, 183-195.
17. Steinberg, C.; Muenster, U. Geochemistry and Ecological Role of Humic Substances. In *Humic Substances in Soil, Sediment, and Water*, Aiken, G. R.; McKnight, D. M.; Wershaw, R. L.; MacCarthy, P., Eds.; Wiley-Interscience: New York, NY, 1985.
18. Wetzel, R. G. *Limnology: Lake and River Ecosystems*; 3; Academic Press: San Diego, 2001.
19. Chen, K. L.; Elimelech, M. Influence of humic acid on the aggregation kinetics of fullerene (C-60) nanoparticles in monovalent and divalent electrolyte solutions. *J. Colloid Interf. Sci.* **2007**, *309*, 126-134.
20. Chen, K. L.; Elimelech, M. Interaction of fullerene (C-60) nanoparticles with humic acid and alginate coated silica surfaces: Measurements, mechanisms, and environmental implications. *Environ. Sci. Technol.* **2008**, *42*, 7607-7614.
21. Ghosh, S.; Mashayekhi, H.; Pan, B.; Bhowmik, P.; Xing, B. S. Colloidal behavior of aluminum oxide nanoparticles as affected by pH and natural organic matter. *Langmuir* **2008**, *24*, 12385-12391.
22. Baalousha, M. Aggregation and disaggregation of iron oxide nanoparticles: Influence of particle concentration, pH and natural organic matter. *Sci. Total Environ.* **2009**, *407*, 2093-2101.
23. Liu, X.; Wazne, M.; Han, Y.; Christodoulatos, C.; Jasinkiewicz, K. L. Effects of natural organic matter on aggregation kinetics of boron nanoparticles in monovalent and divalent electrolytes. *J. Colloid Interf. Sci.* **2010**, *348*, 101-107.
24. Saleh, N. B.; Pfefferle, L. D.; Elimelech, M. Influence of biomacromolecules and humic acid on the agregation knetics of sigle-walled carbon nanotubes. *Environ. Sci. Technol.* **2010**, *44*, 2412-2418.
25. Thio, B. J. R.; Zhou, D. X.; Keller, A. A. Influence of natural organic matter on the aggregation and deposition of titanium dioxide nanoparticles. *J. Hazard. Mat.* **2011**, *189*, 556-563.
26. Domingos, R. F.; Tufenkji, N.; Wilkinson, K. J. Aggregation of titanium dioxide nanoparticles: role of a fulvic acid. *Environ. Sci. Technol.* **2009**, *43*, 1282–1286.
27. King-Heiden, T. C.; Wiecinski, P. N.; Mangham, A. N.; Metz, K. M.; Nesbit, D.; Pedersen, J. A.; Hamers, R. J.; Heideman, W.; Peterson, R. E. Quantum dot nanotoxicity assessment using the zebrafish embryo. *Environ. Sci. Technol.* **2009**, *43*, 1605-1611.
28. Zhu, Z. J.; Carboni, R.; Quercio, M. J.; Yan, B.; Miranda, O. R.; Anderton, D. L.; Arcaro, K. F.; Rotello, V. M.; Vachet, R. W. Surface properties dictate uptake, distribution, excretion, and toxicity of nanoparticles in fish. *Small*, **2010**, *6*, 2261-2265.
29. Truong, L.; Moody, I. S.; Stankus, D. P.; Nason, J. A.; Lonergan, M. C.; Tanguay, R. L. Differential stability of lead sulfide nanoparticles influences biological responses in embryonic zebrafish. *Arch. Toxicol.* **2011**, *85*, 787-798.
30. Federici, G.; Shaw, B. J.; Handy, R. D. Toxicity of titanium dioxide nanoparticles to rainbow trout (*Oncorhynchus mykiss*): Gill injury, oxidative stress, and other physiological effects. *Aquat. Toxicol.* **2007**, *84*, 415-430.

31. Griffitt, R. J.; Luo, J.; Gao, J.; Bonzongo, J. C.; Barber, D. S. Effects of particle composition and species on toxicity of metallic nanomaterials in aquatic organisms. *Environ. Toxicol. Chem.* **2008**, *27*, 1972-197.
32. Zhu, X. S.; Zhu, L.; Duan, Z. H.; Qi, R. Q.; Li, Y.; Lang, Y. P. Comparative toxicity of several metal oxide nanoparticle aqueous suspensions to Zebrafish (*Danio rerio*) early developmental stage. *J. Environ. Sci. Health, Part A* **2008**, *43*, 278-284.
33. Hall, S.; Bradley, T.; Moore, J. T.; Kuykindall, T.; Minella, L. Acute and chronic toxicity of nano-scale TiO_2 particles to freshwater fish, cladocerans, and green algae, and effects of organic and inorganic substrate on TiO_2 toxicity. *Nanotoxicol.* **2009**, *3*, 91-97.
34. Ramsden, C. S.; Smith, T. J.; Shaw, B. J.; Handy, R. D. Dietary exposure to titanium dioxide nanoparticles in rainbow trout, (*Oncorhynchus mykiss*): No effect on growth, but subtle biochemical disturbances in the brain. *Ecotoxicol.* **2009**, *18*, 939-951.
35. Bar-Ilan, O.; Louis, K. M.; Yang, S. P.; Pedersen, J. A.; Hamers, R. J.; Peterson, R. E.; Heideman, W. Titanium dioxide nanoparticles produce phototoxicity in the developing zebrafish. *Nanotoxicol.* **2012**, *6*, 670-679.
36. Ma, H. B.; Brennan, A.; Diamond, S. A. Phototoxicity of TiO_2 nanoparticles under solar radiation to two aquatic species: *Daphnia magna* and Japanese medaka. *Environ. Toxicol. Chem.* **2012**, *31*, 1621-1629.
37. Bar-Ilan, O. Toxicity of metal and metal oxide nanoparticles in developing zebrafish. PhD Dissertation. University of Wisconsin, Madison, WI, 2011.
38. Fraysse, B.; Mons, R.; Garric, J. Development of a zebrafish 4-day toxicity of embryo-larval bioassay to assess chemicals. *Ecotoxicol. Environ. Safety* **2006**, *63*, 253-267.
39. Cheng, J. P.; Flahaut, E.; Cheng, S. H. Effect of carbon nanotubes on developing zebrafish (*Danio rerio*) embryos. *Environ. Toxicol. Chem.* **2007**, *26*, 708-716.
40. King-Heiden, T. C.; Dengler, E.; Kao, W. J.; Heideman, W.; Peterson, R. E. Developmental toxicity of low generation PAMAM dendrimers in zebrafish. *Toxicol. Appl. Pharmacol.* **2007**, *225*, 70-79.
41. Henry, T. B.; Menn, F. M.; Fleming, J. T.; Wilgus, J.; Compton, R. N.; Sayler, G. S. Attributing effects of aqueous C-60 nano-aggregates to tetrahydrofuran decomposition products in larval zebrafish by assessment of gene expression. *Environ. Health Perspect. A* **2007**, *115*, 1059-1065.
42. Zhu, X. S.; Zhu, L.; Li, Y.; Duan, Z. H.; Chen, W.; Alvarez, P. J. J. Developmental toxicity in zebrafish (*Danio rerio*) embryos after exposure to manufactured nanomaterials: Buckminsterfullerene aggregates (nC60) and fullerol. *Environ. Toxicol. Chem.* **2007**, *26*, 976-979.
43. Cheng, J. P.; Chan, C. M.; Veca, L. M.; Poon, W. L.; Chan, P. K.; Qu, L. W.; Sun, Y. P.; Cheng, S. H. Acute and long-term effects after single loading of functionalized multi-walled carbon nanotubes into zebrafish (*Danio rerio*). *Toxicol. Appl. Pharmacol.* **2009**, *235*, 216-225.
44. Lee, K. J.; Nallathamby, P. D.; Browning, L. M.; Osgood, C. J.; Xu, X. H. N. In vivo imaging of transport and biocompatibility of single silver nanoparticles in early development of zebrafish embryos. *ACS Nano* **2007**, *1*, 133-143.
45. Asharani, P. V.; Serina, N. G. B.; Nurmawati, M. H.; Wu, Y. L.; Gong, Z.; Valiyaveettil, S. Impact of multi-walled carbon nanotubes on aquatic species. *J. Nanosci. Nanotechno.* **2008**, *8*, 3603-3609.

46. Yeo, M. K.; Kang, M. Effects of nanometer sized silver materials on biological toxicity during zebrafish embryogenesis. *Bull. Korean Chem. Soc.* **2008**, *29*, 1179-1184.
47. Bar-Ilan, O.; Albrecht, R. M.; Fako, V. E.; Furgeson, D. Y. Toxicity assessments of multisized gold and silver nanoparticles in zebrafish embryos. *Small* **2009**, *5*, 1897-1910.
48. Griffitt, R. J.; Hyndman, K.; Denslow, N. D.; Barber, D. S. Comparison of molecular and histological changes in zebrafish gills exposed to metallic nanoparticles. *Toxicol. Sci.* **2009**, *107*, 404-415.
49. Yeo, M. K.; Kim, H. E. Gene expression in zebrafish embryos following exposure to TiO_2 nanoparticles. *Mol. Cell. Toxicol.* **2010,** *6*, 97-104.
50. Yoon, J. W.; Yeo, M. K. The difference of surface charge and crystal shape in TiO_2 nanoparticles induce differential biological effects in zebrafish. *Mol. Cell. Toxicol.* **2009**, *5*, 49-49.
51. Zhu, X. S.; Wang, J. X.; Zhang, X. Z.; Chang, Y.; Chen, Y. S. The impact of ZnO nanoparticle aggregates on the embryonic development of zebrafish (*Danio rerio*). *Nanotechnol.* **2009**, *20*.

Chapter 2: Influence of Dissolved Organic Matter on Titanium Dioxide Nanoparticle Toxicity to Developing Zebrafish[1]

[1] Published as Yang, S .P.; Bar-Ilan, O.; Peterson, R. E.; Heideman, W.; Hamers, R. J.; Pedersen, J. A. Influence of humic acid on titanium dioxide nanoparticle toxicity to developing zebrafish. *Environ. Sci. Technol.* **2013**, Early Online.

2.1 Abstract

Titanium dioxide nanoparticle (TiO_2 NP) suspension stability can be altered by adsorption of dissolved organic matter (DOM). This is expected to impact their environmental fate and bioavailability. To date, the influence of DOM on the toxicity of TiO_2 NPs to aquatic vertebrates has not been reported. We examined the impact of Suwannee River humic acid (HA) on the toxicity of TiO_2 NPs to developing zebrafish (*Danio rerio*) in the presence and absence of simulated sunlight. Adsorption of HA increased suspension stability and decreased TiO_2 NP exposure. In the absence of simulated sunlight, a small but significant increase in lethality was observed in fish exposed to TiO_2 NPs in the presence of HA. Under simulated sunlight illumination, photocatalytic degradation of HA reduced suspension stability. Despite the lower levels of Ti associated with fish in the treatments containing HA, under simulated sunlight illumination, median lethal concentrations were lower and oxidative DNA damage was higher relative to fish exposed to TiO_2 NPs in the absence of HA. TiO_2 NPs were more toxic in the presence of HA. This study demonstrates the importance of considering environmental factors (i.e., exposure to sunlight, adsorption of DOM) when assessing the risks posed by engineered nanomaterials in the environment.

2.2 Introduction

Current applications of titanium dioxide nanoparticles (TiO_2 NPs) range from personal care products to photovoltaics to environmental remediation.[1] As production volumes and applications for TiO_2 NPs increase, so does the potential for their release into the environment.[2] Because TiO_2 is a wide band gap semiconductor, reactive oxygen species (ROS) can be generated upon adsorption of energy equal to or larger than the band gap and

gap energies for TiO_2 NPs fall within the UV to violet region (e.g., 3.0-5.0 eV; 250-415nm) with this range reflecting TiO_2 NP size and crystal phase differences.[3]

Supra-band gap irradiation of TiO_2 promotes electrons from the valence to conduction band leaving a hole (h^+) in the valence band. Although the electron and hole can interact in several manners (e.g., recombination, conduction of electricity), ROS are formed at the surface when the free electron or hole interacts with electron acceptors/donors in the surrounding medium.[4] In aqueous environments, free electrons reduce molecular oxygen to generate superoxide radical ($O_2{\cdot}^-$) while the hole can oxidize water to form hydroxyl radical ($OH{\cdot}$).[4]

Bulk TiO_2 is considered biologically inert and is often used as a pigment in consumer products (e.g., personal care products, foods).[5] Studies comparing bulk and nanoscale TiO_2, however, have reported increases in toxicity with the nanoscale material.[6-8] Furthermore, the ability for TiO_2 NPs to produce ROS upon UV illumination increases their toxicity to plankton and fish cell cultures.[9-13] We have shown that exposure of developing zebrafish (*Danio rerio*) to TiO_2 NPs in the presence of simulated sunlight significantly decreased survival and increased the incidence of malformations.[14-15] Formation of superoxide *in vivo*, increased expression of an antioxidant response-element-driven reporter, and increased DNA damage with concurrent exposure to light were consistent with oxidative stress as the mechanism of toxicity.[14]

Once released into aquatic environments, TiO_2 NPs may acquire a coating of dissolved organic mater (DOM) molecules, a complex mixture of molecules resulting from microbial degradation of plant, algae and bacterial matter. Adsorption of DOM increases

the suspension stability of unfunctionalized TiO_2 NPs.[16-19] Increased stability of TiO_2 NP suspensions is expected to increase residence times in the water column, facilitate advective transport in aqueous environments, increase exposure to free-swimming aquatic organisms, and reduce delivery to benthic species. DOM can to diminish nanoparticle toxicity by reducing bioavailability to microcrustaceans and bacteria.[20-23] Furthermore, DOM can act as both a source and a sink for ROS in aqueous environments.[24-27] However, to date, the effect of DOM on TiO_2 NP toxicity to aquatic vertebrates has not been reported.

The objective of this study was to determine the extent that adsorption of DOM alters the inherent and photo-enhanced toxicity of TiO_2 NPs toward developing zebrafish. To accomplish this, we exposed embryonic and larval zebrafish to a commercial TiO_2 NP preparation in the absence and presence of simulated sunlight illumination. We examined the influence of DOM on TiO_2 NP suspension stability and uptake by and toxicity toward developing zebrafish. We chose to examine unfunctionalized Degussa P25 TiO_2 NPs because of their use in commerce. We used two polarity fractions of DOM, Suwannee River humic acid (HA) and fulvic acid (FA), and a natural organic matter isolate (NOM) as a models for aquatic DOM because they have been well-characterized and used in prior NP aggregation studies.[16] Developing zebrafish were chosen as the animal model because their rapid, well-studied development, small size, and high fecundity makes them suitable for assessing the toxicity of nanomaterials.[8, 14-15, 22, 28-37]

2.3 Materials and Methods

Materials

Aeroxide P25 TiO_2 nanoparticles (3:1 anatase: rutile) were purchased from Evonik Degussa (Essen, Germany). Primary particle diameter was previously determined to be 21±1 nm by high resolution transmission electron microscopy.[14] A 2000 mg·L^{-1} TiO_2 NP stock suspension was prepared in ultrapure water (18 MΩ·cm resistivity; Barnstead NANOpure Ultrapure Water System, Dubuque, IA), sonicated for 1h (Bransonic 2510 ultrasonicator; 100 W; 40 kHz), and stored in the dark for ≤7d. Prior to making working TiO_2 NP suspensions, the stock was mixed and then sonicated for 2-5 min. Suwannee River humic acid (HA; 2S101H), fulvic acid (FA, 1S101F), and natural organic matter isolate (NOM, 1R101N) were purchased from the International Humic Substance Society, and a stock of 1000 mg·L^{-1} was made in ultrapure water.

Zebrafish exposures were conducted in "fish water." Fish water was prepared by dissolving 58 mg of Instant Ocean™ salt (Aquarium Systems; Mentor, OH) and 47.6 mg $NaHCO_3$ (Fisher Scientific) per in 1 L of ultrapure water yielding a final ionic composition of 4.4 mM Cl^-, 4.6 mM Na^+, 0.78 mM HCO_3^-, 0.22 mM Mg^{2+}, 87 µM K^+, 81 µM Ca^{2+}, 27 µM CO_3^{2-}, 5.7 µM Br^-, 4.2 µM B^{3+}, 0.81 µM Sr^{2+}, 0.43 µ M F^-, 0.35 µM Li^+, and 15 nM I^- (ionic strength = 0.07 mM, pH = 7-7.4).[38]

To study photo-enhanced toxicity, sunlight was simulated using a 250 W blue-spectrum metal halide lamp (XM 250W, 10,000K; electronic ballast; XM Lighting, Anaheim, CA), a lamp commonly used in aquaria.[14] The spectrum for the metal halide lamp was

obtained with a Licor Spectroradiometer LI-800[39] and compared to that of sunlight at Earth's surface using the ASTM G173-03 global tilt reference (Figure 2.1).[40] The lamp was designed to simulate sunlight underwater, hence the difference in irradiance intensities between the two spectra. Despite these differences, the lamp spectrum included wavelengths with energies equal to and exceeding the band gap of the TiO_2 NPs (387-414 nm)[41] and was, therefore, expected to induce charge-hole separation and the production of reactive oxygen species (ROS).

To minimize the evaporation of the exposure solutions, 96-well plates were covered with the plate lid. For exposures conducted in the absence of simulated sunlight, samples were covered in foil and placed under the lamp. The lamp was set for a 14h:10h on: off cycle. Temperatures differences between off and on cycles were small (off: 27-28°C; on: 28-30°C). These temperature differences did not produce measurable differences in aggregation state (data not shown).

Assessment of Suspension Stability

Suspensions of TiO_2 NPs (100 mg·L^{-1}) with and without DOM (30 mg·L^{-1}) were prepared in fish water from stock solutions. Particle diffusivities and electrophoretic mobilities (μ_E) were determined by dynamic and electrophoretic light scattering using a Zetasizer Nano ZS (Malvern Instruments, Worcestershire, UK; 633 nm laser, 173° scattering angle). Particle diffusivities were converted to intensity-averaged hydrodynamic diameters using the Stokes-Einstein equation. Intensity measurements were converted to hydrodynamic diameter (d_h) number distributions using Mie theory.[42] Confidence in the

precise d_h in the number distributions is less than for the intensity-average d_h, but d_h number distributions can be used for comparative purposes between treatments.[43-45]

Suspension stability was assessed under the same conditions employed in the zebrafish toxicity assay. A 96-well plate format was chosen because of the small sample size required. For each NP treatment, 100 μL was added to each well (12 wells per time point/measurement; ~1.2 mL per treatment/time point). At designated time points, the solution was removed from the specified row.

To determine hydrodynamic diameters, sample suspensions (500 μL) were transferred to low-volume, disposable cuvettes (Sarstedt, Part No. 67.758). Three measurements, each consisting of 10 runs, were obtained and averaged to yield hydrodynamic d_h distributions. To determine electrophoretic motilities, 1 mL of the collected suspensions was loaded in a clear, disposable folded capillary cell (Malvern Instruments, Part No. DTS1060); six measurements, each consisting of 15 runs, were conducted and averaged. For both analyses, each experiment was performed a minimum of two times.

Hydrodynamic diameters and electrophoretic mobilities of the HA in the absence of TiO_2 NPs were also determined before (t=0 h) and after (t=24 h) exposure in the absence of illumination with simulated sunlight. Hydrodynamic diameters were not measured for HA after simulated sunlight illumination because such data were not relevant for the TiO_2 NP suspensions containing HA under simulated sunlight illumination. In those treatments, HA

underwent extensive photocatalytic degradation as discussed in the main text and shown in Figure 2.8.

To confirm that HA decreased the hydrodynamic diameter of TiO_2 NP aggregates (Figure 2.4A), we conducted analogous DLS experiments using a filtered HA solution. Distributions of d_h and electrophoretic mobilities were collected for HA solutions in the presence and absence of TiO_2 NPs (100 mg·L^{-1}) and at t=0 and t =24 h in the absence or presence of simulated sunlight illumination (14 h on: 10 h off). Ultrapure water and fish water used to make solutions were filtered through a 0.1 μm syringe filter (Millipore, Part No. SLVV033RS), and stock solutions of HA (1000 mg·L^{-1}) were filtered through a 0.22 μm syringe filters (Millipore, Part No. SLGP033RS).

Photocatalytic Degradation of HA by TiO_2 NPs

We assessed the photocatalytic degradation of HA by TiO_2 NPs using high-pressure size-exclusion chromatography with diode array detection (HPSEC-DAD).[46-47] Humic acid solutions (30 mg·L^{-1}) alone or with TiO_2 NPs (100 mg·L^{-1}) were added to a 96-well plate (100 μL per well; 96 wells per sample) and exposed to and shielded from simulated sunlight. At the end of the experiment, the entire solution from each well was removed, combined, and centrifuged through an Amicon Ultracel 50K centrifugal filter (3000*g*, 30 min; Millipore, MA). The filtrate (2 mL) containing non-adsorbed HA and/or HA degradation products was injected into a Shimadzu HPLC (Shimadzu Instruments, Kyoto, Japan) equipped with a Waters Protein-Pak 125 column.

Sample injection and separation were conducted using a Shimatzu system that consisted of a system controller (SCL-10A), diode array detector (SPD-M10A), and two liquid chromatographs (LC-6AD). Phosphate buffer (0.02 M; pH 6.8; ionic strength adjusted to 0.1 M with NaCl) was used as the mobile phase with an isocratic flow rate of 1.0 $mL \cdot min^{-1}$, and a Waters Protein-Pak 125 (7.8 mm × 30 cm; steel; WAT084601) column was employed. Absorbance was measured at 1 nm increments from 200-700 nm for up to 30 min. Polystyrene sulfonate standards (1 $g \cdot L^{-1}$) with molecular masses of 8000, 18 000, and 35 000 *u* were used for calibration. [47]

Zebrafish Exposures

Zebrafish (AB strain) were bred to obtain fertilized embryos. Zebrafish were exposed continuously to TiO_2 NPs or controls from the embryonic stage (4-6 hours post fertilization (hpf)) until the larval stage (5 days post fertilization (dpf)). One fish was added to each well of a 96-well cell culture plate (BD Biosciences, Part No. 351172) at 4-6 hpf. Fish were maintained at 27-30°C in either the presence or absence of simulated sunlight. Control fish kept in the dark, under normal laboratory lighting and under simulated sunlight developed normally (e.g., similar hatching times and incidence of malformations; Figure 2.2).

Exposure suspensions ([TiO_2 NP]= 0-1000 $mg \cdot L^{-1}$; [DOM]= 0 or 30 $mg \cdot L^{-1}$) were prepared daily in fish water. At 4-6 hpf, 100 µL of dosing suspensions were added to each well. Every subsequent day until 5 dpf, the suspension was removed (including sedimented NPs) and replaced with freshly prepared suspensions.

For each exposure, 12 fish were used and three replicates were performed (36 fish per treatment); each experiment was performed a minimum of three times. Zebrafish were assessed daily for mortality. At designated time points, 10 larvae from each exposure group (n = 3 replicates) were immobilized in 3% methylcellulose and photographed in the lateral orientation at 2.6× magnification. From these micrographs, malformations (e.g., bent spine, stunted growth, tail fin malformation), edema, and failed yolk sac absorption were examined (see Figure 2.3 for representative micrographs). The incidence of pericardial edema and failed yolk sac absorption were quantified. Zebrafish were cared for according to all institutional protocols (protocol M00489-4-11-06).

Determination of TiO_2 NP Exposure

To determine TiO_2 NP exposure levels, surviving zebrafish were collected at the desired time point, rinsed, pooled, and alkaline digested. For each exposure condition, 12 pooled samples were used. Fish were rinsed in 10 mL ultrapure H_2O and transferred to a preweighed centrifuge tube. Excess water was removed, and the sample was allowed to air dry for 2 h. After drying, the wet weight of sample was obtained.

To determine the difference between the amount of TiO_2 NPs associated with the fish (association levels) and the amount internalized by the fish (body burden), fish were either rinsed in ultrapure H_2O (association) or in an Ivory Soap solution to remove NPs on the surface of the fish (body burden). To determine association levels, the fish were rinsed three times in ultrapure H_2O. To determine body burden levels, fish were washed using a method adapted from Lake *et al.*[S548] Briefly, fish were placed in 1 mL of 1 $g \cdot L^{-1}$ Ivory liquid hand soap (Procter and Gamble, Ohio, USA) for 5 min and then rinsed three times in 1 mL

ultrapure H_2O. For both procedures, excess water was removed and samples were stored at −80 °C.

To determine Ti concentrations, alkaline digestion was performed. Fish were digested in 1 mL of 5 M NaOH for 24 h at 65°C. Digestates were added to 1.5 mL of 5 M HNO_3 and diluted to 5 mL with ultrapure H_2O. Ti concentrations were determined using a Varian Vista-MPX inductively coupled plasma-optical emission spectrometer (ICP-OES; 0.75 $L \cdot min^{-1}$ nebulizer flow; 15.0 $L \cdot min^{-1}$ plasma flow; Varian, Inc., CA). Emission was recorded at 334.188, 334.941, 336.122, and 337.280 nm and averaged.

Thiobarbituric Acid Reactive Substance (TBARS) Analysis

Exposure of organisms to reactive oxygen species (ROS) can cause oxidative stress. Lipid hydroperoxides and aldehydes (i.e., thiobarbituric acid reactive substances) are produced when a hydrogen atom is abstracted from an unsaturated fatty acid and double bonds rearrange.[49] Lipid hydroperoxides alter membrane fluidity and membrane protein integrity and are associated with oxidative stress.[49] Lipid peroxidation was assessed using a microplate-format TBARS assay (ZeptoMetrix TBARS Assay Kit; ZeptoMetrix Corp., NY).[50-51] In this assay, thiobarbituric acid undergoes a nucleophilic addition reaction with malondialdehyde (MDA), a well-characterized oxidation product of polyunsaturated fatty acids, to form a fluorescent, covalent adduct.

For this assay, zebrafish (48 fish per replicate; two replicates per experiment) were exposed in the presence or absence of HA (30 $mg \cdot L^{-1}$) to 0 or 1000 $mg \cdot L^{-1}$ TiO_2 NPs in the absence of simulated sunlight (until 4 dpf) or 0 or 250 $mg \cdot L^{-1}$ TiO_2 NPs in the presence of

simulated sunlight (until 3 dpf). The chosen time points were 24 h prior to the largest observed decrease in survival, and the selected concentrations corresponded to the largest change in survival between TiO_2 NP exposures in the presence and absence of HA (data not shown).

At the indicated time point, surviving fish were collected and rinsed twice with 10 mL ultrapure water. Fish were transferred to a centrifuge tube, and excess water was removed. Samples were flash-frozen in liquid nitrogen and stored at −80 °C until analysis.

Thawed samples were added to 250 µL phosphate buffered saline (PBS) and homogenized (three 20s beatings at 4.0 $m \cdot s^{-1}$) with a Fast Prep-24 Homgenizer (MP Biomedicals, Ohio, USA) using 1.4 mm ceramic beads (Mo Bio Laboratories Inc, California, USA). A ZeptoMetrix TBARS Assay Kit (ZeptoMetrix Corporation, New York, USA) was used, and the microplate technique was employed. Fluorescence was measured using a FLx800 Fluorescence Microplate Reader (Biotek, Vermont, USA) with λ_{ex} = 530 nm and λ_{em} = 550 nm.

The amount of MDA produced was normalized to protein content. Protein content was quantified using a bicinchoninic acid assay (Pierce Biotechnology, Illinois, USA). Aliquots of fish samples were diluted 1:5 in PBS (two protein samples per fish sample), and the microplate procedure for the assay was used. Absorbance was measured at λ = 540 nm with a Dynatech Laboratories MRX microplate reader (Dynatech Laboratories, Virginia, USA). Each experiment was performed a minimum of three times.

Determination of 8-Hydroxy-2-deoxy Guanosine (8-OHdG) Levels

One of the hallmarks of oxidative stress is the formation of DNA adducts. A commonly assayed DNA adduct is 8-hydrox-2-deoxy-guanosine (8-OHdG).[52-54] Concentrations of 8-OHdG in zebrafish were determined by an enzyme-linked immunosorbent assay.

For this assay, zebrafish (40 fish were used; two replicates per experiment) were exposed to controls (i.e., fish water, HA only) or TiO_2 NPs (250 and 500 $mg \cdot L^{-1}$) in the presence and absence of HA in the light until 3 dpf. This time point was chosen because it was 24 h prior to the largest observed decrease in survival, and this concentration was selected because it corresponded to the largest change in survival between TiO_2 NP exposures in the presence and absence of HA ($p \leq 0.05$; data not shown). At 3 dpf, the fish were collected, flash frozen, and stored at −80 °C until analysis.

DNA was extracted using Promega Wizard SV Genomic DNA extraction kit and quantified using a Nanodrop ND-1000 Spectrophotometer (Thermo Fisher, Delaware, USA). After extraction, DNA was digested using nuclease P1 and used in a 96-well competitive assay kit following manufacturer's instructions (StressMarq Biosciences; British Columbia, Canada). Absorbance at $\lambda = 405$ nm was read using a BioTex Synergy Mx microplate reader (Biotek, Vermont, USA). 8-OHdG concentration was normalized to DNA concentration. Each experiment was performed a minimum of two times.

Statistical Analyses

Median lethal concentrations (LC_{50} values) were calculated using a trimmed Spearman-Karber analysis with 12.5% trim (USEPA Trimmed Spearmen-Karber Analysis Program, Version 1.5).[55] Differences in LC_{50} values were considered significant if their 95% confidence intervals did not overlap. Data are presented as mean ± SEM unless otherwise noted. Unpaired *t*-tests were employed to determine *p*-values. The level of significance for all analyses was $p \leq 0.05$.

2.4 Results and Discussion

Effect of HA on the Inherent Toxicity of TiO_2 NPs

Stability of TiO_2 NP Suspensions. We expected suspension stability to affect the exposure of developing zebrafish to TiO_2 NPs. We therefore examined the aggregate size (hydrodynamic diameter, d_h) and electrophoretic mobility (μ_E) of TiO_2 NPs in the absence and presence of Suwannee River HA before (t=0h) and after (t=24h) exposure in the absence of simulated sunlight illumination.

In the absence of HA, aggregates (100 $mg \cdot L^{-1}$) displayed a monomodal size distribution with d_h=0.2 μm and $\mu_E = -1.73(\pm 0.04) \times 10^4$ $cm^2 \cdot V^{-1} \cdot s^{-1}$ (Figure 2.4A-B). After exposure in the absence of HA, the TiO_2 aggregate size distribution remained monomodal but d_h increased to 1.5 μm (Figure 2.4A) and μ_E decreased to $-1.45(\pm 0.04) \times 10^4$ $cm^2 \cdot V^{-1} \cdot s^{-1}$ (Figure 2.4B). These data indicate that, in the absence of HA, TiO_2 NP aggregated over the course the exposure period.

In the presence of HA, TiO_2 NP suspensions were visibly more stable. The distribution of d_h values from TiO_2 NPs in the presence of HA differed from that in its absence (Figure 2.4A). At t=0 h, the d_h distribution had a mode at ~0.05 μm with a shoulder extending to ~0.2 μm. At t=24 h, the d_h distribution shifted to slightly larger values: the mode was ~0.09 μm and the shoulder extended to ~0.2 μm.

Non-adsorbed HA in the TiO_2 NP suspension may have contributed to the observed scattering. In the absence of TiO_2 NPs, modal d_h values for HA at t=0 h and t=24 h were 0.014±0.0072 μm and 0.049±0.0093 μm (Table 2.1). Hence, part of the scattering in Figure 2.4A may be attributable to that of HA. The suspension included HA- TiO_2 NP complexes and free HA (as demonstrated by the HP-SEC results; Figure 2.8). Nonetheless, the data clearly show that the size of TiO_2 NPs in the presence of HA is smaller than that of the particles in its absence (modal d_h=0.2 μm at t=0 h and 1.5 μm at t=24 h).

In the presence of HA, the measured μ_E were more negative than for TiO_2 NPs (Figure 2.4B) or HA alone (Table 2.1) suggesting that HA molecules adsorbed to the NP. Adsorption of HA molecules also decreased TiO_2 NP sedimentation rate (data not shown). In the absence of HA, TiO_2 NP aggregates sedimented rapidly; in the presence of HA, the bulk of TiO_2 NPs remained in suspension over the course of the exposure period.

These results are consistent with HA adsorption to TiO_2 NP surfaces reducing aggregate size. Similar influence of DOM on TiO_2 NP suspension stability in the absence of UV illumination has been reported previously.[17-19,56] The observation that TiO_2 NP suspension stability differed in the presence and absence of HA led to the expectation that exposure to the zebrafish would also differ.

Effect of HA on Ti Association with Developing Zebrafish. Developing zebrafish reside near the sediment-water interface. We hypothesized that fish exposed to unstable suspensions (i.e., those in the absence of DOM) would have a greater TiO_2 NP exposure (i.e., association levels; body burdens) than those exposed to stable suspensions (i.e., those in the presence of DOM). To test this hypothesis, we examined TiO_2 NP association levels and body burdens after exposure in the presence and absence of HA.

Differences between association levels and body burdens did exist indicating that washing may have removed some bound NPs from the surface of the zebrafish. For instance, at a nominal exposure concentration of 100 $mg \cdot L^{-1}$ TiO_2 NPs, association levels were significantly higher than body burden levels both in the presence and absence of HA. In the absence of HA, body burden was 16 ± 1.8 $\mu g\ Ti \cdot g\ fish^{-1}$ while the association level was 87.4 ± 8.2 $\mu g\ Ti \cdot g\ fish^{-1}$; in the presence of HA, body burden was 11.1 ± 1.6 $\mu g\ Ti \cdot g\ fish^{-1}$ and association level was 25.7 ± 5.9 $\mu g\ Ti \cdot g\ fish^{-1}$ (Table 2.2).

Despite the observed differences between association levels and body burdens, scanning electron microscopy indicated relatively little TiO_2 was adhered to the surface of the larvae (data not shown). Furthermore, it was unclear how washing altered the integrity of the fish tissue. For these reasons, association levels instead of body burdens were used in the remainder of the study.

Consistent with expectations, levels of Ti associated with the fish were significantly lower in those exposed to TiO_2 NPs in the presence than in the absence of HA ($p \leq 0.05$; Figure 2.5A). For example, exposure to the nominal 100 $mg \cdot L^{-1}$ TiO_2 NP dose resulted in

association levels of 87±8.2 $\mu g_{Ti} \cdot g_{fish}^{-1}$ in the absence of HA and 26±5.9 $\mu g_{Ti} \cdot g_{fish}^{-1}$ in the presence of HA (Figure 2.5A). This decrease in amount of Ti associated with the fish in the presence of HA also occurred at the nominal 10 and 250 $mg \cdot L^{-1}$ TiO_2 NP doses (data not shown).

Although the chorion can be a barrier to TiO_2 NP uptake,[14] we found that the decrease in Ti association with the fish in the presence of HA was not due to a delay in hatching ($p \leq 0.05$). For example, fish exposed to TiO_2 NPs (100 $mg \cdot L^{-1}$) in the absence of DOM hatched at 2.7±0.15 dpf while those exposed in the presence of HA hatched at 2.9±0.16 dpf. To our knowledge, this is the first study to demonstrate that acquisition of a HA coating and concomitant changes in suspension stability leads to altered nanoparticle uptake by fish.

Effect of HA on TiO_2 NP Toxicity. By increasing suspension stability, adsorption of HA reduced TiO_2 NP uptake. We therefore hypothesized that reduced uptake would lead to reduced toxicity. To test this hypothesis, we examined the effect of HA on survival and the incidence of failed yolk sac absorption and edema in developing zebrafish after TiO_2 NP exposure.

In the absence of HA, TiO_2 NPs produced very low mortality (Figure 2.5B). Acquisition of a HA coating produced small, but statistically significant decreases in survival at all nominal TiO_2 NP exposure concentrations ($p \leq 0.05$; Figure 2.5B). Nonetheless, the low mortalities over the concentration range examined precluded calculation of LC_{50} values.

The increased mortality in the presence of HA occurred despite the lower levels of Ti associated with the fish in this treatment. For example, zebrafish exposed to TiO_2 NPs (nominal concentration of 100 $mg \cdot L^{-1}$ until 5 dpf) in the presence of HA exhibited lower levels of Ti associated with them relative to those exposed in the absence of HA (Figure 2.5A). Despite this lower body burden, TiO_2 NP exposure in the presence of HA resulted in higher mortality (Figure 2.5B). These results suggest that HA-coated TiO_2 NPs are more toxic than TiO_2 NPs lacking this coating.

Zebrafish exposed to TiO_2 NPs (1000 $mg \cdot L^{-1}$ nominal concentration until 4 dpf) in both the presence and absence of HA exhibited a higher incidence of failed yolk sac absorption and pericardial edema relative to control fish ($p \leq 0.05$; Figure 2.5C-D). Fish exposed to TiO_2 NPs in the presence of HA had lower incidence of failed yolk sac absorption and edema relative to those exposed to TiO_2 NPs in the absence of HA ($p \leq 0.05$; Figure 2.5C-D).

Due to differences in TiO_2 NP suspension stability, the exposure scenarios in the treatments with and without HA were not equivalent. We therefore examined toxicity relative to the amounts of TiO_2 NPs associated with the fish. The levels of Ti associated with fish exposed to TiO_2 NPs (1000 $mg \cdot L^{-1}$ nominal concentration until 4 dpf) in the absence and presence of HA were 130±17 and 73±8.9 $\mu g_{Ti} \cdot g_{fish}^{-1}$, respectively (data not shown). When normalized to the amount of Ti associated with the fish, no difference in incidence of failed yolk sac absorption or edema were observed between fish exposed to TiO_2 NP in the presence and absence of HA ($p > 0.05$; data not shown).

Effect of HA on TiO_2 NP-Induced Oxidative Stress. Oxidative stress has been proposed as the primary mechanism of TiO_2 NP toxicity.[57-59] We therefore hypothesized that HA-coated TiO_2 NPs produced more oxidative stress in developing zebrafish than did uncoated TiO_2 NPs. To test this hypothesis, we evaluated lipid peroxidation using the thiobarbituric acid reactive substance (TBARS) assay.

Zebrafish exposed to TiO_2 NPs (nominal concentration of 1000 $mg \cdot L^{-1}$ until 4 dpf) in the presence and absence of HA exhibited higher TBARS concentrations than fish exposed to controls ($p \leq 0.05$; Figure 2.5E). On a nominal dose basis, the presence of HA did not influence TBARS levels in fish exposed to TiO_2 NPs ($p > 0.05$; Figure 2.5E). However, when TBARS concentrations were examined relative to the amount of Ti associated with the fish, those exposed in the presence of HA had higher TBARS concentrations than those exposed in the absence of HA ($p \leq 0.05$; Figure 2.6).

These results indicate that exposure to TiO_2 NPs can cause lipid peroxidation in fish in absence of UV illumination. These findings are not unexpected; lipid peroxidation has been reported previously in fish exposed to TiO_2 NPs in the absence of UV illumination.[8, 60] However, the ability for adsorbed HA to increase the degree of lipid peroxidation relative to amount of TiO_2 NPs associated with the fish is unexpected. These results again suggest that HA-coated TiO_2 NPs are more toxic than are uncoated TiO_2 NPs and indicate that increased oxidative stress may be the cause of the increased mortality observed in the presence of HA.

Effect of HA on Photo-enhanced Toxicity of TiO_2 NPs

Stability of TiO_2 NP Suspensions. We examined the effect of simulated sunlight illumination on the stability of TiO_2 NP suspensions in the absence and presence of HA. In the absence of HA, TiO_2 NPs aggregated over the course of the 24-h exposure period (14h light:10h dark). At the beginning of the period, the TiO_2 aggregates (100 $mg \cdot L^{-1}$) exhibited a monomodal size distribution with a modal d_h=0.2 μm (Figure 2.7A) and had μ_E=−1.8(±0.04) $\times 10^4$ $cm^2 \cdot V^{-1} \cdot s^{-1}$ (Figure 2.7B). At the end of the period, TiO_2 NP aggregate size remained monomodally distributed with a modal d_h=1.0 μm (Figure 2.7A) and had μ_E=−1.57(±0.03) $\times 10^4$ $cm^2 \cdot V^{-1} \cdot s^{-1}$ (Figure 2.7B).

By the end of the 24 h period, TiO_2 NP d_h and μ_E did not differ substantially between suspensions with and without HA. For example, at 100 $mg \cdot L^{-1}$ TiO_2 NPs, aggregates had monomodal distributions with modes at 0.6 and 1.0 μm in the presence and absence of HA, respectively (Figure 2.7A). Furthermore, at 100 $mg \cdot L^{-1}$ TiO_2 NPs, μ_E=−1.8(±0.04) and −1.6(±0.03) $\times 10^4$ $cm^2 \cdot V^{-1} \cdot s^{-1}$ in the presence and absence of HA, respectively (Figure 2.7B). Adsorption of HA molecules reduced the sedimentation rate of TiO_2 NPs at the beginning of the illumination period (e.g., for initial ~4 h for the 100 $mg \cdot L^{-1}$ treatment), but the sedimentation rate increased as the illumination period lengthened until it was indistinguishable from the uncoated TiO_2 NPs (data not shown).

These results show that, while the presence of HA increased suspension stability initially, suspensions in both the presence and absence of HA were unstable after simulated sunlight illumination. Previous studies have not investigated the effect of sunlight on the stability of TiO_2 NP suspensions in the presence of DOM. However, TiO_2 NPs have been

shown to photocatalytically degrade organic molecules including those in DOM.[61-63] As such, this decrease in suspension stability was not unexpected.

Photocatalytic Degradation of HA by TiO_2 NPs. We hypothesized that photocatalytic degradation of DOM by TiO_2 NPs was responsible for the diminished suspension stability observed in the presence of HA upon simulated sunlight illumination. We therefore employed HPSEC-DAD (λ= 200-700 nm) to examine the size distribution and UV-Vis absorbance profiles of HA before and after simulated sunlight illumination in the absence and presence of TiO_2 NPs.

Before simulated sunlight illumination and in the absence of TiO_2 NPs, HA had a broad apparent M_r distribution (100-30,000 Da) encompassing most of the absorbance range examined (200 to 650 nm; Figure 2.8A); most of the signal intensity derived from molecules with apparent M_r of ~2000 Da and absorbance in the 200-220 nm range. After one 24-h exposure period (14h light:10h dark), the M_r distribution for HA was unchanged (Figure 2.8B).

Prior to illumination, the apparent M_r distribution for HA in the presence of TiO_2 NPs (100 mg·L^{-1}; Figure 2.8C) was similar to that in the absence of the nanoparticles (Figure 2.8A). After one 24-h exposure period (14h light:10h dark), however, the apparent M_r distribution changed dramatically in the presence of TiO_2 NPs (100 mg·L^{-1}; Figure 2.8D). The majority of the chromophoric molecules eluted at times corresponding to apparent M_r of 260 and 500 Da. The absorbance region had also narrowed to 200-450 nm with the bulk of the absorbance at 200-210 nm. The contraction of the absorbance range and decrease in

apparent M_r occurred gradually and in a TiO_2 NP concentration-dependent manner (data not shown).

Simulated sunlight illumination altered the apparent M_r distribution and UV-Vis absorption range of HA in the presence of TiO_2 NPs. Together with the DLS and electrophoretic mobility data, these results suggest that HA molecules adsorb to TiO_2 NPs imparting a more negative charge to the nanoparticle surface and producing aggregates of smaller size than in the absence of HA. Upon illumination with simulated sunlight, photocatalytically produced holes, ·OH, or both oxidize chromophores and fragment HA molecules. Decomposition of HA molecules on the TiO_2 NP surfaces reduces the degree of negative surface charge on the particles destabilizing the suspension. These results are consistent with previous studies examining photocatalytic degradation of DOM by TiO_2 NPs.[60-63]

Effect of HA on Ti Association with Developing Zebrafish. Adsorption of HA increased TiO_2 NP suspension stability during part of the light exposure period. We therefore hypothesized that the level of Ti associated with fish would be lower in those exposed in the presence of HA. Consistent with expectations, the levels of Ti associated with fish exposed to TiO_2 NPs in the presence of HA were lower than for those exposed in the absence of HA. For example, at 100 $mg \cdot L^{-1}$ TiO_2 NP exposures, the amount of Ti associated with the fish decreased from 78±4.8 $\mu g_{Ti} \cdot g_{fish}^{-1}$ in the absence of HA to 54±1.0 $\mu g_{Ti} \cdot g_{fish}^{-1}$ in its presence (Figure 2.9A).

As the chorion has been shown to be a barrier to TiO_2 NP exposure,[14] we examined whether differences in hatching time were responsible for differences in levels of Ti associated with the fish in the absence and presence of HA. The presence of HA caused a small (~0.3d) delay in hatching time ($p \leq 0.05$). Fish exposed to TiO_2 NPs (100 $mg \cdot L^{-1}$) in the absence of HA hatched at 2.2±0.02 dpf while those exposed in the presence of HA hatched at 2.5±0.04 dpf. The delayed hatching in the exposures containing HA is consistent with the lower amount of Ti associated with fish in this treatment.

Effect of HA on TiO_2 NP Toxicity. The lower levels of Ti associated with zebrafish exposed to TiO_2 NPs in the presence of HA led us to hypothesize that the presence of HA would result in diminished toxicity. To test this hypothesis, we examined the effect of HA on survival and the incidence of failed yolk sac absorption and edema in developing zebrafish exposed to TiO_2 NP under simulated sunlight illumination.

In the absence of HA, TiO_2 NPs produced a dose-dependent decrease in survival and had an LC_{50} of 290 $mg \cdot L^{-1}$ ($CI_{95\%}$: 260-323 $mg \cdot L^{-1}$; Figure 2.9B). In the presence of HA, TiO_2 NPs caused a dose-dependent decrease in survival and a trend towards increased toxicity was apparent. The presence of HA reduced the LC_{50} to 156 $mg \cdot L^{-1}$ ($CI_{95\%}$: 118-207 $mg \cdot L^{-1}$; Figure 2.9B).

The increased mortality in the presence of HA occurred despite the lower levels of Ti associated with the fish in this treatment. For example, zebrafish exposed to TiO_2 NPs at a nominal concentration of 100 $mg \cdot L^{-1}$ until 5 dpf in the presence of HA exhibited lower Ti body burdens relative to those exposed in the absence of HA (Figure 2.9A). Despite this

lower body burden, TiO_2 exposures in the presence of the presence of HA resulted in higher mortality (Figure 2.9B).

To determine if this increase in mortality was caused by photodegradation products of HA produced in the presence of TiO_2 NPs, we illuminated HA- TiO_2 NP suspensions, removed the NPs by centrifugal filtration, and exposed the fish to remaining solution under illumination. We found that the mortality in these exposures did not differ from fish exposed to fish water or HA in the absence of TiO_2 NPs (p >0.05; data not shown). These results indicate that products of HA photocatalytic degradation are not responsible for the mortality observed in the presence of HA upon simulated sunlight illumination.

Fish exposed to TiO_2 NPs in both the presence and absence of HA (250 $mg \cdot L^{-1}$ until 3 dpf) exhibited increased incidence of failed yolk sac absorption but not pericardial edema relative to control fish ($p \leq 0.05$; Figure 2.9C-D). Fish exposed to TiO_2 NPs in the presence of HA showed increased incidence of failed yolk sac absorption relative to those exposed to TiO_2 NPs in the absence of HA ($p \leq 0.05$; Figure 2.9D).

Effect of HA on TiO_2 NP-Induced Oxidative Stress. Co-exposure to TiO_2 NPs and simulated sunlight can significantly increase oxidative stress in developing zebrafish.[14-15] We therefore hypothesized that increased TiO_2 NP toxicity in the presence of HA was caused by increased oxidative stress. To test this hypothesis, we evaluated lipid peroxidation (using the TBARS assay) and oxidative DNA damage (using the 8-OHdG assay) induced by illuminated TiO_2 NPs in the presence and absence of HA.

In zebrafish exposed to TiO_2 NPs in the light (250 $mg \cdot L^{-1}$ until 3 dpf), TBARS levels did not differ from those exposed to controls (p >0.05; data not shown). Furthermore, TBARS levels in fish exposed to TiO_2 NPs in the presence and absence of HA did not differ (p >0.05; data not shown). We note that the TBARS levels in fish illuminated in the absence of TiO_2 NPs was much higher than in control fish held in the dark.

In contrast, zebrafish exposed to TiO_2 NPs (250 $mg \cdot L^{-1}$ until 3 dpf) in the presence and absence of HA exhibited higher levels of oxidative DNA damage (8-OHdG) than control fish (Figure 2.9E). Furthermore, those exposed to TiO_2 NPs in the presence of HA had levels of 8-OHdG (7.9±0.5 $pg_{8\text{-}OHdG} \cdot mg_{DNA}^{-1}$) higher by a factor of 1.5 than those exposed to TiO_2 NPs in the absence of HA (5.1±0.6 $pg_{8\text{-}OHdG} \cdot mg_{DNA}^{-1}$; Figure 2.9E). Levels of Ti associated with fish under the exposure conditions of this experiment were 67±7.0 and 170±15 $\mu g_{Ti} \cdot g_{fish}^{-1}$ in the absence and presence of HA, respectively. Normalized to levels of Ti associated with the fish, fish exposed to TiO_2 NPs in the presence of HA had 8-OHdG levels higher than those exposed in the absence of HA by a factor of 2.8 ($p \leq 0.05$; Figure 2.10).

As a semiconductor, TiO_2 NPs can produce oxidative DNA damage through several mechanisms.[54] Fish exposed to TiO_2 NPs in the presence of HA had higher 8-OHdG levels than those exposed in the absence of HA. These results are consistent with HA increasing TiO_2 NP toxicity by increasing oxidative stress.

Effect of DOM Type on Inherent and Photo-Enhanced Toxicity of TiO_2 NPs.

Exposure in the Absence of Simulated Sunlight. To determine if DOM type affected TiO_2 NP toxicity, we also examined the influence of Suwannee River fulvic acid (FA) and

natural organic matter isolate (NOM) on the TiO_2 NP suspension stability and uptake by and toxicity to developing zebrafish.

The presence of DOM, regardless of type, increased TiO_2 NP suspension stability before exposure. For all three DOM types, aggregates had polymodal distributions with modes from 0.03 to 0.2 μm prior to exposure and μ_E from -2.59 to – 2.66 $\times 10^4$ $cm^2 \cdot V^{-1} \cdot s^{-1}$ (Figure 2.11A-B). After exposure, all three DOM types still increased suspension stability. Aggregates again had polymodal distributions with modes from 0.03 to 0.2 μm and μ_E from -2.47 to – 2.57 $\times 10^4$ $cm^2 \cdot V^{-1} \cdot s^{-1}$ (Figure 2.11A-B).

No difference in the levels of Ti associated with the fish were found in the presence of HA, FA, and NOM. For instance, at 100 $mg \cdot L^{-1}$ TiO_2 NPs, body burdens in the presence of HA, FA, and NOM were 26 ± 5.9, 39 ± 9.9, and 37 ± 4.8 $\mu g_{Ti} \cdot g_{fish}^{-1}$, respectively (Figure 2.12A). However, these levels were significantly lower than that that in the absence of DOM (87.4 ± 8.2 $\mu g_{Ti} \cdot g_{fish}^{-1}$; $p \leq 0.05$; Figure 2.5A).

Despite the similarities in suspension stability and exposure levels, differences in toxicity were observed between the three DOM types. In the dark, the presence of HA and NOM caused significantly more failed yolk sac absorption and edema than the presence of FA ($p \leq 0.05$). For instance, 38.1 ± 4.8 % and 40.0 ± 3.2 % of fish exposed to TiO_2 NPs (1000 $mg\ L^{-1}$ until 4 dpf) in the presence of HA and NOM, respectively, exhibited failed yolk sac absorption while in the presence of FA only 18.9 ± 3.5% exhibited this endpoint (Figure 2.12B). Furthermore, 8.3 ± 2.6 and 6.7 ± 2.1 % of fish exposed to TiO_2 NPs (1000 $mg\ L^{-1}$ until 4 dpf) in the presence of HA and NOM, respectively, exhibited edema while in the

presence of FA only 2.8 ± 0.8% exhibited this endpoint (Figure 2.12B). Differences in mortality were also observed between the various DOM types. The presence of HA caused significantly more mortality than FA and NOM at all TiO_2 NP concentrations (Figure 2.12C; *p≤0.05*).

Exposure in the Presence of Simulated Sunlight. As discussed previously, the presence of DOM, regardless of type, increased TiO_2 NP suspension stability before exposure. After exposure, however, suspension stability was reduced in the presence of all three DOM types. Despite this decrease in stability, aggregates in the presence of HA, FA, and NOM did not differ substantially in size nor μ_E. For instance, at 100 $mg \cdot L^{-1}$, aggregates were monomodal with modes from 0.5 to 1.0 μm and had μ_E from -1.60 to – 1.73 $\times 10^4$ $cm^2 \cdot V^{-1} \cdot s^{-1}$ (Figure 2.13A-B).

While differences in suspension stability were not observed between the DOM types, differences in exposure levels were. For instance, at 100 $mg \cdot L^{-1}$ TiO_2 NPs, the presence of HA significantly reduced the amount of Ti associated with the fish compared to the presence of FA and NOM (HA: 54±1.0; FA: 94±5.7, NOM: 95±4.8 $\mu g_{Ti} \cdot g_{fish}^{-1}$; p≤0.05; Figure 2.14A).

Differences in toxicity were also observed between the three DOM types. The presence of HA and NOM caused significantly more failed yolk sac absorption than the presence of FA while the presence of HA caused significantly more edema than that of FA and NOM (p≤0.05). For instance, 46.7±2.8% and 40.0±0.0% of fish exposed to TiO_2 NPs (250 mg L^{-1} until 3 dpf) in the presence of HA and NOM, respectively, exhibited failed yolk

sac absorption while in the presence of FA only 30.0±0.0% exhibited this endpoint (Figure 2.14B). Of the fish exposed to TiO_2 NPs in the presence of HA, 6.67±1.1% exhibited edema while only 3.33±1.1 % of fish in the presence of FA and no fish in the presence of NOM exhibited this endpoint (Figure 2.14B).

Differences in mortality were also observed between the various DOM types. The presence of HA caused significantly more mortality than FA and NOM at several TiO_2 NP concentrations (*$p \leq 0.05$*; Figure 2.14C). Furthermore, the LC_{50} in the presence of HA was also significantly lower than the LC_{50} in the presence of FA (250 $mg \cdot L^{-1}$; $CI_{95\%}$: 223-281 $mg \cdot L^{-1}$) and NOM (244 $mg \cdot L^{-1}$; $CI_{95\%}$: 216-276 $mg \cdot L^{-1}$).

Upon both dark and light exposure, the differences in toxicity observed between the three DOM types were not associated with differences in Ti association levels. In fact, fish exposed to TiO_2 NPs in the presence of HA had significantly lower association levels than those exposed in the presence of FA and NOM upon simulated sunlight exposure ($p \leq 0.05$; Figure 2.14A). However, fish exposed in the presence of HA exhibited greater incidence of toxic endpoints (i.e., failed yolk sac absorption, edema, mortality) ($p \leq 0.05$; Figure 2.14B-C).

Differences in molecular structure and composition may account for these the differences in exposure and toxicity observed between the three DOM types. Several groups have shown that nanoparticle surface chemistry can impact biodistribution and toxicity.[64-66] For example, surface chemistry (e.g., charge, hydrophilicity) was shown to impact the uptake, distribution, and toxicity of gold nanoparticles in Japanese medaka (*Oryzias latipes*).[67]

Suwannee River HA and FA are polarity fractions of Suwannee River DOM and differ substantially in molecular structure and composition. The HA used in the study has higher aromaticity than FA and NOM, and, although it has similar carboxylic and phenolic content than NOM, FA has a greater carboxylic and lower phenolic content.[68]

Thus, differences in surface chemistry caused by adsorption of the different DOM types may be responsible for the differences in toxicity. In fact, solutions containing HA typically had lower μ_e than solutions containing FA and NOM. HA also has a larger electron accepting capacity than FA,[69] and it is possible that differences in electron accepting capacity may have altered biological responses (i.e., antioxidant response) associated with TiO_2 NP toxicity.

2.5 Environmental implications

To our knowledge, this is the first study to examine the impact of DOM on the toxicity of TiO_2 NPs to an aquatic vertebrate. Nanoparticles are expected to acquire coatings of organic molecules upon entry into aquatic environments. We found that humic acid coating increased TiO_2 NP suspension stability and reduced exposure to zebrafish (i.e., levels of Ti associated with fish). In the absence of simulated sunlight illumination, fish exposed to TiO_2 NPs in the presence of HA exhibited a small but significant increase in mortality. Under simulated sunlight illumination, photocatalytic degradation of HA reduced suspension stability. Median lethal concentrations (LC_{50} values) decreased in the TiO_2 NP exposures with HA (i.e., mortality increased), and fish in these exposures exhibited higher levels of oxidative DNA damage than those exposed to TiO_2 NPs in the absence of HA. Relative to the amount of TiO_2 NPs associated with the fish, those with HA coatings were

more toxic. While the presence of HA caused increased toxicity after exposure in both the presence and absence of simulated sunlight, the same trends were not observed in the presence of FA and NOM suggesting that NOM composition can affect toxicity. While further research will be required to elucidate the mechanism responsible for this finding, our results are consistent with oxidative stress as the cause of TiO_2 NP-induced toxicity and this appears accentuated by the presence of HA.

Predicting concentration of TiO_2 NPs in environmental matrices is challenging. Probabilistic material flow analysis for TiO_2 NPs in U.S. consumer products (e.g., cosmetics, plastics, paint) had led to predicted TiO_2 NP concentrations in surface waters ranging from 0.002 (15% quantile) to 0.01 (85% quantile) $\mu g \cdot L^{-1}$.[70] The TiO_2 NP concentrations employed in this study are much higher than those currently predicted to be in the environment. However, we recently showed that exposure of developing zebrafish to low concentrations (1 $\mu g \cdot L^{-1}$) of uncoated TiO_2 NPs for up to 23d under simulated sunlight illumination produced significantly increased mortality, oxidative stress, and developmental delays relative to controls.[15] Adsorbed HA increases the suspension stability of these TiO_2 NPs and would be expected to increase exposure to zebrafish once they begin feeding. Hence, subchronic exposure of developing fish to HA-TiO_2 NPs warrants investigation. We note that zebrafish are a commonly used laboratory model in part because they are hardy. More sensitive fish species may exhibit signs of toxicity at lower NP concentrations.

These findings highlight the importance of considering environmental factors (i.e., exposure to sunlight, adsorption of DOM) when assessing the risks posed by engineered

nanomaterials in the environment. Adsorption of DOM to TiO_2 NP may alter exposure to both organisms in the water column (e.g., free swimming fish) and those at the sediment-water interface (e.g., fish embryos).

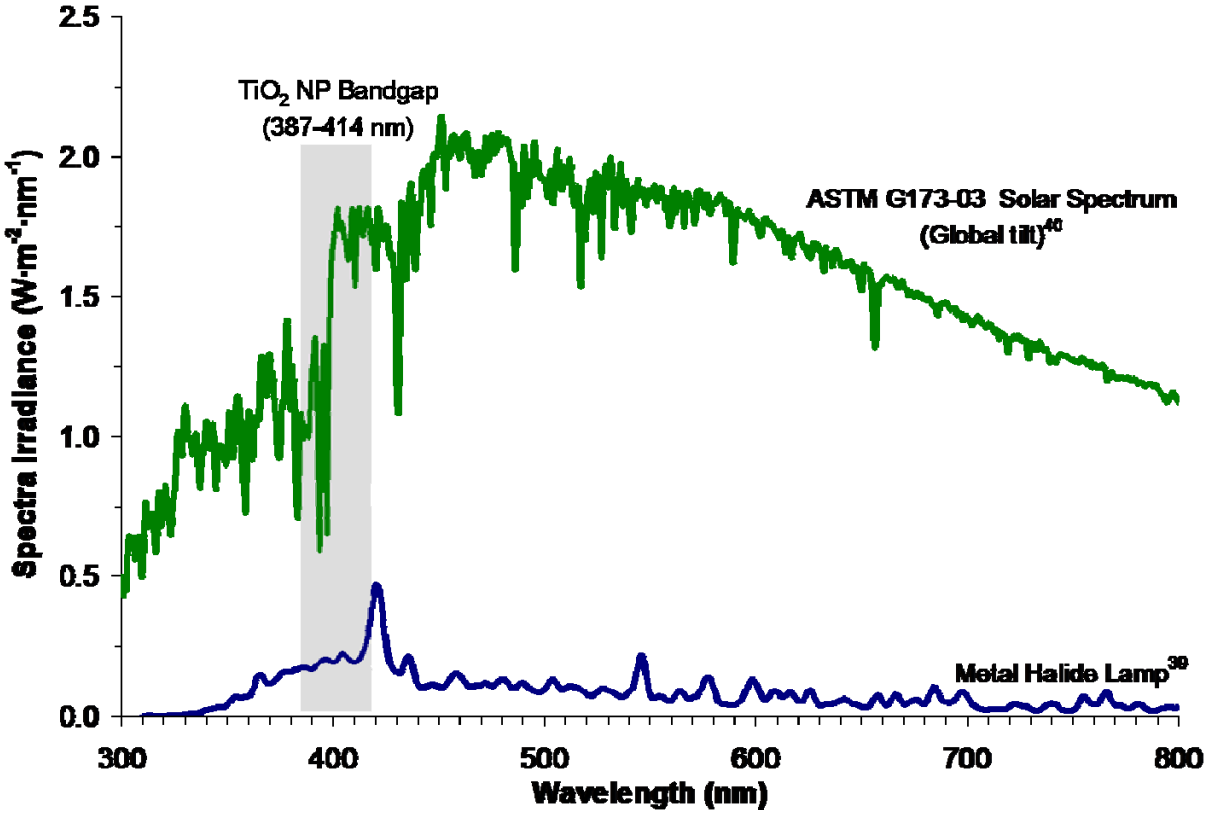

Figure 2.1. Spectral irradiance ($W \cdot m^{-2} \cdot nm^{-1}$) of the metal halide lamp employed in this study (blue line)[39] and the sun (ASTM G173-03 global tilt reference spectrum; green line).[40] The gray box indicates the band gap range of the TiO_2 NPs used in this study.[41]

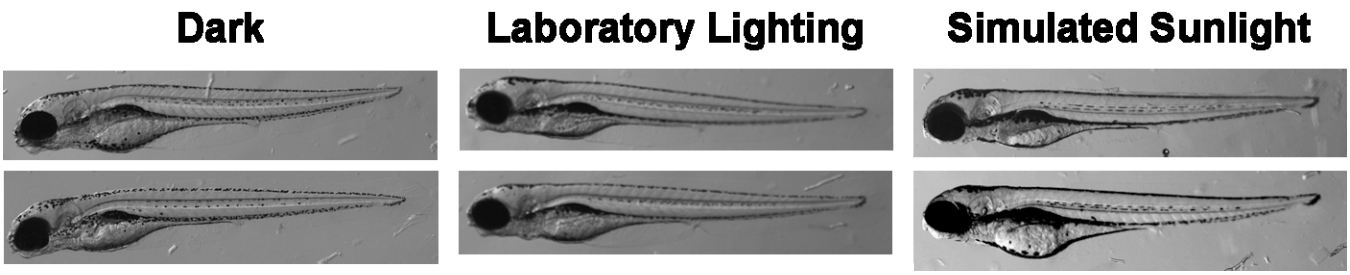

Figure 2.2. Representative micrographs of fish exposed to fish water in the dark, under laboratory lighting, and illuminated with simulated sunlight until 5 dpf.

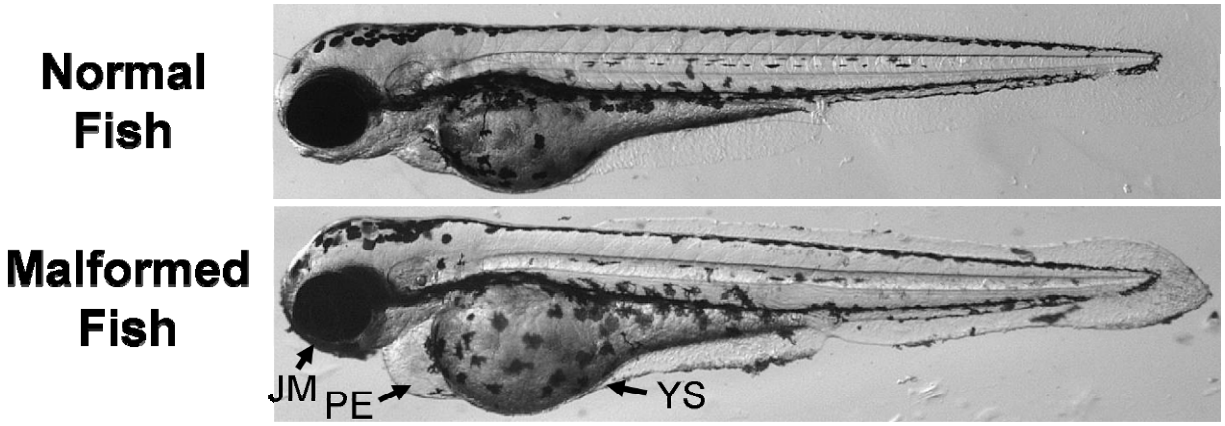

Figure 2.3. Representative micrographs of normal and malformed fish. Observed toxicity endpoints include jaw malformations (JM), reduced yolk sac absorption (YS), and pericardial edema (PE).

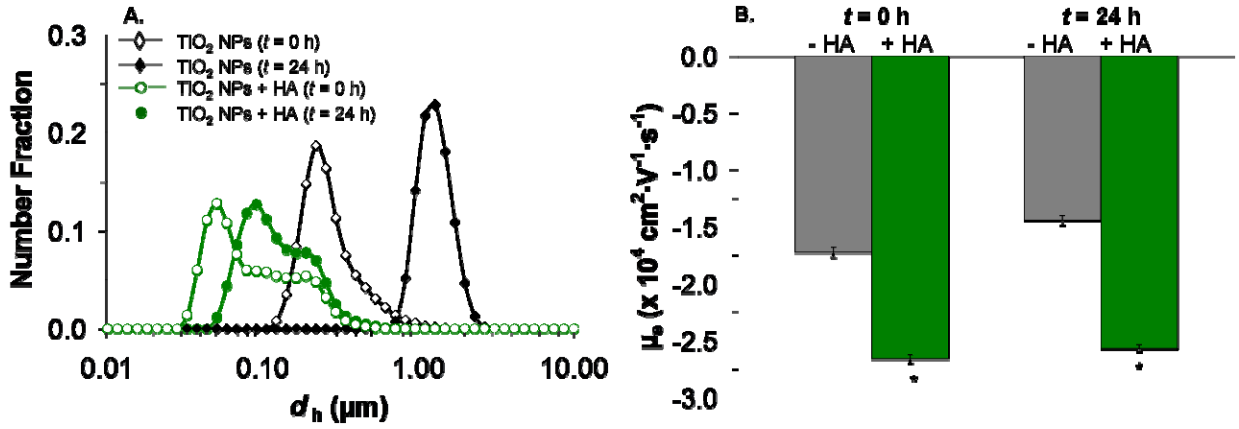

Figure 2.4. Properties of TiO_2 NPs in absence of illumination with simulated sunlight. (A) Hydrodynamic diameter (d_h) number distributions presented as particle size distribution for TiO_2 NPs (100 mg·L^{-1}) in the absence (♦) and presence of HA (●) before (0 h) and after (24 h) exposure. Data points correspond to mean values (n = 2 replicates; 6 measurements/replicate). Lines are provided to guide the eye. **B.** Electrophoretic mobility (μ_E) for TiO_2 NPs (100 mg·L^{-1}) in the presence and absence of HA before (0 h) and after (24 h) exposure. Bars correspond to mean values; error bars represent SEM (n = 2 replicates; 6 measurements/replicate). The * indicates significant decrease relative to TiO_2 NP suspensions without HA. All differences assessed at p = 0.05 level of significance.

Table 2.1. Hydrodynamic diameter (d_h) and electrophoretic mobility (μ_e) of Suwannee River humic acid in fish water.[a-c]

time	d_h (nm)	μ_e ($\times 10^4$ $cm^2 \cdot V^{-1} \cdot s^{-1}$)
0 h	14 ± 7.2	−1.8 ± 0.18
24 h	49 ± 9	−2.0 ± 0.16

[a] Measurements of 30 $mg \cdot L^{-1}$ HA suspensions were obtained before and after 24-h dark exposure period. [b] Abbreviations: d_h, number-average hydrodynamic diameter; μ_E, electrophoretic mobility. [c] All values presented as mean ± SEM.

Table 2.2. Body burden and association levels in fish exposed to TiO_2 NPs[a] in the presence and absence of HA

	Body Burden[b] ($\mu g_{Ti} \cdot g_{fish}^{-1}$)	Association Levels[c] ($\mu g_{Ti} \cdot g_{fish}^{-1}$)
TiO_2 NPs	16 ± 1.8	87 ± 8.2*
HA-TiO_2 NPs	11 ± 1.6	26 ± 5.9*

[a] Fish were exposed to a nominal exposure concentration of 100 $mg \cdot L^{-1}$ TiO_2 NPs until 5 dpf; [b] Body burdens were obtained by rinsing the fish in Ivory soap solution; [c] Association levels were obtained by rinsing the fish in ultrapure H_2O. The * indicates significant difference between association levels and body burden. All differences assessed at $p = 0.05$ level of significance.

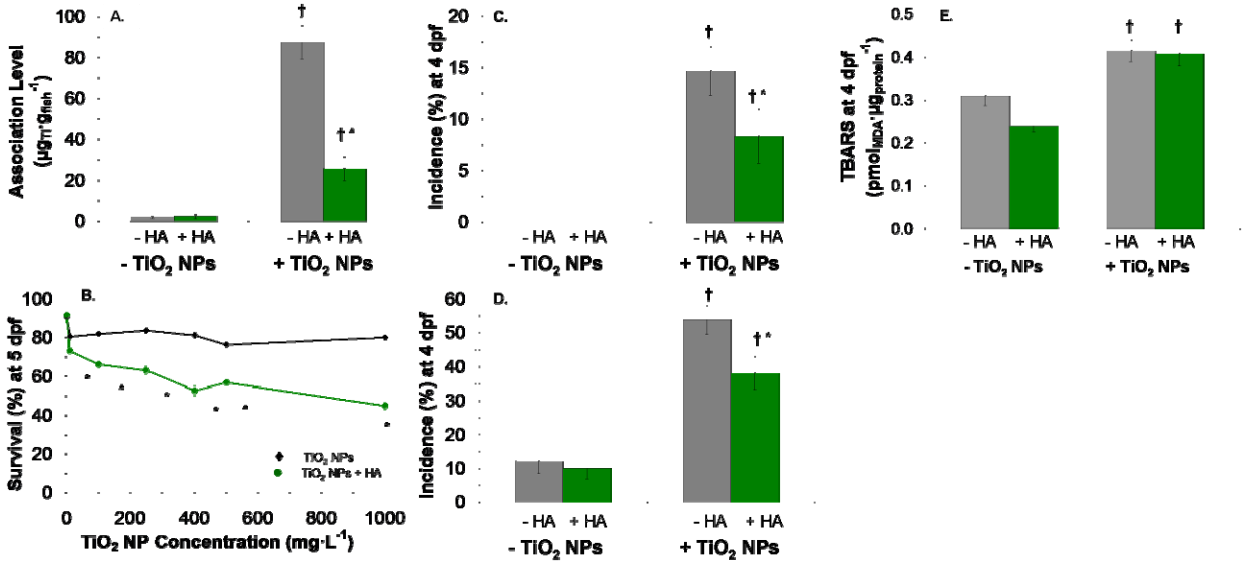

Figure 2.5. Inherent toxicity of TiO_2 NPs in absence of illumination with simulated sunlight. (A) Titanium levels associated with zebrafish at 5 dpf after exposure to control or TiO_2 NPs (100 mg·L^{-1}) in the presence or absence of HA (*n* = 3-6 replicates, 4 measurements per replicate). (B) Dose-response curves at 5 dpf for fish exposed to control or TiO_2 NPs (10-1000 mg·L^{-1}) in the absence or presence of HA (*n* = 3 replicates; 12 fish/replicate; each experiment conducted 3 times). (C) Incidence (%) of edema in fish exposed to control or TiO_2 NPs (1000 mg·L^{-1}) in the presence or absence of HA until 4 dpf (*n* = 2-3 replicates; 10 fish/replicate). (D) Incidence (%) of failed yolk sac absorption in fish exposed to control or TiO_2 NPs (1000 mg·L^{-1}) in the presence or absence of HA until 4 dpf (*n* = 2-3 replicates; 10 fish/replicate). (E) Thiobarbituric acid reactive substance (TBARS) concentrations, expressed as malondialdehyde (MDA; pM) per mass of protein (µg), for fish exposed to control or TiO_2 NPs (1000 mg·L^{-1}) in the absence or presence of HA until 4 dpf (*n* = 2 replicates; 48 fish/replicate; each experiment conducted 3 times). In all plots, bars or data points represent means, error bars are SEM, and lines are provided to guide the eye. Symbols: †, change relative to control; *, change relative to TiO_2 NP suspensions without DOM. All differences assessed at $p = 0.05$ level of significance.

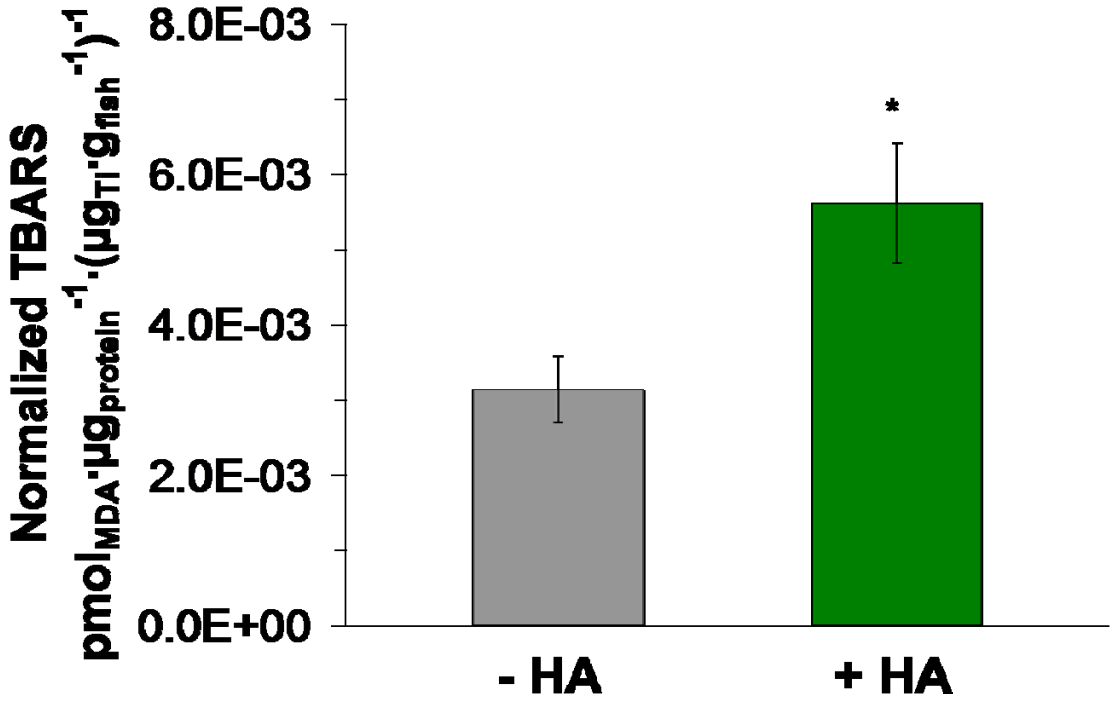

Figure 2.6. Exposure to TiO_2 NPs results in more lipid peroxidation in the presence of humic acid (HA) in the absence of simulated sunlight exposure. Concentrations of thiobarbituric acid reactive substance (TBARS) normalized to levels of Ti associated with fish exposed to TiO_2 NPs (nominal concentration: 1000 $mg \cdot L^{-1}$) in the absence or presence of HA until 4 dpf in the dark (n = 2 replicates; 48 fish/replicate; each experiment conducted 3 times). TBARS is expressed as malondialdehyde (MDA; pmol) per mass of protein ($\mu g_{protein}$), and the level of Ti associated with the fish expressed as (μg_{Ti}) per mass of fish (μg_{fish}). Bars represent means, and error bars are SEM. The * indicates change relative to TiO_2 NP suspensions without HA. All differences assessed at p = 0.05 level of significance.

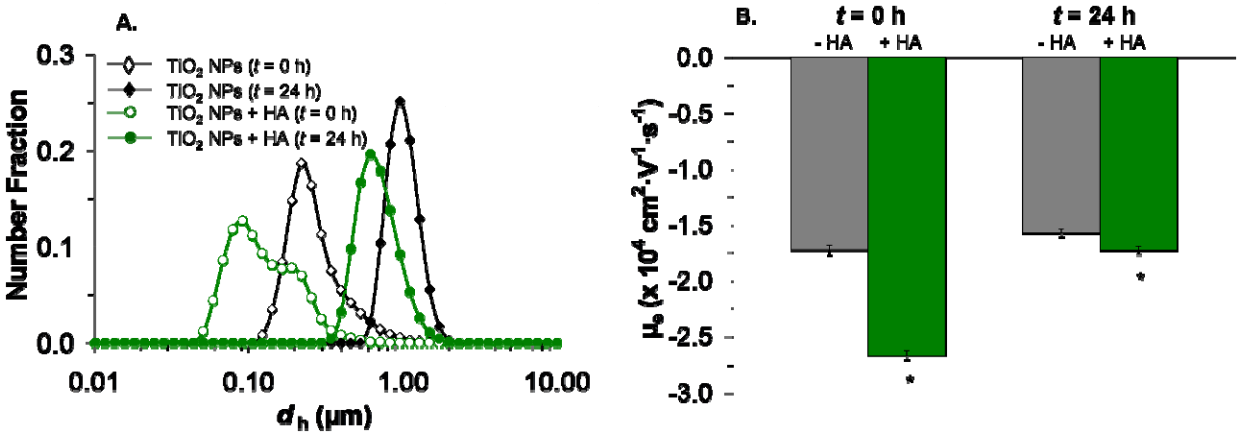

Figure 2.7. Properties of TiO_2 NPs under illumination with simulated sunlight. (A) Hydrodynamic diameter (d_h) number distributions presented as particle size distribution for TiO_2 NPs (100 mg·L^{-1}) in the absence (♦) and presence of HA (●) before (0 h) and after (24 h) exposure. Data points correspond to mean values (n = 2 replicates; 6 measurements/replicate). Lines are provided to guide the eye. **B.** Electrophoretic mobility (μ_E) for TiO_2 NPs (100 mg·L^{-1}) in the presence and absence of HA before (0 h) and after (24 h) exposure. Bars correspond to mean values; error bars represent SEM (n = 2 replicates; 6 measurements/replicate). The * indicates significant decrease relative to TiO_2 NP suspensions without HA. All differences assessed at p = 0.05 level of significance.

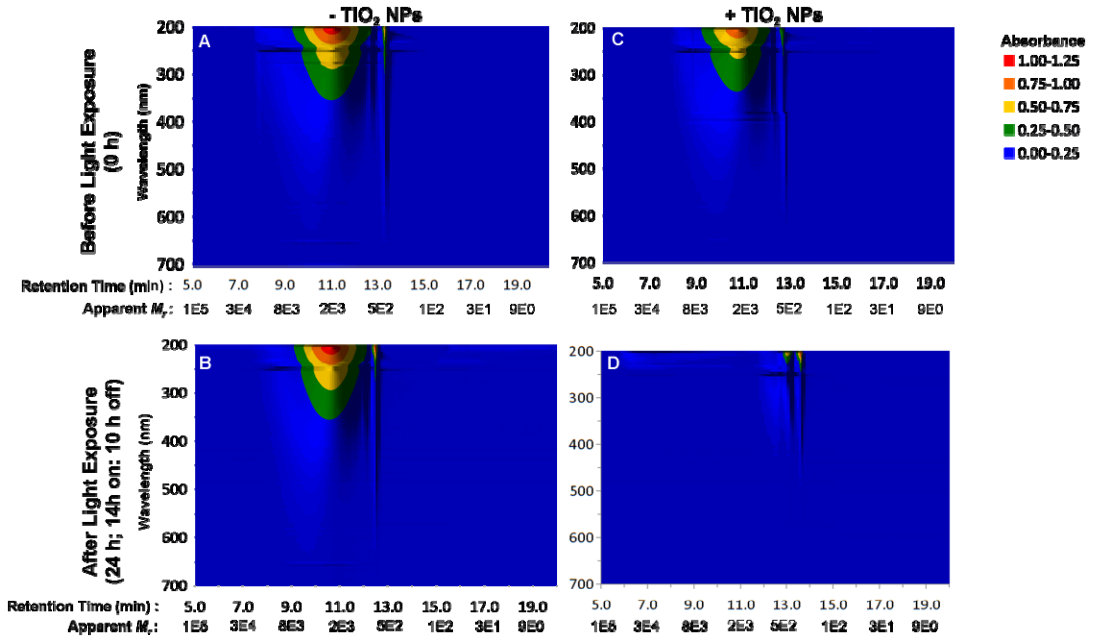

Figure 2.8. TiO_2 NPs photocatalytically degrade humic acid (HA). Representative high-performance size-exclusion chromatograms for HA as a function of retention time (min) and apparent relative molecular mass (M_r) before (A) and after (B) illumination in the absence of TiO_2 NPs and before (C) and after (D) illumination in the presence of TiO_2 NPs (100 mg·L^{-1}).

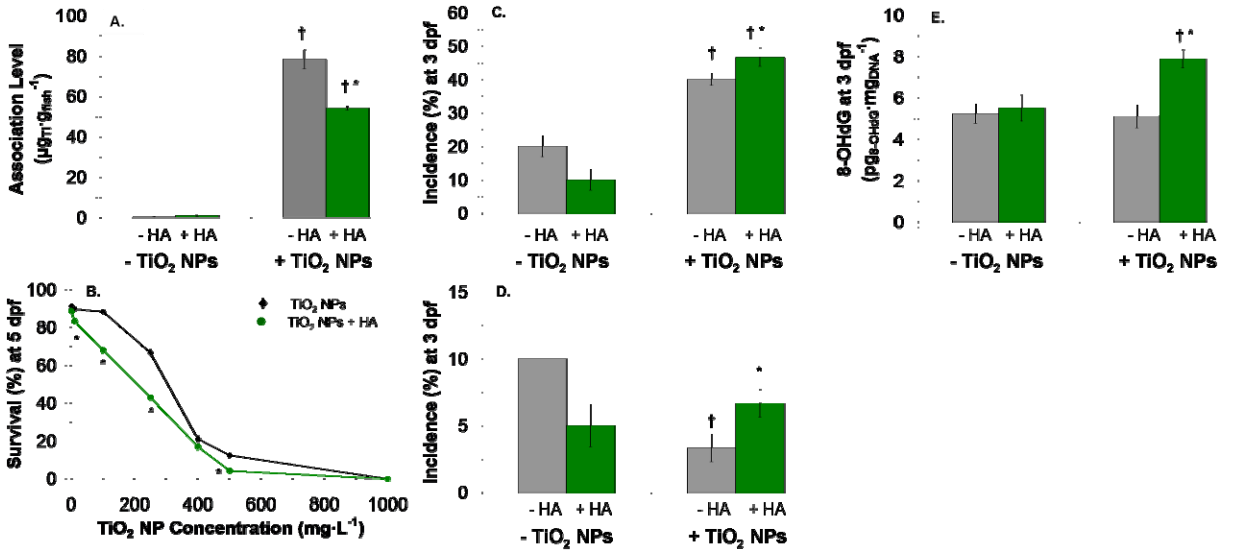

Figure 2.9. Photo-enhanced toxicity of TiO_2 NPs under illumination with simulated sunlight. (A) Titanium levels associated with zebrafish at 5 dpf after exposure to control and TiO_2 NPs (100 mg·L^{-1}) in the presence or absence of HA (*n* = 3-6 replicates, 4 measurements per replicate). (B) Dose-response curves at 5 dpf for fish exposed to control or TiO_2 NPs (10-1000 mg·L^{-1}) in the absence or presence of HA (*n* = 3 replicates; 12 fish/replicate; each experiment conducted 3 times). (C) Incidence (%) of edema in fish exposed to control or TiO_2 NPs (250 mg·L^{-1}) in the presence or absence of HA until 3 dpf (*n* = 2-3 replicates; 10 fish/replicate). (D) Incidence (%) of failed yolk sac absorption in fish exposed to control or TiO_2 NPs (250 mg·L^{-1}) in the presence or absence of HA until 3 dpf (*n* = 2-3 replicates; 10 fish/replicate). (E) Oxidative DNA damage, expressed as expressed as mass of 8-hydrox-2-deoxy-guanosine (8-OHdG) normalized to mass of DNA ($pg_{8\text{-}OHdG}$·mg_{DNA}^{-1}), in fish exposed to controls and TiO_2 NPs (250 mg·L^{-1}) in the presence and absence of HA in the light until 3 dpf (*n* = 2 replicates; 40 fish/replicate; each experiment conducted 2 times). In all plots, bars or data points represent means, error bars are SEM, and lines are provided to guide the eye. Symbols: †, change relative to control; *, change relative to TiO_2 NP suspensions without DOM. All differences assessed at *p* = 0.05 level of significance.

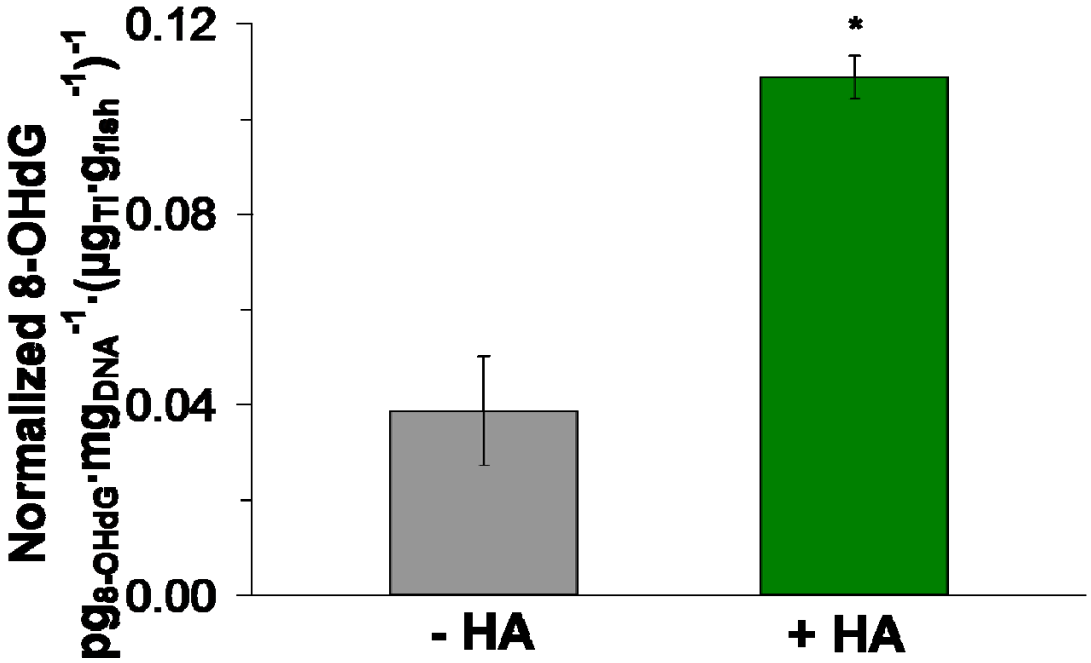

Figure 2.10. Under simulated sunlight illumination, exposure to TiO_2 NPs results in more oxidative DNA damage in the presence of humic acid (HA). Amount of 8-OHdG normalized to the amount of Ti associated with fish exposed to TiO_2 NPs (nominal concentration: 250 $mg \cdot L^{-1}$) in the presence and absence of HA in the light until 3 dpf (n = 2 replicates; 40 fish/replicate; each experiment conducted 2 times). Oxidative DNA damage expressed as mass of 8-OHdG normalized to mass of DNA ($pg_{8\text{-}OHdG} \cdot mg_{DNA}^{-1}$), and association levels expressed as mass of Ti normalized to wet weight of fish ($\mu g_{Ti} \cdot \mu g_{fish}^{-1}$). Bars represent means, and error bars are SEM. The * indicates change relative to TiO_2 NP suspensions without HA. All differences assessed at p = 0.05 level of significance.

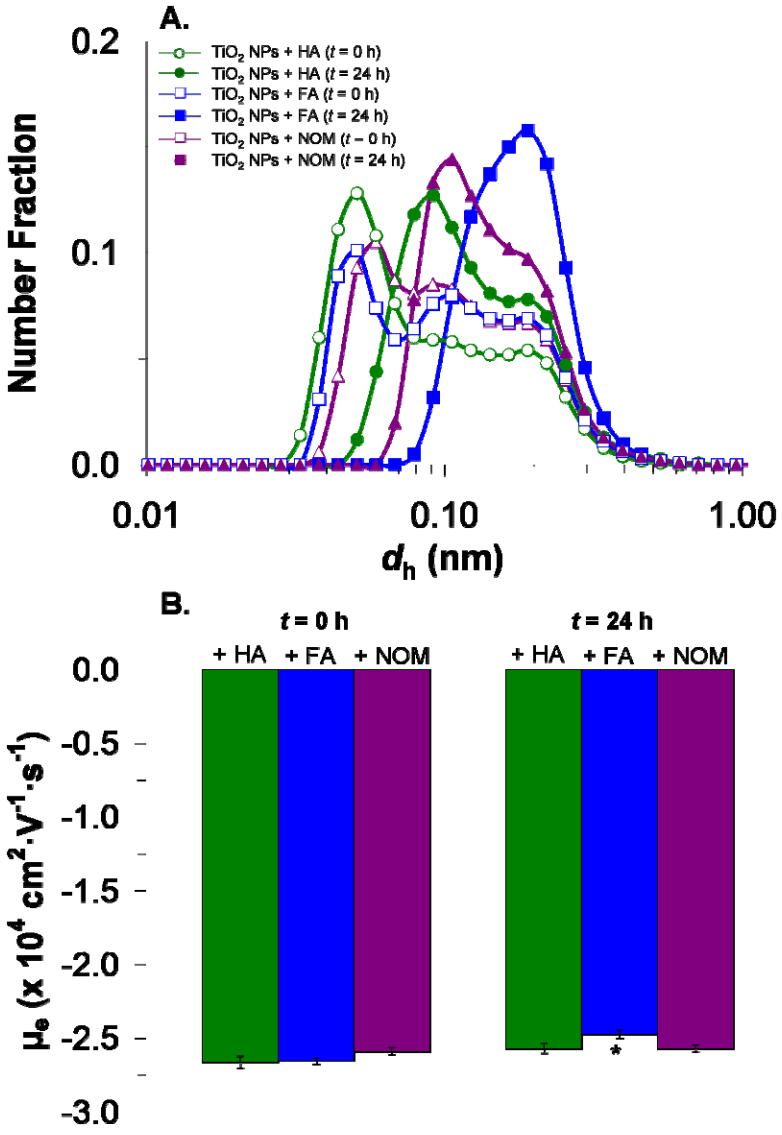

Figure 2.11. Influence of DOM type on TiO_2 NPs properties in the absence of illumination with simulated sunlight. (A) Hydrodynamic diameter (d_h) number distributions presented as particle size distribution for TiO_2 NPs (100 mg·L^{-1}) in the presence of HA (●), FA (■), and NOM (▲) before (0 h) and after (24 h) exposure. Data points correspond to mean values (n = 2 replicates; 6 measurements/replicate). Lines are provided to guide the eye. (B) Electrophoretic mobility (μ_E) for TiO_2 NPs (100 mg·L^{-1}) in the presence of HA, FA, and NOM before (0 h) and after (24 h) exposure. Bars correspond to mean values; error bars represent SEM (n = 2 replicates; 6 measurements/replicate). The * indicates significant difference compared to suspensions containing HA. All differences assessed at p = 0.05 level of significance.

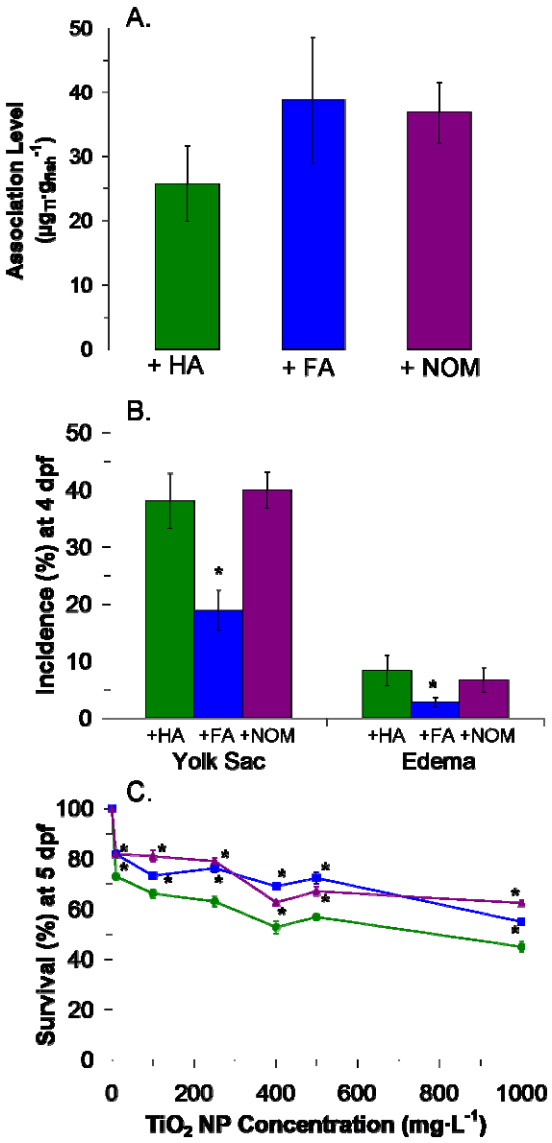

Figure 2.12. Influence of DOM type on the inherent toxicity of TiO_2 NPs in the absence of illumination with simulated sunlight. (A) Titanium levels associated with zebrafish at 5 dpf after exposure to TiO_2 NPs (100 mg·L^{-1}) in the presence of HA, FA, and NOM (n = 3-6 replicates, 4 measurements per replicate). (B) Incidence (%) of failed yolk sac absorption and edema in fish exposed to TiO_2 NPs (1000 mg·L^{-1}) in the presence HA, FA, and NOM until 4 dpf (n = 2-3 replicates; 10 fish/replicate). (C) Dose-response curves at 5 dpf for fish exposed to TiO_2 NPs (10-1000 mg·L^{-1}) in the presence of HA, FA, and NOM (n = 3 replicates; 12 fish/replicate; each experiment conducted 3 times). In all plots, bars or data points represent means, error bars are SEM, and lines are provided to guide the eye. The asterisk (*) indicates significant difference compared to suspensions containing HA (p< 0.05).

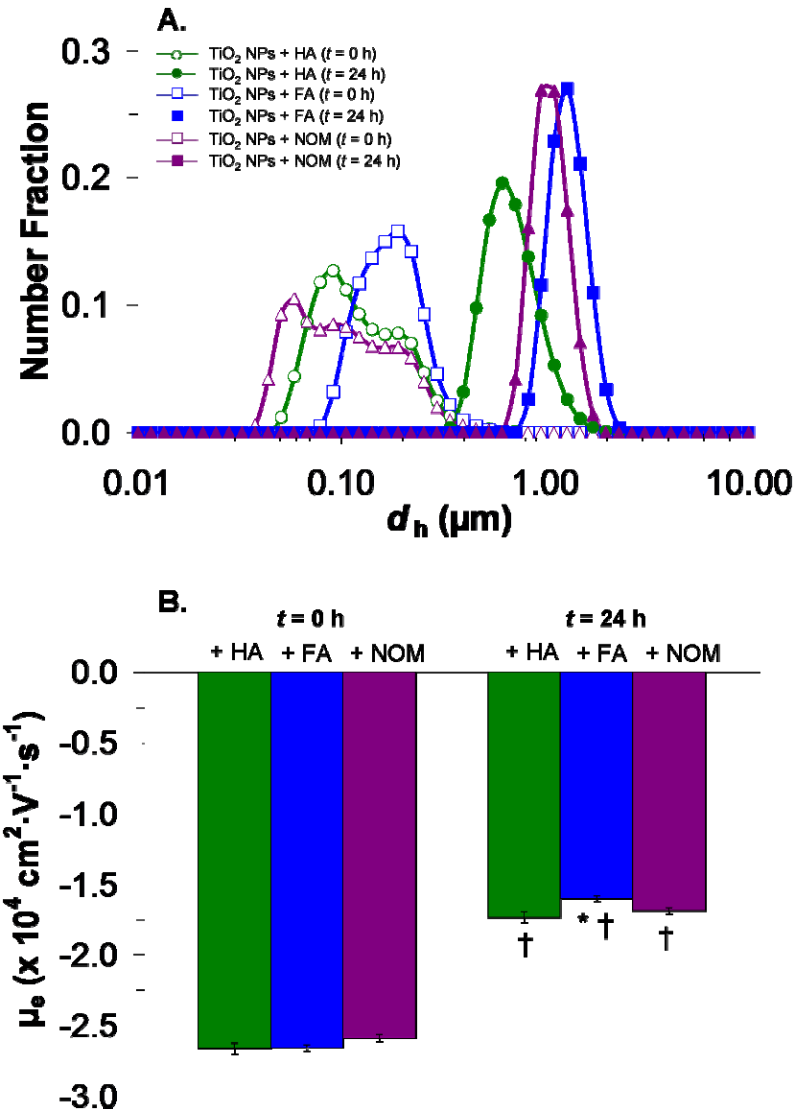

Figure 2.13. Influence of DOM type on TiO_2 NPs properties in the presence of illumination with simulated sunlight. (A) Hydrodynamic diameter (d_h) number distributions presented as particle size distribution for TiO_2 NPs (100 mg·L^{-1}) in the presence of HA (●), FA (■), and NOM (▲) before (0 h) and after (24 h) exposure. Data points correspond to mean values (n = 2 replicates; 6 measurements/replicate). Lines are provided to guide the eye. (B) Electrophoretic mobility (μ_E) for TiO_2 NPs (100 mg·L^{-1}) in the presence of HA, FA, and NOM before (0 h) and after (24 h) exposure. Bars correspond to mean values; error bars represent SEM (n = 2 replicates; 6 measurements/replicate). The † indicates significant difference between before and after exposure and * indicates significant difference compared to suspensions containing HA. All differences assessed at p = 0.05 level of significance.

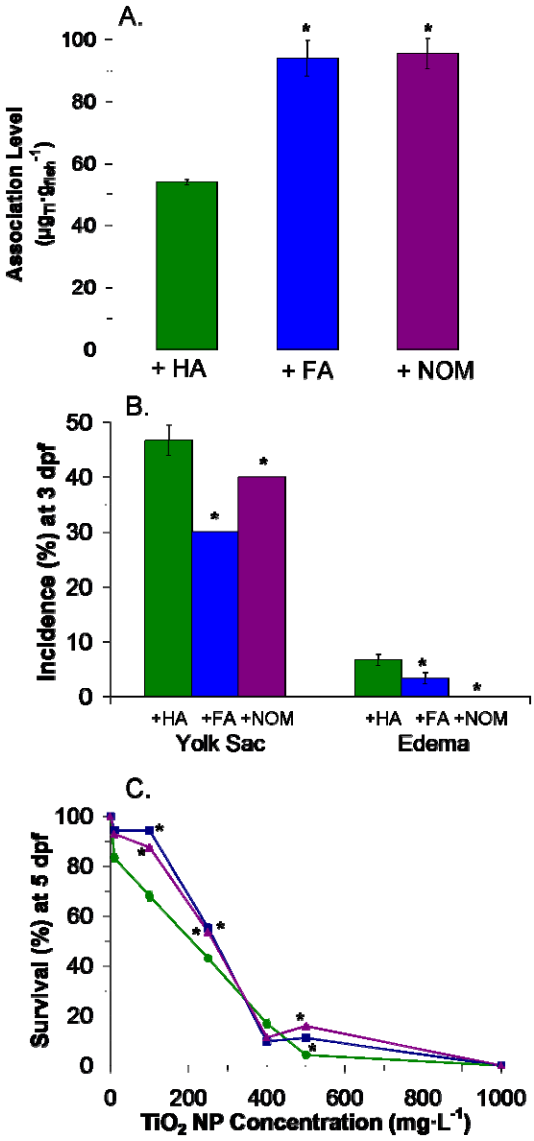

Figure 2.14. Influence of DOM type on the photo-enhanced toxicity of TiO_2 NPs in the presence of illumination with simulated sunlight. (A) Titanium levels associated with zebrafish at 5 dpf after exposure to TiO_2 NPs (100 mg·L^{-1}) in the presence of HA, FA, and NOM (*n* = 3-6 replicates, 4 measurements per replicate). (B) Incidence (%) of failed yolk sac absorption and edema in fish exposed to TiO_2 NPs (250 mg·L^{-1}) in the presence HA, FA, and NOM until 3 dpf (*n* = 2-3 replicates; 10 fish/replicate). (C) Dose-response curves at 5 dpf for fish exposed to TiO_2 NPs (10-1000 mg·L^{-1}) in the presence of HA, FA, and NOM (*n* = 3 replicates; 12 fish/replicate; each experiment conducted 3 times). In all plots, bars or data points represent means, error bars are SEM, and lines are provided to guide the eye. The * indicates significant difference compared to suspensions containing HA. All differences assessed at $p = 0.05$ level of significance.

References

1. Boxall, A.; Chaudhry, Q.; Sinclair, S.; Jones, A.; Aitken, J., R; Watts, C. Current and future predicted environmental exposure to engineered nanoparticles. Department for Environment, Food and Rural Affairs: London, 2007.
2. Kaegi, R.; Ulrich, A.; Sinnet, B.; Vonbank, R.; Wichser, A.; Zuleeg, S.; Simmler, H.; Brunner, S.; Vonmont, H.; Burkhardt, M.; Boller, M. Synthetic TiO_2 nanoparticle emission from exterior facades into the aquatic environment. *Environ. Pollut.* **2008,** *156*, 233-239.
3. Guisbiers, G.; Van Overschelde, O.; Wautelet, M. Theoretical investigation of size and shape effects on the melting temperature and energy bandgap of TiO_2 nanostructures. *Appl. Phys. Lett.* **2008**, *92*, 103121-103123.
4. Hoffmann, M. R.; Martin, S. T.; Choi, W. Y.; Bahnemann, D. W. Environmental applications of semiconductor photocatalysis. *Chem. Rev.* **1995**, *95*, 69-96.
5. *State of the Science Literature Review: Nano Titanium Dioxide Environmental Matters;* Scientific, Technical, Research, Engineering and Modeling Support (STREAMS) Final Report EP-C-05-059; U.S. Environmental Protection Agency Office of Research and Development: Washington, DC, 2010.
6. Kang, J. L.; Moon, C.; Lee, H. S.; Lee, H. W.; Park, E. M.; Kim, H. S.; Castranova, V. Comparison of the biological activity between ultrafine and fine titanium dioxide particles in RAW 264.7 cells associated with oxidative stress. *J. Toxicol. Environ. Health* **2008,** *71*, 478-485.
7. Zhu, R. R.; Wang, S. L.; Chao, J.; Shi, D. L.; Zhang, R.; Sun, X. Y.; Yao, S. D. Bio-effects of nano-TiO_2 on DNA and cellular ultrastructure with different polymorph and size. *Mat. Sci. Eng. C-Bio S* **2009,** *29*, 691-696.
8. Xiong, D. W.; Fang, T.; Yu, L. P.; Sima, X. F.; Zhu, W. T. Effects of nano-scale TiO_2, ZnO and their bulk counterparts on zebrafish: Acute toxicity, oxidative stress and oxidative damage. *Sci. Total Environ.* **2011**, *409*, 1144-1452.
9. Battin, T. J.; Kammer, F. V. D.; Weilhartner, A.; Ottofuelling, S.; Hofmann, T. Nanostructured TiO_2: Transport behavior and effects on aquatic microbial communities under environmental conditions. *Environ. Sci. Technol.* **2009**, *43*, 8098-8104
10. Hund-Rinke, K.; Simon, M. Ecotoxic effect of photocatalytic active nanoparticles TiO_2 on algae and daphnids. *Environ. Sci. Pollut. Res.* **2006**, *13*, 225-232.
11. Reeves, J. F.; Davies, S. J.; Dodd, N. J. F.; Jha, A. N. Hydroxyl radicals ((OH)-O-center dot) are associated with titanium dioxide (TiO_2) nanoparticle-induced cytotoxicity and oxidative DNA damage in fish cells. *Mutat. Res. Fundam. Mol. Mech. Mutag.* **2008**, *640*, 113-122.
12. Dodd, N. J. F.; Jha, A. N. Titanium dioxide induced cell damage: A proposed role of the carboxyl radical. *Mutat. Res. Fundam. Mol. Mech. Mutag.* **2009**, 660, 79-82.
13. Vevers, W. F.; Jha, A. N. Genotoxic and cytotoxic potential of titanium dioxide (TiO_2) nanoparticles on fish cells in vitro. *Ecotoxicol.* **2008**, 17, 410-420.

14. Bar-Ilan, O.; Louis, K. M.; Yang, S. P.; Pedersen, J. A.; Hamers, R. J.; Peterson, R. E.; Heideman, W. Titanium dioxide nanoparticles produce phototoxicity in the developing zebrafish. *Nanotoxicol.* **2012**, 670-679.
15. Bar-Ilan, O. Toxicity of metal and metal oxide nanoparticles in developing zebrafish. PhD Dissertation. University of Wisconsin, Madison, WI, 2011.
16. Domingos, R. F.; Tufenkji, N.; Wilkinson, K. J. Aggregation of titanium dioxide nanoparticles: role of a fulvic acid. *Environ. Sci. Technol.* **2009**, *43*, 1282–1286.
17. Yang, K.; Lin, D. H.; Xing, B. S. Interactions of humic acid with nanosized inorganic oxides. *Langmuir* **2009**, *25*, 3571-3576.
18. Zhang, Y.; Chen, Y. S.; Westerhoff, P.; Crittenden, J. Impact of natural organic matter and divalent cations on the stability of aqueous nanoparticles. *Water Res.* **2009**, *43*, 448 4249-4257.
19. Keller, A. A.; Wang, H. T.; Zhou, D. X.; Lenihan, H. S.; Cherr, G.; Cardinale, B. J.; Miller, R.; Ji, Z. X. Stability and aggregation of metal oxide nanoparticles in natural aqueous matrices. *Environ. Sci. Technol.* **2010**, *44*, 1962-1967.
20. Edgington, A. J.; Roberts, A. P.; Taylor, L. M.; Alloy, M. M.; Reppert, J.; Rao, A. M.; Mao, J. D.; Klaine, S. J. The influence of natural organic matter on the toxicity of multiwalled carbon nanotubes. *Environ. Toxicol. Chem.* **2010**, *29*, 2511-2518.
21. Fabrega, J.; Fawcett, S. R.; Renshaw, J. C.; Lead, J. R. Silver nanoparticle impact on bacterial growth: effect of pH, concentration, and organic matter. *Environ. Sci. Technol.* **2009**, *43*, 7285-7290.
22. Chen, J., Dong, X., Xin, Y., Zhao, M. Effects of titanium dioxide nano-particles on growth and some histological parameters of zebrafish (*Danio rerio*) after a long-term exposure. *Aquat. Toxicol.* **2011**, *101*, 493-499.
23. Jiang, G. X.; Shen, Z. Y.; Niu, J. F.; Bao, Y. P.; Chen, J.; He, T. D. Toxicological assessment of TiO_2 nanoparticles by recombinant Escherichia coli bacteria. *J. Environ. Monitor.* **2011**, *13*, 42-48.
24. Latch, D. E.; McNeill, K. Microheterogeneity of singlet oxygen distributions in irradiated humic acid solutions. *Science* **2006**, *311*, 1743-1747.
25. Vione, D.; Falletti, G.; Maurino, V.; Minero, C.; Pelizzetti, E.; Malandrino, M.; Ajassa, R.; Olariu, R. I.; Arsene, C. Sources and sinks of hydroxyl radicals upon irradiation of natural water samples. *Environ. Sci. Technol.* **2006**, *40*, 3775-3781.
26. Cory, R. M.; Cotner, J. B.; McNeill, K. Quantifying interactions between singlet oxygen and aquatic fulvic acids. *Environ. Sci. Technol.* **2009**, *43*, 718-723.
27. McKay, G.; Dong, M. M.; Kleinman, J. L.; Mezyk, S. P.; Rosario-Ortiz, F. L. Temperature dependence of the reaction between the hydroxyl radical and organic matter. *Environ. Sci. Technol.* **2011**, *45*, 6932-6937.
28. Henry, T. B.; Menn, F. M.; Fleming, J. T.; Wilgus, J.; Compton, R. N.; Sayler, G. S. Attributing effects of aqueous C-60 nano-aggregates to tetrahydrofuran decomposition products in larval zebrafish by assessment of gene expression. *Environ. Health Perspect. A* **2007**, *115*, 1059-1065.
29. Zhu, X. S.; Zhu, L.; Li, Y.; Duan, Z. H.; Chen, W.; Alvarez, P. J. J. Developmental toxicity in zebrafish (*Danio rerio*) embryos after exposure to manufactured nanomaterials:

Buckminsterfullerene aggregates (nC60) and fullerol. *Environ. Toxicol. Chem.* **2007**, *26*, 976-979.
30. Harper, S.; Usenko, C.; Hutchison, J. E.; Maddux, B. L. S.; Tanguay, R. L. In vivo biodistribution and toxicity depends on nanomaterial composition, size, surface functionalisation and route of exposure. *J. Exp. Nanosci.* **2008**, *3*, 195-206.
31. Zhu, X. S.; Zhu, L.; Duan, Z. H.; Qi, R. Q.; Li, Y.; Lang, Y. P. Comparative toxicity of several metal oxide nanoparticle aqueous suspensions to Zebrafish (*Danio rerio*) early developmental stage. *J. Environ. Sci. Health, Part A: Environ. Sci. Eng.* **2008**, *43*, 278-284.
32. Bar-Ilan, O.; Albrecht, R. M.; Fako, V. E.; Furgeson, D. Y. Toxicity assessments of multisized gold and silver nanoparticles in zebrafish embryos. *Small* **2009**, 5, 1897-1910.
33. Cheng, J. P.; Chan, C. M.; Veca, L. M.; Poon, W. L.; Chan, P. K.; Qu, L. W.; Sun, Y. P.; Cheng, S. H. Acute and long-term effects after single loading of functionalized multi-walled carbon nanotubes into zebrafish (*Danio rerio*). *Toxicol. Appl. Pharmacol.* **2009**, 235, 216-225.
34. Jiang, J. K.; Oberdorster, G.; Biswas, P. Characterization of size, surface charge, and agglomeration state of nanoparticle dispersions for toxicological studies. *J. Nanopart. Res.* **2009**, 11, 77-89.
35. King-Heiden, T. C.; Wiecinski, P. N.; Mangham, A. N.; Metz, K. M.; Nesbit, D.; Pedersen, J. A.; Hamers, R. J.; Heideman, W.; Peterson, R. E. Quantum dot nanotoxicity assessment using the zebrafish embryo. *Environ. Sci. Technol.* **2009**, 43, 1605-1611.
36. Yeo, M. K.; Kim, H. E. Gene expression in zebrafish embryos following exposure to TiO_2 nanoparticles. *Mol. Cell. Toxicol.* **2010,** *6*, 97-104.
37. Jovanovic, B.; Ji, T. M.; Palic, D. Gene expression of zebrafish embryos exposed to titanium dioxide nanoparticles and hydroxylated fullerenes. *Ecotoxicol. Environ. Saf*. **2011**, *74*, 1518-1525.
38. Orr, M. What does that number really mean? Aquarium water testing methods, results and interpretation. *SeaScope*. **2008**, 24, 3-4. http://www.instantocean.com/~/media/UPG/Files/Instant%20Ocean/SeaScope/Volume%2024%20Fall.ashx
39. Joshi, S. Pennsylvania State University, University Park, PA. Unpublished work, **2011**
40. ASTM, *Standard tables for terrestrial direct normal solar spectral irradiance for air mass 1.5*. **1987**, American Society for Testing and Materials, Philadelphia, PA. http://rredc.nrel.gov/solar/spectra/am1.5/
41. Bickley, R. I., Gonzalezcarreno, T.; Lees, J. S., Palmisano, L., Tilley, R. J. D. A structural investigation of titanium-dioxide photocatalysts. *J. Solid State Chem.* **1991**, *92*, 178-190.
42. Malvern Instruments, Intensity-Volume-Number: What Size is Correct; Technical Note MRK1357-01
43. Ma, X.; Benson, C. H.; McKenzie, D.; Aiken, J. M.; Pedersen, J. A. Adsorption of pathogenic prion protein to quartz sand. *Environ. Sci. Technol.* **2007**, *41*, 2324-2330.
44. Metz, K. M.; Mangham, A. N.; Bierman, M. J.; Jin, S.; Hamers, R. J.; Pedersen, J. A. Engineered nanomaterial transformation under oxidative environmental

conditions: development of an in vitro biomimetic assay. *Environ. Sci. Technol.* **2009**, *43*, 1598-1604.
45. Wiecinski, P. N.; Metz, K. M.; Mangham, A. N.; Jacobson, K. H.; Hamers, R. J.; Pedersen, J. A. Gastrointestinal biodurability of engineered nanoparticles: Development of an in vitro assay. *Nanotoxicology* **2009**, *3*, 202-U66.
46. Chin, Y. P.; Aiken, G.; Oloughlin, E. Molecular-weight, polydispersity, and spectroscopic properties of aquatic humic substances. *Environ. Sci. Technol.* **1994**, *28*, 1853-1858.
47. Pelekani, C.; Newcombe, G.; Snoeyink, V. L.; Hepplewhite, C.; Assemi, S.; Beckett, R. Characterization of natural organic matter using high performance size exclusion chromatography. *Environ. Sci. Technol.* **1999**, *33*, 2807-2813.
48. Lake, J. L.; Ryba, S. A.; Serbst, J. R.; Libby, A. D. Mercury in fish scales as an assessment method for predicting muscle tissue mercury concentrations in largemouth bass. *Arch. Environ. Contam. Toxicol.* 2006, *50*, 539-544.
49. Almroth, B. C.; Sturve, J.; Berglund, A.; Forlin, L. Oxidative damage in eelpout (*Zoarces viviparus*), measured as protein carbonyls and TBARS, as biomarkers. *Aquat. Toxicol.* **2005**, *73*, 171-180.
50. Hu, J.; Liang, Y.; Chen, M. J.; Wang, X. R. Assessing the toxicity of TBBPA and HBCD by zebrafish embryo toxicity assay and biomarker analysis. *Environ. Toxicol.* **2009**, *24*, 334-342.
51. Khan, F. R.; Bury, N. R.; Hogstrand, C. Cadmium bound to metal rich granules and exoskeleton from *Gammarus pulex* causes increased gut lipid peroxidation in zebrafish following single dietary exposure. *Aquat. Toxicol.* **2010**, *96*, 124-129.
52. Kelly, K. A.; Havrilla, C. M.; Brady, T. C.; Abramo, K. H.; Levin, E. D. Oxidative stress in toxicology: established mammalian and emerging piscine model systems. *Environ. Health Perspect.* **1998**, *106*, 375-384.
53. Armstrong, D. *Oxidative stress biomarkers and antioxidant protocols*; Humana Press Inc.: Totowa, New Jersey, 2002; Vol. 186.
54. Petersen, E. J.; Nelson, B. C. Mechanisms and measurements of nanomaterial-induced oxidative damage to DNA. *Anal. Bioanal. Chem.* **2010**, *398*, 613-650.
55. Hamilton, M. A.; Russo, R. C.; Thurston, R. V. Trimmed Spearman-Karber method for estimating median lethal concentration in toxicity bioassays. *Environ. Sci. Technol.* **1977**, *11*, 714-719.
56. Tso, C. P.; Zhung, C. M.; Shih, Y. H.; Tseng, Y. M.; Wu, S. C.; Doong, R. A. Stability of metal oxide nanoparticles in aqueous solutions. *Water Sci. Technol.* **2010**, *61*, 127-133.
57. Heinlaan, M.; Ivask, A.; Blinova, I.; Dubourguier, H. C.; Kahru, A. Toxicity of nanosized and bulk ZnO, CuO and TiO_2 to bacteria *Vibrio fischeri* and crustaceans *Daphnia magna* and *Thamnocephalus platyurus*. *Chemosphere* **2008**, *71*, 1308-1316.
58. Sharma, V. K. Aggregation and toxicity of titanium dioxide nanoparticles in aquatic environment-A review. *J. Environ. Sci. Health A* **2009**, *44*, 1485-1495.

59. Iavicoli, I.; Leso, V.; Fontana, L.; Bergamaschi, A. Toxicological effects of titanium dioxide nanoparticles: a review of in vitro mammalian studies. *Eur. Rev. Med. Pharmacol. Sci.* **2011**, *15*, 481-508.
60. Federici, G.; Shaw, B. J.; Handy, R. D. Toxicity of titanium dioxide nanoparticles to rainbow trout (*Oncorhynchus mykiss*): Gill injury, oxidative stress, and other physiological effects. *Aquat. Toxicol.* **2007**, *84*, 415-430.
61. Coleman, H. M.; Marquis, C. P.; Scott, J. A.; Chin, S. S.; Amal, R. Bactericidal effects of titanium dioxide-based photocatalysts. *Chem. Eng. J.* **2005**, *113*, 55-63.
62. Lee, P. F.; Sun, D. D.; Leckie, J. O. Adsorption and photodegradation of humic acids by nano-structured TiO_2 for water treatment. *J. Adv. Oxid. Technol.* **2007**, *10*, 72-78.
63. Gumy, D.; Giraldo, S. A.; Rengifo, J.; Pulgarin, C. Effect of suspended TiO_2 physicochemical characteristics on benzene derivatives photocatalytic degradation. *Appl. Catalysis B* **2008**, *78*, 19-29.
64. Goodman, C. M.; McCusker, C. D.; Yilmaz, T.; Rotello, V. M. Toxicity of gold nanoparticles functionalized with cationic and anionic side chains. *Bioconjugate Chem.* **2004**, *15* (4), 897-900.
65. Clift, M. J. D.; Rothen-Rutishauser, B.; Brown, D. M.; Duffin, R.; Donaldson, K.; Proudfoot, L.; Guy, K.; Stone, V. The impact of different nanoparticle surface chemistry and size on uptake and toxicity in a murine macrophage cell line. *Toxicol. Appl. Pharmacol.* **2008**, *232* (3), 418-427.
66. Schipper, M. L.; Iyer, G.; Koh, A. L.; Cheng, Z.; Ebenstein, Y.; Aharoni, A.; Keren, S.; Bentolila, L. A.; Li, J. Q.; Rao, J. H.; Chen, X. Y.; Banin, U.; Wu, A. M.; Sinclair, R.; Weiss, S.; Gambhir, S. S. Particle size, surface coating, and PEGylation influence the biodistribution of quantum dots in living mice. *Small* **2009**, *5* (1), 126-134.
67. Zhu, Z. J.; Carboni, R.; Quercio, M. J.; Yan, B.; Miranda, O. R.; Anderton, D. L.; Arcaro, K. F.; Rotello, V. M.; Vachet, R. W. Surface properties dictate uptake, distribution, excretion, and toxicity of nanoparticles in fish. *Small* **2010**, *6* (20), 2261-2265.
68. International Humic Substance Society (IHSS) Website; http://www.humicsubstances.org/
69. Aeschbacher, M.; Sander, M.; Schwarzenbach, R. P. Novel Electrochemical Approach to Assess the Redox Properties of Humic Substances. *Environ. Sci. Technol.* **2010**, *44* (1), 87-93.
70. Gottschalk, F.; Sonderer, T.; Scholz, R. W.; Nowack, B. Modeled environmental concentrations of engineered nanomaterials (TiO_2, ZnO, Ag, CNT, Fullerenes) for different regions. *Environ. Sci. Technol.* **2009**, *43*, 9216-9222.

Chapter 3: Impact of Intentional Functionalization on the Inherent and Photo-Enhanced Toxicity of Titanium Dioxide Nanoparticles to Developing Zebrafish

3.1 Abstract

Physicochemical factors, such as surface functionalization, can impact the environmental fate and toxicity of nanomaterials. Applications of titanium dioxide (TiO_2) nanoparticles (NPs) range from cosmetics to photovoltaics to environmental remediation. While release of these materials into the environment is likely, the effect of surface functionalization on the inherent and photo-enhanced toxicity of TiO_2 NPs to aquatic vertebrates has not yet been examined. In this study, we investigated the extent to which intentional functionalization with organic ligands (i.e., citrate, ascorbate, and 3,4-dihydroxybenzaldehyde) affected the toxicity of TiO_2 NPs to developing zebrafish (*Danio rerio*). In general, functionalization altered the toxicity of TiO_2 NPs both in the absence and presence of simulated sunlight illumination. Functionalization also increased TiO_2 NP suspension stability and altered TiO_2 NP association levels. While exposure to TiO_2 NPs increased oxidative DNA damage and differences in damage were apparent between bare and functionalized TiO_2 NPs, illumination did not increase oxidative DNA damage for any of the TiO_2 NP preparations. These results demonstrate the importance of examining the extent to which physicochemical factors (e.g., intentional functionalization) and environmental factors (e.g., sunlight exposure) impact nanomaterial toxicity to develop safer nanomaterials for future applications.

3.2 Introduction

Nanotechnology has the potential to dramatically benefit society by reducing energy costs as well as increasing manufacturing productivity and efficiency.[1] One of the unique

features of nanotechnology is the tunability of properties such as size, shape, phase, and surface charge. By controlling these factors, the optical, electrical, and magnetic properties of the material can be engineered for specific applications. For example, materials can be engineered to have improved light harvesting abilities and multiple-exciton generation making them suitable for photocatalytic as well as photovoltaic applications.[1] Furthermore, the high surface to volume ratio of nanomaterials makes them of interest as catalysts for processes ranging from minimizing chemical waste to improving feedstock utilization.[1]

To ensure the safety of such technologies, it is crucial to investigate how the unique nano-scale properties may affect the toxicity of the material of interest. Because of their small size, cellular uptake of nanomaterials is more likely than for their bulk counterparts.[2] Furthermore, the high surface to volume ratio as well as the unique optical and electronic properties makes it possible for nanomaterials to interact with biological tissues in manners different than bulk materials.[2] Possible interactions include the formation of reactive species due to UV activation of electron hole pairs, dissolution of the nanomaterial resulting in the release of toxic byproducts, and redox cycling activated by the presence of biological components.[2]

In fact, studies have shown that nano-sized materials can cause enhanced toxicity compared to bulk counterparts.[3-8] For example, Xiong *et al.* found that the acute median lethal concentration (96-h LC_{50}) of nano-TiO_2 nanoparticles (NPs) for adult zebrafish (*Danio rerio*) was 124.5 mg L^{-1} while bulk TiO_2 caused no mortality even at concentrations up to 300 mg L^{-1}.[8] Fish exposed to TiO_2 NPs also had increased levels of lipid peroxidation

and alterations in antioxidant biomarkers compared to those exposed to the bulk material. The authors hypothesized that the difference in toxicity between the bulk and nano-sized material was due to the ability for TiO_2 NPs to cause oxidative stress.

As a wide bandgap semiconductor, absorption of energy equal to or higher than the bandgap by TiO_2 NPs can promote an electron from the valence band to the conduction band leaving behind a hole in the valence band.[9] This reaction is exploited in applications ranging from cosmetics to photovoltaics to environmental remediation.[9] However, the ability to absorb UV light is also a cause for concern as TiO_2 NPs can produce reactive oxygen species (ROS) upon photo-activation. In aqueous environments, the hole can oxidize water to form hydroxyl radical (·OH) and the electron can reduce molecular oxygen to form superoxide anion ($O_2{\cdot}^-$).[9] Excess ROS can override antioxidant mechanisms leading to oxidative stress resulting in cellular damage (e.g., DNA damage, lipid peroxidation, protein oxidization), disease (e.g., cancer, diabetes, cardiovascular disease) and, ultimately, death.[10]

We found that exposure (both acute (i.e., 5 d) and subchronic (i.e., 21 d)) to uncoated commercially available TiO_2 NPs (Degussa P25) under illumination with simulated sunlight increased mortality and the incidence of morphological malformations (e.g., stunted growth, edema, malformed head and tail) in developing zebrafish (*Danio rerio*).[11-12] These increases in toxicity corresponded with increases in oxidative DNA damage, *in vivo* superoxide concentrations, and activation of an antioxidant response element (ARE) reporter.[11-12] We concluded that the enhanced toxicity was caused by

increased oxidative stress in response to increased ROS production by TiO_2 NPs upon simulated sunlight illumination.

While these studies used TiO_2 NPs lacking intentional coatings, nanoparticles are often functionalized with organic ligands during synthesis to control physicochemical properties including size, stability, and reactivity. Differences in ligand properties can alter NP toxicity. For example, King-Heiden *et al.* found that quantum dots (CdSe:ZnS core:shell) functionalized with methoxy-terminated polyethylene glycol (PEG) produced less incidence/severity of morphological malformations in larval zebrafish than those with carboxy- and methoxy-terminated PEG.[13] The authors hypothesized that these differences were caused by differences in tissue distribution of the quantum dots as body burden levels were similar among the three terminations.[13]

These studies indicate that, to reduce the potential for adverse effects, it is crucial to evaluate not only the toxicity of the nanomaterial itself but also how environmental (e.g., ionic strength, presence of organic ligands, sunlight exposure) and physicochemical properties (e.g., surface coatings, size) can influence toxicity. Thus, the overall objective of this study was to examine the influence of intentional functionalization on inherent and photo-enhanced toxicity of TiO_2 NPs towards developing zebrafish. To accomplish this, we exposed embryo/larval zebrafish to uncoated and citrate, ascorbate, and DHBA-functionalized-TiO_2 NPs in the presence and absence of simulated sunlight illumination. The influence of functionalization on TiO_2 NP suspension stability, exposure, and oxidative DNA damage was also examined. The zebrafish is an ideal model to assess the toxicity of

nanomaterials because their small size and high fecundity permits low sample volumes and large sample sizes.[14] Furthermore, the genome is fully sequenced allowing for comparisons to other aquatic species as well as humans.[14]

3.3 Materials and Methods

Materials

$TiCl_4$ (Part No. 208556), anhydrous benzyl alcohol (Part No. 305197), sodium citrate (Part No. 51804), (+)-sodium L-ascorbate (Part No. A7631), 3,4-dihydroxybenzaldehye (Part No. D108405), and dialysis membranes (12.4 kDa cellulose; Part No. D9777) were purchased from Sigma Aldrich (St Louis, MO). Ethanol (Part No. 2716) was purchased from Decon Laboratories Inc. (King of Prussia, PA). The commercially prepared, uncoated TiO_2 NP preparation (Part No. SN3301) was purchased from Sun Innovations (Fremont, CA). LC/MS grade water (Part No. W6-1) was purchased from Fisher Scientific (Thermo Fisher, Delaware, USA).

Zebrafish exposures were conducted in "fish water" as described in Chapter 2. To study photo-enhanced toxicity, sunlight was simulated using a 250 W blue-spectrum metal halide lamp as described in Chapter 2.

Nanoparticle Synthesis and Functionalization

TiO_2 NPs were synthesized using a method adapted from Kotsokechagia *et al.*[16] Briefly, $TiCl_4$ was added to anhydrous ethanol in a round-bottom flask. Anhydrous benzyl alcohol was added, and the solution was heated (85 °C, 6.5 h). The particles were

precipitated with diethyl ether (1:2 (v:v) diethyl ether: nanoparticle suspension) and centrifuged until the supernatant was clear. The supernatant was decanted, and the particles were resuspended in a 1:1 (v:v) ultrapure H_2O: ethanol solution at pH 1.

TiO_2 NPs synthesized in-house were functionalized with citrate, ascorbate, or 3,4-dihydroxybenzaldehyde (DHBA), and aliquots of the commercially obtained TiO_2 NPs were functionalized with citrate. Citrate was chosen because it is commonly employed to increase NP stability,[17-18] ascorbate was chosen for its antioxidant properties,[19] and DHBA was chosen because the aldehyde moiety can undergo Schiff base reactions with thiol and amine groups allowing DHBA to be a linker molecule for a variety of terminal groups.[20]

To functionalize the in-house synthesized TiO_2 NPs, uncoated suspensions were precipitated with a 3:1 (v:v) diethyl ether: methanol mixture and centrifugation. To functionalize the citrate-TiO_2 NPs, an aqueous solution of sodium citrate (20 mL at 5-10 mM) at pH 8 was subsequently added to the sedimented NPs and sonicated for 90 min. For the ascorbate-TiO_2 NPs, an aqueous solution of sodium L-ascorbate (20 mL at 6 mM) was prepared at pH 10. The solution was added to the sedimented NPs and agitated (final pH = 8). For the DHBA-TiO_2 NPs, an aqueous solution of DHBA (20 mL at 7 mM) was prepared at pH 10 and heated to 80 °C. This solution was added to the sedimented NPs and agitated (final pH = 8). Samples were dialyzed against ultrapure H_2O for two 24 h periods using a 12.4 kDa cellulose membrane to remove excess ligand..

To functionalize the commercially obtained TiO_2 NPs (citrate (SI)), an aqueous solution (20 mL at 10 mM) of citrate at pH 8 was added to the TiO_2 NP powder (20 mg) and

sonicated for 60 min. Samples were dialyzed against ultrapure H_2O for one 48 h period using a 12.4 kDa cellulose membrane.

Nanoparticle Characterization

Transmission Electron Microscopy (TEM). Primary particle size was determined by TEM. Samples of in-house synthesized TiO_2 NPs prior to functionalization were deposited onto a copper mesh grid and imaged using a Philips CM200 Ultra Twin TEM. ImageJ was used to determine particle size.

Raman spectroscopy. Raman spectroscopy was used to determine the crystal phase of the in-house synthesized TiO_2 NPs. Samples of in-house synthesized TiO_2 NPs prior to functionalization were dripped onto a glass slide and oven-dried (80 °C). Raman spectra were acquired with a Thermo Scientific DXR Raman Microscope. Spectra were obtained from 50 to 3500 cm^{-1} using a 532 nm laser with a 10.0 mW power. Using a 10× objective, 10 exposures were obtained with a collection time of 5 s.

Fourier transform infrared spectroscopy (FTIR). We employed FTIR to examine nanoparticle-ligand interactions. A small amount of the functionalized nanoparticle suspension was placed onto a ZnSe salt plate and oven-dried (80 °C). Measurements, consisting of 100 scans, were obtained in transmission mode using a Bruker Model Vertex70 spectrometer. For comparison purposes, spectra were also obtained for the neat ligands.

Assessment of TiO_2 NP Stock Concentration. To determine the concentration of the TiO_2 NP stocks, inductively coupled plasma-optical emission spectroscopy (ICP-OES) was used. Prior to analysis, samples were digested in aqua regia (1:1 concentrated

hydrocholoric acid (HCl): concentrated nitric acid (HNO_3)).[21] Briefly, nanoparticle suspensions were diluted twice in ultrapure H_2O; first by a factor of 1:10 and then by a factor of 1:1000. Aqua regia (2 mL) was added to a 10 µL aliquot of the diluted sample. The sample was then heated at 125 °C for 2 h. Samples were then diluted to 10 mL using 10% HNO_3. Ti concentrations were determined using a Varian Vista-MPX inductively coupled plasma-optical emission spectrometer (0.75 $L \cdot min^{-1}$ nebulizer flow; 15.0 $L \cdot min^{-1}$ plasma flow; Varian, Inc., California, USA). Emission was recorded at 334.188, 334.941, 336.1[15], and 337.280 nm and averaged.

Quantification of Reactive Oxygen Species (ROS). We assessed ROS generation using a microplate assay kit (OxiSelect™ *In Vitro* ROS/RNS Assay Kit, Cell Biolabs Inc., San Diego, CA). In this assay, total free radical formation was assessed using the fluorogenic probe dichlorodihydrofluorescin (DCHF). In the presence of free radicals (e.g., ·OH, hydrogen peroxide (H_2O_2), peroxyl radical, nitric oxide, peroxynitrite anion), DCHF is oxidized to the fluorescent molecule, dichlorofluorescin (DCF).[22] As cellular peroxidases are necessary for H_2O_2 to oxidize DCHF to DCF and ·OH is formed upon reduction of H_2O_2 by peroxidases, it is highly likely that DCHF actually detects the presence of ·OH and not H_2O_2.[22]

The feasibility of using DCHF to detect free radicals generated by engineered nanomaterials has been in question.[23] Concerns about this system include interaction of NPs with optical measurements, potential for the cellular peroxidase to alter the fluorescence signal in the presence of NPs, and interaction of NPs with the probe. To address such concerns, we spiked TiO_2 NPs aliquots with a known amount of DCF in the

presence and absence of the catalyst (i.e., peroxidase component). Bare and functionalized TiO_2 NPs did not alter the DCF signal in either the presence or absence of the catalyst (data not shown). Furthermore, no signal was detected for TiO_2 NPs samples lacking the DCF spike (data not shown). Together, these results indicate that the TiO_2 NPs did not interfere with the optical measurement, the catalyst did not impact the DCF signal in the absence or presence of TiO_2 NPs, and the TiO_2 NPs did not interfere with the DCF signal. As such, we determined this assay suitable for use in this study.

For this study, a modified assay protocol was developed. Bare and functionalized TiO_2 NPs (500 $mg \cdot L^{-1}$) were exposed to the absence and presence of a 254 nm illumination (Pen-Ray® grid lamp, UVP LLC, Upland, CA) for ~40 mins. Prior to the termination of exposure (5 min), the catalyst was added. The quenched, stabilized probe was subsequently added and the samples incubated (15 min). After incubation, fluorescence was measured (λ_{ex} = 485/20 nm, λ_{em} = 528/20 nm; FLx800 Fluorescence Microplate Reader, Biotek, Vermont, USA).

As the majority of radical species produced by TiO_2 NPs upon photo-activation are expected to be hydroxyl radicals,[24] we converted fluorescence intensity to ·OH equivalents. To do so, a calibration curve was prepared with H_2O_2 concentrations ranging from 10 to 100 μM. To reduce background ROS levels, LC-MS grade H_2O was used to prepare the samples and standards.

Assessment of Suspension Stability. Suspension stability was assessed under the same conditions employed in the zebrafish toxicity assay. Suspensions of 10 $mg \cdot L^{-1}$ TiO_2

NPs were prepared from stocks in fish water. Particle diffusivities were determined by dynamic light scattering (Zetasizer Nano ZS, Malvern Instruments, Worcestershire, UK; 633 nm laser, 173° scattering angle) as described in Chapter 2. Because the size distributions of these samples were monomodal, we reported mean number-averaged hydrodynamic diameters, d_h. Measurements were obtained prior to and after one 24 h exposure period in the presence and absence of illumination. Each experiment was performed a minimum of three times.

Toxicological and TiO_2 NP Exposure Assessment

Zebrafish Exposures. Zebrafish toxicity assays were performed as described in Chapter 2. Briefly, fertilized zebrafish (AB strain) eggs were exposed to fish water or bare or functionalized TiO_2 NPs (1-500 $mg \cdot L^{-1}$; n = 12 fish, three replicates per concentration) from 4-6 hours post-fertilization (hpf; embryonic stage) until 5 days post-fertilization (dpf; larval stage). Each experiment was conducted at least twice. Zebrafish were assessed daily for mortality.

At 5 dpf, fish exposed to fish water and bare or functionalized TiO_2 NPs (250 $mg \cdot L^{-1}$) in the absence and presence of illumination were immobilized in 3% methylcellulose and photographed in the lateral orientation at 2.6× magnification (n = 10 fish; each experiment was conducted at least twice). From these micrographs, malformations (e.g., bent spine, stunted growth, tail fin malformation), edema, and failed yolk sac absorption were examined as described in Chapter 2. The incidence of pericardial edema and failed yolk sac absorption were quantified.

The protocol for animal use and maintenance was approved by the Research Animal Resources Center of UW-Madison, which follows the National Institutes of Health Guide to the Care and Use of Laboratory Animals (protocol # M00489-4-11-06).

Determination of TiO_2 NP Association with Zebrafish. TiO_2 NP exposure levels were determined using a method adapted for Chapter 2. Briefly, surviving zebrafish exposed to fish water or bare or functionalized TiO_2 NPs (1, 10, and 500 $mg \cdot L^{-1}$) were collected, pooled (four pooled samples per dose/treatment), flash frozen, and stored at −80 °C until digestion.

Fish were digested in aqua regia at 125 °C for 2h. Digestates were diluted to 5 mL with ultrapure H_2O. A Varian Vista-MPX inductively coupled plasma-optical emission spectrometer (0.75 $L \cdot min^{-1}$ nebulizer flow; 15.0 $L \cdot min^{-1}$ plasma flow; Varian, Inc., California, USA) was employed to determine Ti concentrations. Emission was recorded at 334.188, 334.941, 336.115, and 337.280 nm and averaged.

Oxidative Stress Assessment

Determination of 8-Hydroxy-2-deoxy guanosine (8-OHdG) levels. To assess the oxidative stress, we measured the formation of the commonly assayed DNA adduct, 8-OHdG.[10,25-26] An increase in oxidative DNA adduct formation is a hallmark of oxidative stress. We previously employed this technique with zebrafish exposed to bare and humic acid (HA)-coated TiO_2 NPs.[11-12,15]

Briefly, zebrafish (*n* = 48; at least two replicates per experiment) were exposed to fish water or bare or functionalized TiO_2 NPs (500 mg·L^{-1}) in the presence and absence of simulated sunlight illumination until 3 dpf. Surviving fish were collected, flash frozen, and stored at -80 °C until analysis. DNA was extracted using a Promega Wizard SV Genomic DNA extraction kit and quantified as described in Chapter 2. After extraction, 8-OHdG levels were determined by an enzyme-linked immunosorbent assay and normalized to DNA quantity as described in Chapter 2.

Statistical analyses

Median lethal concentrations (LC_{50} values) were calculated using a trimmed Spearman-Karber analysis (USEPA Trimmed Spearmen-Karber Analysis Program, Version 1.5).[27] Data are presented as mean ± SEM unless otherwise noted. Unpaired *t*-tests were employed to determine *p*-values. The level of significance for all analyses was $p \leq 0.05$.

3.3 Results

Nanoparticle Characterization

Transmission electron microscopy (TEM) of in-house synthesized and commercially obtained TiO_2 NPs indicated that they were roughly spherical with primary particle diameters of 6.0±1.0 nm (Figure 31A) and 12±3.7 nm,[12] respectively, prior to functionalization. Raman spectra of in-house synthesized TiO_2 NPs prior to functionalization exhibited the characteristic peaks for anatase (154, 406, 518, and 643 cm^{-}

[1]) and lacked those for rutile (Figure 3.1B).[28-30] The manufacturer reported the same crystal phase for the commercially obtained, bare TiO_2 NPs.[12]

Confirmation of Ligand Binding. We employed FTIR to confirm ligand binding to the TiO_2 NPs. We compared the spectrum of the functionalized TiO_2 NP to that of the neat ligand. For neat sodium citrate, peaks for the asymmetric and symmetric carbonyl stretching vibrations (ν_{asym}(C=O) and ν_{sym}(C=O)) were at 1583 cm^{-1} and 1396 cm^{-1} (Figure 3.2A). For citrate-TiO_2 NPs, the ν_{asym}(C=O) and ν_{sym}(C=O) peaks shifted to 1615 and 1389 cm^{-1}, respectively (Figure 3.2A). This shift indicates that the carboxyl groups are bound to Ti atoms at the nanoparticle surface instead of Na^+ ions.[17] Another indication of the adsorption of citrate to the TiO_2 NP surface is the presence of the C-O stretch (ν(C-O)) in both spectra (neat: 1282 cm^{-1}; TiO_2 NPs: 1248 cm^{-1}; Figure 3.2A).[17] Thus, these results are consistent with previous studies examining the attachment of citric acid to TiO_2 NPs.

For ascorbate, the carbonyl stretch (ν(C=O)) was present in both the neat ligand (1699 cm^{-1}) and TiO_2 NP (1712 cm^{-1}) spectra (Figure 3.2B).[31] Also present in both neat ligand and TiO_2 NP spectra were the C=C stretch (neat: 1582 cm^{-1}; TiO_2 NPs: 1641 cm^{-1}) and the δ(COH) band (neat: 1301 cm^{-1}; TiO_2 NPs: 1313 cm^{-1}) (Figure 3.2B).[31] The presence of these bands in the TiO_2 NP spectra indicates that ascorbate is bound to the surface on the nanoparticle.

For DHBA, the carbonyl stretch (ν(C=O)) of the aldehyde is present in the spectra of both the neat ligand (1644 cm^{-1}) and TiO_2 NPs (1664 cm^{-1}) indicating the presence of an aldehyde group on the nanoparticle surface (Figure 3.2C).[32] Consistent with studies

examining the attachment of catechol to the surface of TiO_2, the δ(OH) band (1383 cm^{-1}) diminishes upon adsorption to TiO_2 NPs (Figure 3.2C).[33] Also consistent with previous studies is the shift in the C-O stretching bands. These bands transition from a split band (1294 and 1271 cm^{-1}) in the neat ligand into an intense band with a shoulder (1289 peak with shoulder at 1258 cm^{-1}) upon adsorption to TiO_2 NPs (Figure 3.2C).[33-34] Further evidence of the absorption of DHBA to the surface of the TiO_2 NPs is the presence of the C=C stretching vibration (ν_{sym}(C=C)) in both spectra (neat: 1328 cm^{-1}; TiO_2 NPs: 1335 cm^{-1}; Figure 3.2C).[34] The presence of these features in the TiO_2 NP spectra indicates that DHBA is bound to the surface on the nanoparticle.

Quantification of ROS Production. To examine if functionalization alters the ability for TiO_2 NPs to produce ROS, we measured ·OH equivalents after exposure in the absence and presence of illumination with a 254 nm lamp. As expected, we saw minimal ROS formation in the absence of illumination (Figure 3.3). In the presence of illumination, we found that functionalization decreased ·OH formation. For instance, in the presence of illumination bare TiO_2 NPs produced 220±6.0 μM ·OH equivalents while citrate-TiO_2 NPs produced 360±10.0 μM ·OH equivalents ($p \leq 0.05$; Figure 3.3).

Despite this decrease in ROS formation with functionalization, both bare and functionalized-TiO_2 NPs produced more ·OH equivalents in the presence of illumination than in the absence ($p \leq 0.05$; Figure 3.3). For instance, bare TiO_2 NPs produced <0.6 μM ·OH equivalents in the absence of illumination and 220±6.0 μM ·OH equivalents in the presence of illumination ($p \leq 0.05$; Figure 3.3).

Assessment of Aggregation State. We have previously shown that nanoparticle suspension stability can impact uptake.[15] We therefore assessed the aggregation state of all TiO_2 NP preparations before and after exposure in the absence and presence of simulated sunlight illumination.

In general, functionalization reduced aggregation. For example, before exposure, bare TiO_2 NPs (10 mg·L^{-1}) were larger (d_h=320±37 nm) than citrate-TiO_2 NPs (d_h=15±1.1 nm; p≤0.05; Table 3.1). Furthermore, after exposure in the absence of illumination, bare TiO_2 NPs (10 mg·L^{-1}) were still larger (d_h =187±32 nm) than citrate-TiO_2 NPs (d_h=26±2.7 nm; p≤0.05; Table 3.1).

However, simulated sunlight exposure increased aggregation for the functionalized particles. For example, in the absence of illumination, the citrate-TiO_2 NPs aggregates (10 mg·L^{-1}) were smaller (d_h=26±2.7 nm) than those subject to illumination (d_h=180±75 nm; p≤0.05; Table 3.1). In fact, after illumination, the aggregation state of the functionalized TiO_2 NP suspensions was closer to that of the bare TiO_2 NPs (i.e., suspension contained larger, unstable aggregates).

<u>TiO_2 NP Association with Developing Zebrafish</u>

Functionalization did not drastically alter Ti association with zebrafish larvae. Differences in association levels were observed between bare and functionalized TiO_2 NPs, however, no overall trend was apparent (Figures 3.4-3.6). For example, in the absence of illumination, fish exposed to a nominal dose of 10 mg·L^{-1} of citrate-TiO_2 NPs had a lower Ti association level (11±1.1 $\mu g_{Ti} \cdot g_{fish}^{-1}$) than those exposed to the same nominal dose of bare

TiO_2 NPs (19±4.2 $\mu g_{Ti} \cdot g_{fish}^{-1}$; $p \leq 0.05$; Figure 3.4A). Conversely, fish exposed to a nominal dose of 500 $mg \cdot L^{-1}$ of citrate-TiO_2 NPs had a higher Ti association level (110±33 $\mu g_{Ti} \cdot g_{fish}^{-1}$) than those exposed to the same nominal dose of bare TiO_2 NPs (15±3.6 $\mu g_{Ti} \cdot g_{fish}^{-1}$; $p \leq 0.05$; Figure 3.4A).

Additionally, illumination did not drastically alter association levels. While differences in association levels were observed between fish exposed to bare and functionalized-TiO_2 NPs the absence and presence of illumination, no overall trend was observed (Figures 3.7). For example, fish exposed to nominal dose of 10 $mg \cdot L^{-1}$ citrate-TiO_2 NPs in the absence of illumination had an equivalent Ti association level (11±1.1 $\mu g_{Ti} \cdot g_{fish}^{-1}$) to those exposed under illumination (11±1.7 $\mu g_{Ti} \cdot g_{fish}^{-1}$; $p > 0.05$; Figure 3.7B). On the other hand, fish exposed to nominal dose of 500 $mg \cdot L^{-1}$ citrate-TiO_2 NPs in the absence of illumination had a higher Ti association level (110±33 $\mu g_{Ti} \cdot g_{fish}^{-1}$) than those exposed under illumination (560±170 $\mu g_{Ti} \cdot g_{fish}^{-1}$; $p \leq 0.05$; Figure 3.7B).

Nanoparticle Toxicity

Morphological Malformations. In the absence of simulated sunlight illumination, fish exposed to all TiO_2 NP preparations exhibited low incidence of malformations (i.e., failed yolk sac absorption, edema; see Figure 2.3 for representative micrographs). Fish exposed to citrate, citrate (SI)-, and DHBA-TiO_2 NPs displayed higher incidence of failed yolk sac absorption than unexposed controls ($p \leq 0.05$), but fish exposed to bare and ascorbate-TiO_2 NPs did not ($p > 0.05$; Table 3.2). Additionally, fish exposed to citrate and DHBA-TiO_2 NPs

displayed higher incidence of edema than those exposed to control ($p \leq 0.05$), but fish exposed to bare, citrate (SI), and ascorbate-TiO_2 NPs did not ($p > 0.05$; Table 3.2).

Despite this low level of toxicity, citrate and DHBA functionalization increased the incidence of malformations ($p \leq 0.05$; Table 3.2). For example, none of the fish exposed to the bare TiO_2 NPs (250 $mg \cdot L^{-1}$) displayed failed yolk sac absorption or edema, but 20±0% of fish exposed to the same nominal dose of citrate-TiO_2 NPs displayed failed yolk sac absorption and 5.0±2.2% displayed edema (Table 3.2). This trend was not apparent for citrate (SI) and ascorbate-TiO_2 NPs ($p > 0.05$; Table 3.2).

In the presence of simulated sunlight illumination, low incidences of malformations were still observed. In fact, only bare TiO_2 NPs produced higher incidence of failed yolk sac absorption than control ($p \leq 0.05$) and none of the preparations displayed more edema than control ($p > 0.05$; Table 3.2). While differences between bare and citrate-TiO_2 NPs were not apparent ($p > 0.05$; Table 3.2), bare TiO_2 NPs caused more failed yolk sac absorption and edema than citrate (SI)-, ascorbate and DHBA-TiO_2 NPs ($p \leq 0.05$; Table 3.2).

Only fish exposed to bare TiO_2 NPs exhibited photo-enhanced toxicity (Table 3.2). For example, in the absence of illumination, none of fish exposed to bare TiO_2 NPs (250 $mg \cdot L^{-1}$) displayed failed yolk sac absorption while 15±1.6% displayed the endpoint under illumination ($p \leq 0.05$; Table 3.2). On the other hand, 20±0.0% exposed to citrate-TiO_2 NPs (250 $mg \cdot L^{-1}$) displayed failed yolk sac absorption in the absence of illumination while 15±2.2% displayed the endpoint under illumination ($p > 0.05$; Table 3.2).

Survival. In the absence of simulated sunlight illumination, fish exposed to all TiO_2 NP preparations exhibited low mortality. Increases in survival relative to control were apparent for each preparation but varied with nominal dose (Figures 3.8A-3.10A). For instance, bare TiO_2 NPs produced more mortality than control at all nominal doses while citrate-TiO_2 NPs did so at nominal doses ≥100 $mg \cdot L^{-1}$ ($p \leq 0.05$; Figure 3.8A). The low mortalities over the concentration range examined precluded calculation of LC_{50} values for all preparations. Nevertheless, citrate and DHBA functionalization increased mortality ($p \leq 0.05$; Figures 3.8A and 3.10A). On the other hand, citrate (SI) and acorbate-TiO_2 NPs did not cause such differences ($p > 0.05$; Figures 3.8A and 3.9A).

In the presence of simulated sunlight illumination, low levels of toxicity were still observed with all TiO_2 NP preparations. Increases in survival relative to control were apparent for each preparation but varied with nominal dose (Figures 3.7B-3.10B). For instance, bare TiO_2 NPs produced more mortality than control at all nominal doses except 100 $mg \cdot L^{-1}$ while citrate-TiO_2 NPs did so at nominal doses ≥100 $mg \cdot L^{-1}$ ($p \leq 0.05$; Figure 3.7B). As such, bare TiO_2 NPs produced more toxicity than functionalized particles at high doses (≥250 $mg \cdot L^{-1}$; $p \leq 0.05$; Figures 3.8B-3.10B). In fact, the LC_{50} of bare TiO_2 NPs was 316 $mg \cdot L^{-1}$ ($CI_{95\%}$: 283-353 $mg \cdot L^{-1}$) while that for the functionalized TiO_2 NPs was >500 $mg \cdot L^{-1}$.

Not all preparations exhibited photo-enhanced toxicity. Bare TiO_2 NPs produced photo-enhanced toxicity at several nominal doses as did ascorbate and DHBA-TiO_2 NPs at the highest nominal dose and citrate (SI)-TiO_2 NPs at the lowest dose ($p \leq 0.05$; Figure 3.11).

On the other hand, citrate-TiO_2 NPs did not produce photo-enhanced toxicity at any nominal doses (p>0.05; Figure 3.11B).

Nanoparticle-Induced Oxidative Stress

In general, exposure to TiO_2 NPs increased oxidative DNA damage. In the absence of illumination, fish exposed to bare TiO_2 NPs had higher 8-OHdG levels than controls (p≤0.05; data not shown); under illumination, fish exposed to all TiO_2 NPs preparations had higher 8-OHdG levels than controls (p≤0.05; data not shown). Additionally, functionalization decreased oxidative DNA damage (p≤0.05; Figure 3.12). For instance, when normalized to the amount of TiO_2 NPs associated with the fish, fish exposed to citrate TiO_2 NPs had less oxidative DNA damage relative to those exposed to bare TiO_2 NPs in both the absence and presence of illumination (p≤0.05; Figure 3.12).

We anticipated that fish exposed to bare TiO_2 NPs under illumination would have more 8-OHdG than those exposed in the absence of illumination as fish exposed in the presence displayed more toxicity. However, this was not the case. In fact, we did not observe photo-enhanced oxidative DNA damage with any of the TiO_2 NP preparations *(*p>0.05; Figure 3.12).

3.4 Discussion

In this study, we examined the extent to which intentional functionalization with organic ligands impacted the toxicity of TiO_2 NPs to developing zebrafish. We also examined the extent to which simulated sunlight illumination altered the toxicity of these

materials. To explore these interactions, we functionalized in-house synthesized TiO_2 NPs with an aqueous suspension of citrate, ascorbate, and DHBA and a commercially obtained preparation with citrate. We examined toxicity by assessing mortality as a function of TiO_2 NP concentration and the incidence of malformations (i.e., failed yolk sac absorption, edema). We assessed oxidative stress using 8-OHdG as a biomarker for oxidative DNA damage.

In general, functionalization increased TiO_2 NP suspension stability (i.e., reduced aggregate size). This is likely caused by an increase in the electrostatic repulsion between particles due to the presence of the charged ligand on the NP surface.[35] This decrease in aggregation state with functionalization is consistent with our previous study and others that have examined the influence of organic coatings on TiO_2 NP stability.[15, 17, 36]

We also found that illumination decreased suspension stability (i.e., increased aggregate size) for the functionalized TiO_2 NPs. This decrease in stability is not unexpected as TiO_2 NPs have been reported to degrade organic molecules upon UV illumination.[9,37-38] We previously found that the aggregation of HA coated-TiO_2 NPs (Degussa P25) increased after illumination.[15] We determined that this increase in aggregation was due to photocatalytic degradation of the HA molecules.

In our previous study, we found that fish exposed to stable suspensions (i.e., TiO_2 NP suspensions containing DOM) had lower association levels than those exposed to unstable suspensions (i.e., TiO_2 NP suspensions lacking DOM) since developing zebrafish reside near the sediment-water interface.[15] Thus, we hypothesized that fish exposed to the

functionalized TiO_2 NPs in this study would have lower association levels than those exposed to bare particles. Contrary to our expectations, functionalization did not uniformly decrease TiO_2 NP association level in either the absence or presence of illumination.

One significant difference between these studies is the size of the coating. DOM is a breakdown product of plant residues and is composed of a variety of organic moieties. We found that the molecular weight of the HA molecules utilized ranged from 100-300,000 Da with the majority of molecules around ~2000 Da.[15] On the other hand, the ligands utilized in this study had few organic moieties and were much smaller (130-190 Da). It is possible that, in addition to increasing stability, steric hindrance by the DOM molecules reduced TiO_2 NP association levels. As the ligands utilized in this study were much smaller, increases in suspension stability were likely caused by electrostatic, and not electrosteric, repulsion. It is possible that such drastic differences in association levels between bare and coated TiO_2 NPs in this study are not apparent because the small size of the ligands provides the particles a better chance of interacting with the zebrafish.

Although illumination decreased the stability of the functionalized TiO_2 NPs, the influence of illumination on exposure was varied with ligand and nominal dose. This gradual change would likely not dramatically impact association. In fact, we previously found that while TiO_2 NPs photocatalytically degraded HA and this degradation resulted in decreased stability over the course of the exposure period, a decrease in association level was still present with HA in the presence of illumination.[15] It is likely that the increase in

aggregation occurred slowly over the course of the exposure period. Thus, the lack of a distinct difference in association level in the presence of illumination is not unexpected.

Differences in toxicity between bare and functionalized TiO_2 NPs varied based on ligand and illumination conditions. In the absence of illumination, we did not detect ROS with any of the TiO_2 NPs preparations. Nevertheless, certain functionalizations (i.e., citrate, DHBA) increased TiO_2 NP toxicity and all preparations except for citrate-TiO_2 NPs produced elevated 8-OHdG levels compared to controls. While citrate and DHBA-TiO_2 NPs caused more mortality than bare particles, bare TiO_2 NPs produced more 8-OHdG than all functionalizations.

In the presence of illumination, functionalized TiO_2 NPs produced more ROS than bare TiO_2 NPs. Contrary to our expectations, bare TiO_2 NPs produced more mortality than functionalized TiO_2 NPs. Furthermore, 8-OHdG levels for the bare TiO_2 NPs were higher than that for the functionalized TiO_2 NPs. Additionally, illumination increased ROS production for all preparations and increased the toxicity of bare, DHBA, and ascorbate-TiO_2 NPs at at least one dose. However, this increase in ROS production and toxicity did not correspond with an increase in 8-OHdG. Most surprisingly, citrate-TiO_2 NPs exhibited photo-enhanced ROS generation but not photo-enhanced toxicity or 8-OHdG levels.

King-Heiden *et al.* found that poly-L-lysine (PLL)-functionalized quantum dots (QDs) caused more mortality to developing zebrafish than polyethylene glycol (PEG)-functionalized QDs.[13] They also found that fish exposed to only PLL were smaller than fish exposed to water and concluded that PLL itself was at least partially responsible for

increased toxicity observed with this ligand.[13] Thus, to ensure that the ligand itself was not responsible for the observed toxicity, we exposed fish to graded concentrations of neat citric acid, ascorbic acid, and DHBA. The maximum concentration of ligand possible was calculated using Equation 1.

$$\text{Max Ligand Concentration} = \frac{\text{TiO}_2\text{ NP concentration}}{\text{density of TiO}_2 * \text{volume of 1 particle} * \text{surface area of 1 particle} * \text{ligand number density} * \text{Avogadro's number}} \quad (1)$$

In this equation, the TiO_2 NP concentration ranged from 0.001 to 0.50 $g \cdot L^{-1}$ (the highest dose); density of TiO_2 was 4.23 $g \cdot cm^{-3}$; volume and surface area of 1 particle were $4/3\pi r^3$ and $4\pi r^2$, respectively, with r assumed to be 3.0×10^{-9} m; maximum ligand number density was assumed to be 5.0×10^{18} molecules$\cdot m^{-2}$; and Avogadro's number was 6.0×10^{23} molecules$\cdot mol^{-1}$. This gave a maximum ligand concentration of 0.2-1 mM. A dosing solution range of 0.01 to 1 mM was employed.

For ascorbic acid and citric acid, toxicity did not differ from controls (data not shown). Dose-dependent increase in mortality was observed only for DHBA; the LC_{50} was 0.72 mM ($CI_{95\%}$: 0.67-0.76 mM; 9.8% trim) in the absence of illumination and 0.39 mM ($CI_{95\%}$: 0.28-0.55 mM; 6.9% trim) in the presence of illumination.

Although mortality was observed in fish exposed to neat DHBA, the ligand concentrations utilized were based on the assumption that the ligand was completely removed from the nanoparticle surface during exposure. This scenario is highly unlikely as stocks were dialyzed twice to remove free ligand and FT-IR analysis indicated that all ligands adsorb to the NP surface (Figure 3.2). By, instead, converting association levels

(Figure 3.7) to maximum ligand concentrations using Equation 1, the amount of ligand associated with the fish by the end of the 5 d exposure period was < 0.1 μM. Given these findings, the toxicity observed was not likely to have been caused by the ligand itself.

As differences in association levels were transient and varied with ligand and nominal dose, it is unlikely that they account for the differences in toxicity observed between bare and functionalized TiO_2 NP or the differences in toxicity observed for both bare and functionalized TiO_2 NP in the absence and presence of illumination. We previously found that, while the presence of HA reduced TiO_2 NP association levels, HA actually increased TiO_2 NP toxicity in both the absence and presence of illumination indicating that differences in toxicity between bare and HA-coated particles were not caused by differences association levels.[15] Thus, the lack of relationship between association level and toxicity found in this study is not surprising.

For many nanomaterials, oxidative stress is the primary mechanism responsible for toxicity.[2] In a recent review, Petersen *et al* summarized several mechanisms by which nanomaterials can cause oxidative stress.[26] First, the nanomaterial and/or surface moieties may possess inherent, redox active properties resulting in excess ROS generation. Second, the nanomaterial may accumulate within the organism causing inflammation. This inflammation can activate response by the immune system and result in excess ROS generation. Finally, the nanomaterial may be taken up by cells and cause damage to subcellular organelles disrupting a variety of biological processes and generating excess ROS.

Manifestations of oxidative stress *in vivo* include altered antioxidant enzyme levels, lipid peroxidation, and DNA damage. Antoxidant enzymes (e..g, superoxide dismutase, catalase, glutathione) scavenge ROS. Excess ROS can overwhelm antioxidant enzymes altering biological response and leading to oxidative stress.[25] Lipid hydroperoxides and aldehydes are produced when a hydrogen atom is abstracted from an unsaturated fatty acid and double bonds rearrange.[39] This abstraction can be caused by a variety of molecular species including molecular oxygen and ·OH. Lipid hydroperoxides alter membrane fluidity and membrane protein integrity. Excess ROS can also cause DNA damage forming single-strand breaks (SSBs), double-strand breaks (DSBs), and oxidatively-induced base lesions.[26] This damage can interfere with cellular processes including transcription and replication and ultimately lead to cell death.[26]

The detection of oxidative DNA damage by TiO_2 NPs in the absence of UV light suggests that the particles cause oxidative stress as several other groups have reported.[3,15,40-43] For instance, Fedrici *et al* found that rainbow trout (*Oncorhynchus mykiss*) exposed to TiO_2 NPs (Degussa P25; ≤1 mg·L^{-1} for up to 14 d) under standard laboratory lighting displayed elevated lipid peroxidation (i.e., thiobarbituric acid reactive substances; TBARS) levels in the gills, intestine, and brain and increased total glutathione levels in the gills.[40] Furthermore, we previously found that the increased toxicity (e.g., decreased survival; increased incidence of edema and failed yolk sac absorption) in fish exposed to HA-coated TiO_2 NPs (Degussa P25; ≤1000 mg·L^{-1} until 5 dpf) in the absence of illumination corresponded with an increase in lipid peroxidation (i.e., TBARS).[15]

As absorption of energy equal to or greater than the bandgap (380-420 nm) is required for ROS production by TiO_2 NPs and we detected minimal *in vitro* ROS production in the absence of illumination, the results from our and previous studies suggests that TiO_2 NPs may cause oxidative stress through a mechanism not dependent on photo-activated ROS production. For instance, TiO_2 NPs may cause toxicity and oxidative DNA damage by either inducing inflammation or causing cellular damage as described by Petersen *et al*.[26] Further studies should examine the extent to which TiO_2 NPs impact the immune system and inflammatory response as well as cytotoxicity and subcellular processes (e.g., mitochrondrial function, adenosine triphosphate (ATP) production) to elucidate the mechanism responsible for TiO_2 NP toxicity in the absence of illumination.

The results that we obtained in the presence of illumination suggest that TiO_2 NPs also produce toxicity through redox-active processes (i.e., photo-activated ROS generation). These results are consistent with other studies that have examined the impact on photo-activation on TiO_2 NP toxicity.[11-12,15, 44-46] Despite this, the oxidative stress results we obtained in the presence of illumination were ambiguous. Bare-TiO_2 NPs increased toxicity but had reduced ROS generation and 8-OHdG levels, and illumination increased ROS production and toxicity for most preparations but did not alter 8-OHdG levels.

Petersen *et al* also proposed two scenarios by which TiO_2 NPs induce DNA damage upon UV illumination.[26] In the first scenario, they postulated that the short half-life of ·OH, produced upon oxidation of water by the photo-generated hole, prevents it from entering the nucleus and directly attacking DNA. Instead, they suggest that O_2^-, produced upon

reduction of molecular oxygen by the photo-generated free electron, dismutases into H_2O_2. H_2O_2 can freely pass into the nucleus and undergo the Fenton's reaction re-forming ·OH. This newly formed ·OH can then directly attack DNA. In the second scenario, the free electron or O_2^- reduces Cu^{2+}, normally present in the cytoplasm, to Cu^+. The Cu^+ ion reacts with H_2O_2 or ·OH forming copper peroxyl species which can enter the nucleus and attack DNA.

These scenarios suggest that *in vitro* ROS detection, especially ·OH, may not be the most accurate predictor of oxidative DNA damage as the ·OH produced *ex vivo* is unlikely to be responsible for the DNA damage detected *in vivo*. A more accurate measure of ROS may be *in vivo* detection. For instance, Bar-Ilan *et al* found that developing zebrafish exposed to TiO_2 NPs (Degussa P25) in the presence of simulated sunlight illumination had higher 8-OHdG levels and increased detection of *in vivo* O_2^-.[11] Future studies evaluating TiO_2 NP toxicity to aquatic species should examine the relationship between *in vitro* and *in vivo* ROS detection and oxidative DNA damage levels.

Although we previously found that HA-coated TiO_2 NPs were much more toxic and caused much more oxidative stress than uncoated-TiO_2 NPs, an increase in toxicity was not apparent with other DOM coatings (i.e., FA, NOM).[15] The formation of oxidative stress requires a variety of complex processes and the ligand may interact with a variety of these steps. Thus, it is not surprising that the four preparations examined in this study did not cause the same response.

While we did not detect differences in 8-OHdG levels between the absence and presence of illumination for any of our TiO_2 NPs preparations, oxidative stress should not be ruled out as the mechanism for the observed toxicity. Several groups have shown that TiO_2 NPs may alter certain oxidative stress endpoints but not others.[8, 15, 40, 43] For instance, we previously found that in the presence of illumination both bare and HA-coated TiO_2 NPs (Degussa P25) produced elevated 8-OHdG levels but not TBARs levels compared to control.[15] These results suggest that the manner in which the TiO_2 NPs produced toxicity resulted in DNA damage but not lipid peroxidation. As such, future studies examining the toxicity of TiO_2 NPs should examine a number of oxidative stress endpoints to more accurately pinpoint toxicological mechanism.

3.5 Conclusions

To our knowledge, this is the first study to examine the influence of multiple ligands on the inherent and photo-enhanced toxicity of TiO_2 NPs to an aquatic vertebrate. We found that functionalization impacted the toxicity of TiO_2 NPs to developing zebrafish upon exposure in both the absence and presence of simulated sunlight illumination. As we observed previously, the presence of an organic coating increased TiO_2 NP suspension stability leading to differences in exposure. However, differences in association levels did not correspond with differences in toxicity. As we previously reported, the results that we obtained when examining oxidative stress as the mechanism of toxicity were ambiguous. While exposure to TiO_2 NPs increased oxidative DNA damage and differences in damage were apparent between bare and functionalized TiO_2 NPs, illumination, surprisingly, did

not increase oxidative DNA damage. Additional research will be required to further examine oxidative stress as the mechanism responsible for the differences in toxicity. This study demonstrates the need to investigate how intentional functionalization may alter the stability, exposure, and toxicity of a nanomaterial when assessing the risks posed by these materials in the environment.

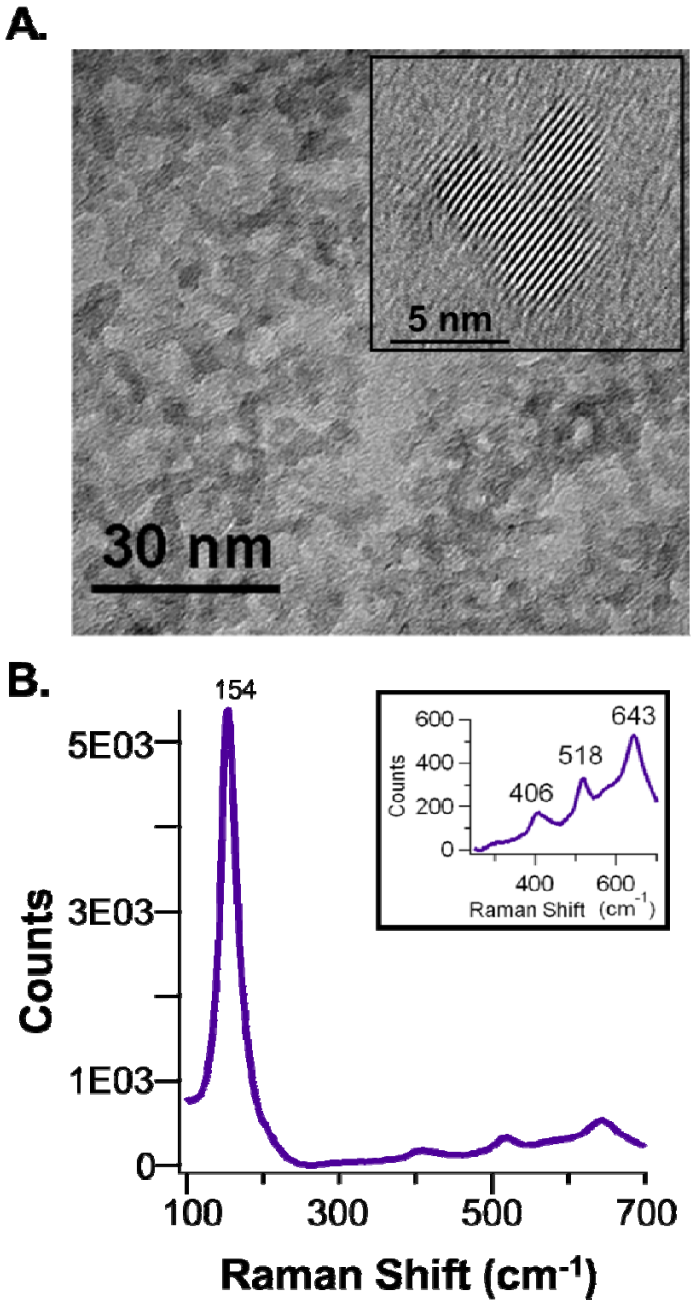

Figure 3.1. TiO_2 NP Primary Particle Size and Crystal Phase. (A) Transmission electron microscopy (TEM) micrographs for house synthesized TiO_2 NPs prior to functionalization showing roughly spherical particles with diameters of 6 ± 1 nm. Insert shows lattice fringes indicating the presence of different TiO_2 faces and, thus, individual particles. (B) Raman spectra for house synthesized TiO_2 NPs prior to functionalization showing only peaks corresponding to the anatase phase.

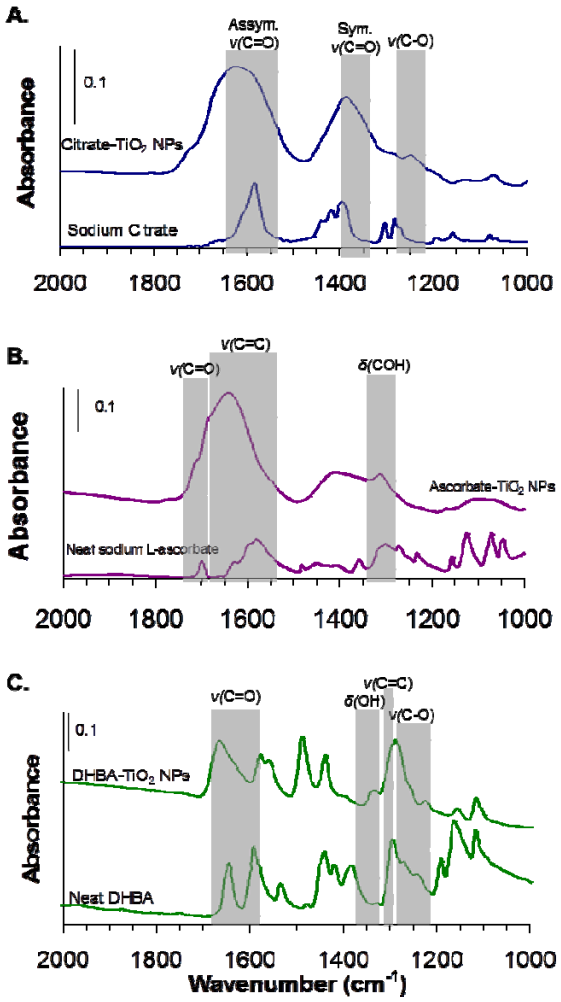

	Wavenumber (cm^{-1}) Neat	Ligand-TiO_2 NPs	Assignment
Sodium Citrate	1583	1622	Asym. ν(C=O)[17]
	1396	1389	Sym. ν(C=O)[17]
	1282	1248	ν(C-O)[17]

	Wavenumber (cm^{-1}) Neat	Ligand-TiO_2 NPs	Assignment
Sodium L-Ascorbate	1699	1712	ν(C=O)[28]
	1582	1641	ν(C=C)[28]
	1301	1313	δ(COH)[28]

	Wavenumber (cm^{-1}) Neat	Ligand-TiO_2 NPs	Assignment
3,4-Dihydroxybenzaldehyde	1644	1664	ν(C=O)[29]
	1383	Diminished	δ(OH)[30]
	1328	1335	ν(C=C)[31]
	1271	1258	ν(C-O)[30-31]
	1294	1289	

Figure 3.2. Fourier Transform Infrared (FTIR) spectroscopy of functionalized TiO_2 NPs. Spectra and peak assignments for (A) citrate-TiO_2 NPs and neat sodium citrate; (B) ascorbate-TiO_2 NPs and neat sodium L-ascorbate; and (C) DHBA-TiO_2 NPs and neat 3,4-dihydroxybenzaldehyde. Shaded areas indicate peak assignments.

Table 3.1. Influence of functionalization on TiO_2 NP aggregate size before and after exposure in the absence and presence of simulated sunlight illumination[a-c]

	d_h (nm)		
	Before Illumination	**- Illumination**	**+ Illumination**
Bare TiO_2 NPs	320 ± 37	190 ± 32	460 ± 51
Citrate-TiO_2 NPs	15 ± 1.1	62 ± 14	180 ± 75
Citrate (SI)-TiO_2 NPs	220 ± 1.5	220 ± 2.9	91; 260[d]
Ascorbate-TiO_2 NPs	35 ± 4.5	62 ± 14	970 ± 200
DHBA-TiO_2 NPs	14 ± 1.7	21 ± 2.4	290 ± 130

[a] Measurements of 10 mg·L^{-1} TiO_2 NP suspensions were obtained before and after 24-h exposure period. [b] Abbreviations: d_h, number-average hydrodynamic diameter. [c] All values presented as mean ± SEM. [d] After exposure in the presence of illumination, citrate (SI)-TiO_2 NPs display a bimodal distribution with peaks at 91 and 260 nm and a tail trailing to 960 nm.

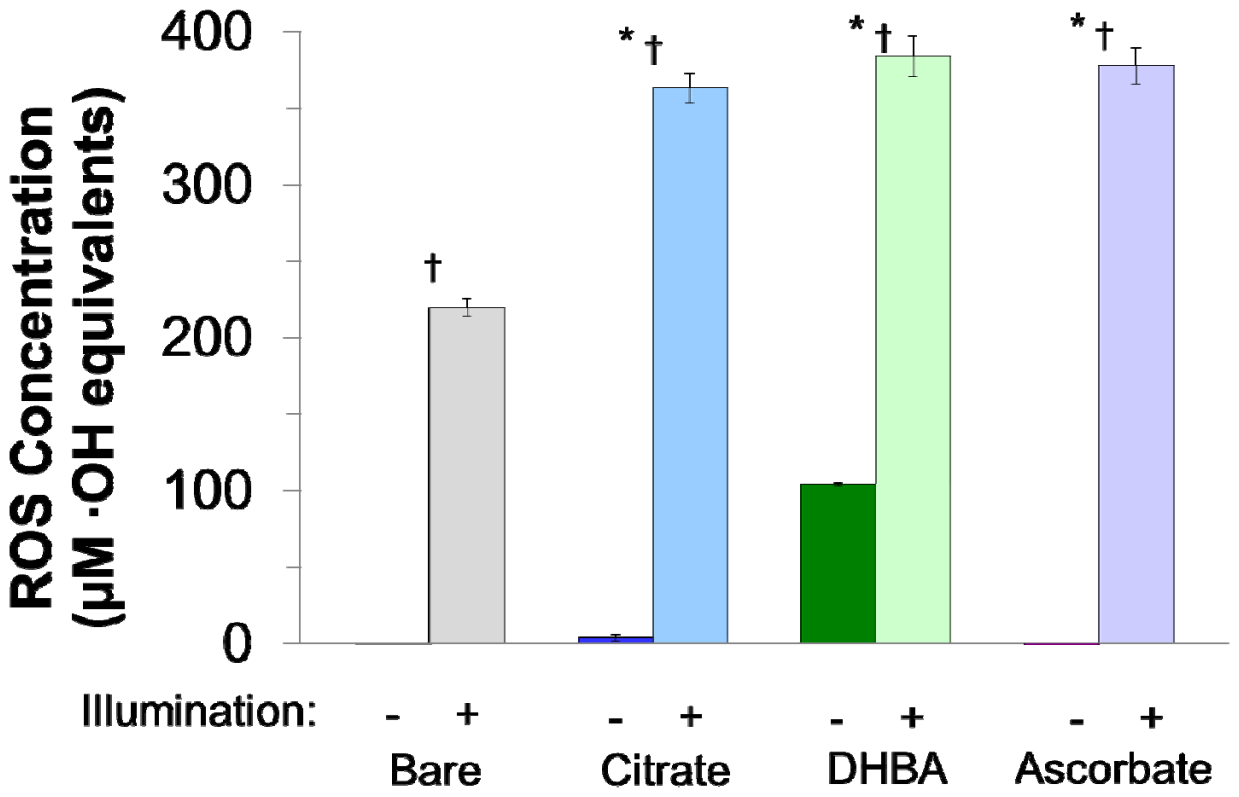

Figure 3.3 Influence of Functionalization and Illumination on ROS Formation by TiO_2 NPs. ROS formation presented as hydroxyl radical (·OH) equivalents for bare, citrate, ascorbate, and DHBA-TiO_2 NPs (500 mg·L^{-1}) in the absence and presence of UV illumination (254 nm; 40 mins). Bars correspond to mean values (4 measurements/preparation) and error bars represent SEM (n = 2 replicates; 6 measurements/replicate). The * indicates significant increase for functionalized-TiO_2 NPs relative to bare TiO_2 NPs and the † indicates significant increase in the presence of illumination relative to the absence. All differences assessed at p = 0.05 level of significance.

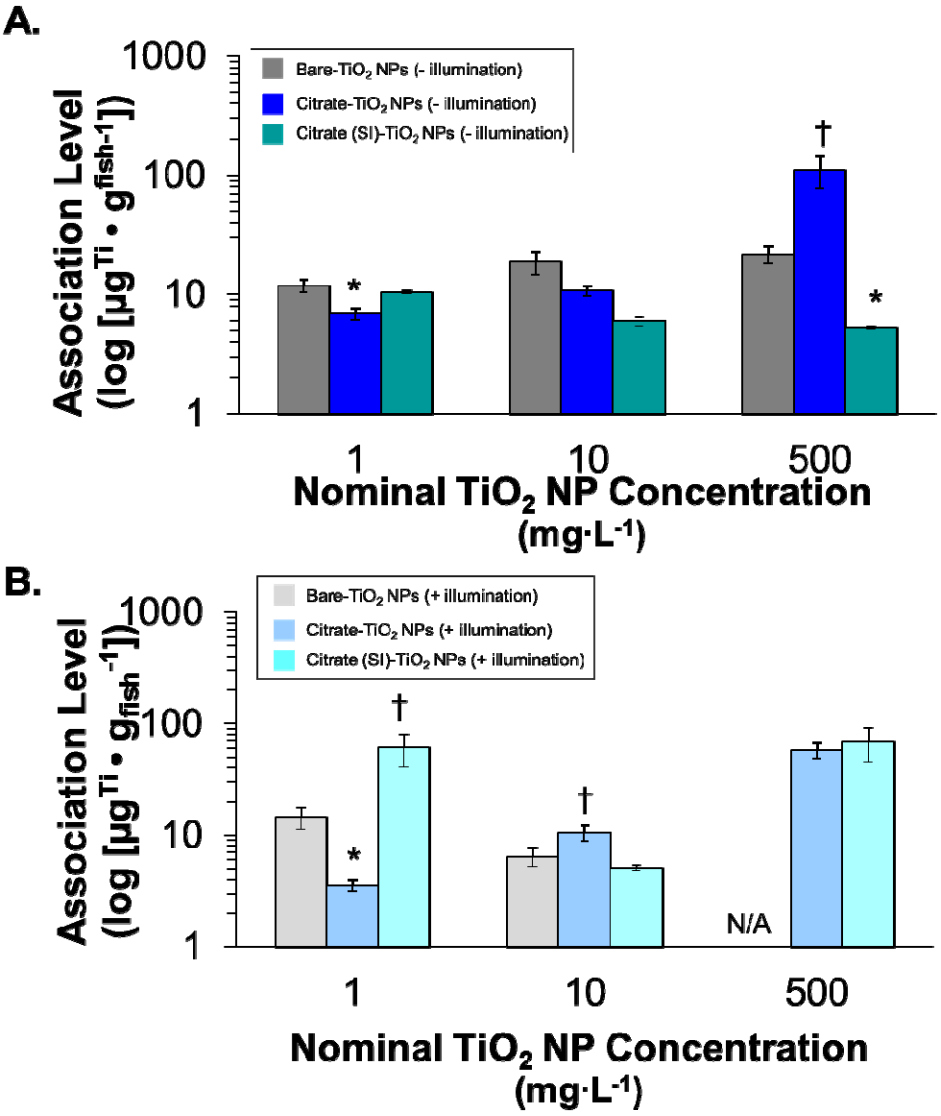

Figure 3.4. Effect of citrate functionalization on TiO_2 NP association level in developing zebrafish. Titanium levels (log) associated with zebrafish at 5 dpf after exposure to bare, citrate, and citrate (SI)-TiO_2 NPs (1, 100, and 500 mg·L^{-1}) in the absence (A) and presence (B) of simulated sunlight illumination (n = 2-6 replicates, 4 measurements per replicate). Measurements at 500 mg·L^{-1} bare TiO_2 NPs under illumination were not available (N/A) due to extensive mortality. Bars correspond to mean values and error bars represent SEM. The * indicates significant decrease in association level for citrate-TiO_2 NPs relative to bare TiO_2 NPs and the † indicates significant increase in association level for citrate-TiO_2 NPs relative to bare TiO_2 NPs. All differences assessed at p = 0.05 level of significance.

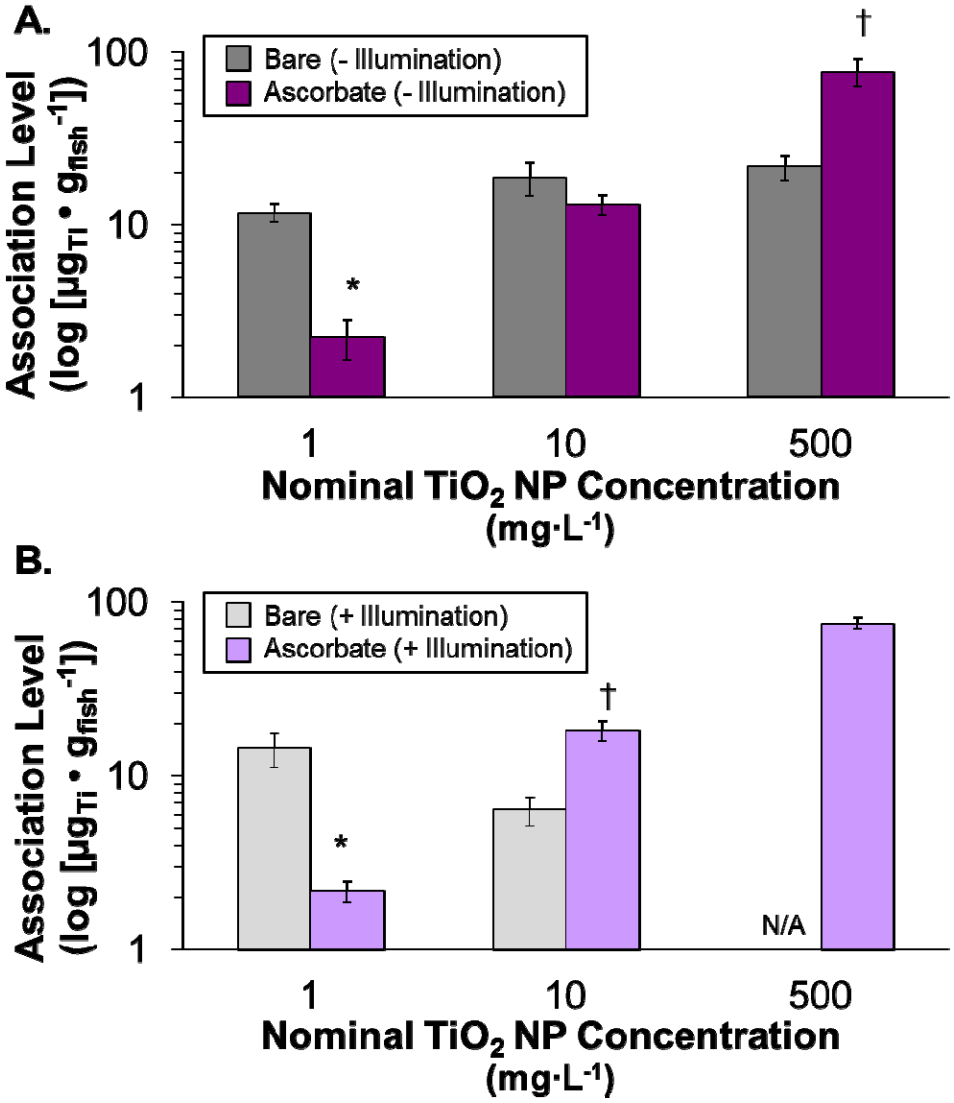

Figure 3.5. Effect of ascorbate functionalization on TiO_2 NP exposure in developing zebrafish. Titanium levels (log) associated with zebrafish at 5 dpf after exposure to bare and ascorbate-TiO_2 NPs (1, 100, and 500 mg·L^{-1}) in the absence (A) and presence (B) of simulated sunlight illumination (n = 2-6 replicates, 4 measurements per replicate). Measurements at 500 mg·L^{-1} bare TiO_2 NPs in the presence of illumination were not available (N/A) due to extensive mortality. Bars correspond to mean values and error bars represent SEM. The * indicates significant decrease in association level for functionalized-TiO_2 NPs relative to bare TiO_2 NPs and the † indicates significant increase in association level for functionalized-TiO_2 NPs relative to bare TiO_2 NPs. All differences assessed at p = 0.05 level of significance.

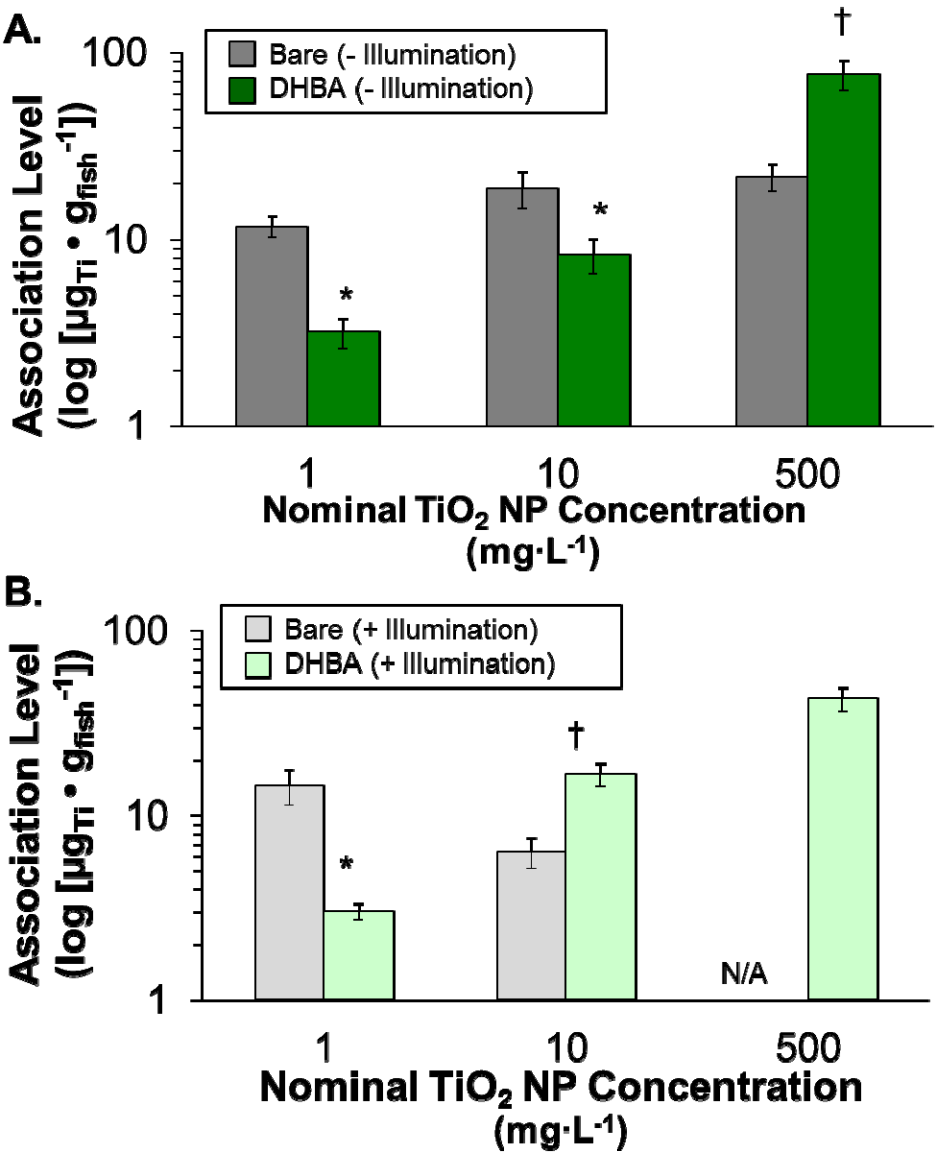

Figure 3.6. Effect of DHBA functionalization on TiO_2 NP exposure in developing zebrafish. Titanium levels (log) associated with zebrafish at 5 dpf after exposure to bare and DHBA-TiO_2 NPs (1, 100, and 500 mg·L^{-1}) in the absence (A) and presence (B) of simulated sunlight illumination (n = 2-6 replicates, 4 measurements per replicate). Measurements at 500 mg·L^{-1} bare TiO_2 NPs in the presence of illumination were not available (N/A) due to extensive mortality. Bars correspond to mean values and error bars represent SEM. The * indicates significant decrease in association level for functionalized-TiO_2 NPs relative to bare TiO_2 NPs and the † indicates significant increase in association level for functionalized-TiO_2 NPs relative to bare TiO_2 NPs. All differences assessed at p = 0.05 level of significance.

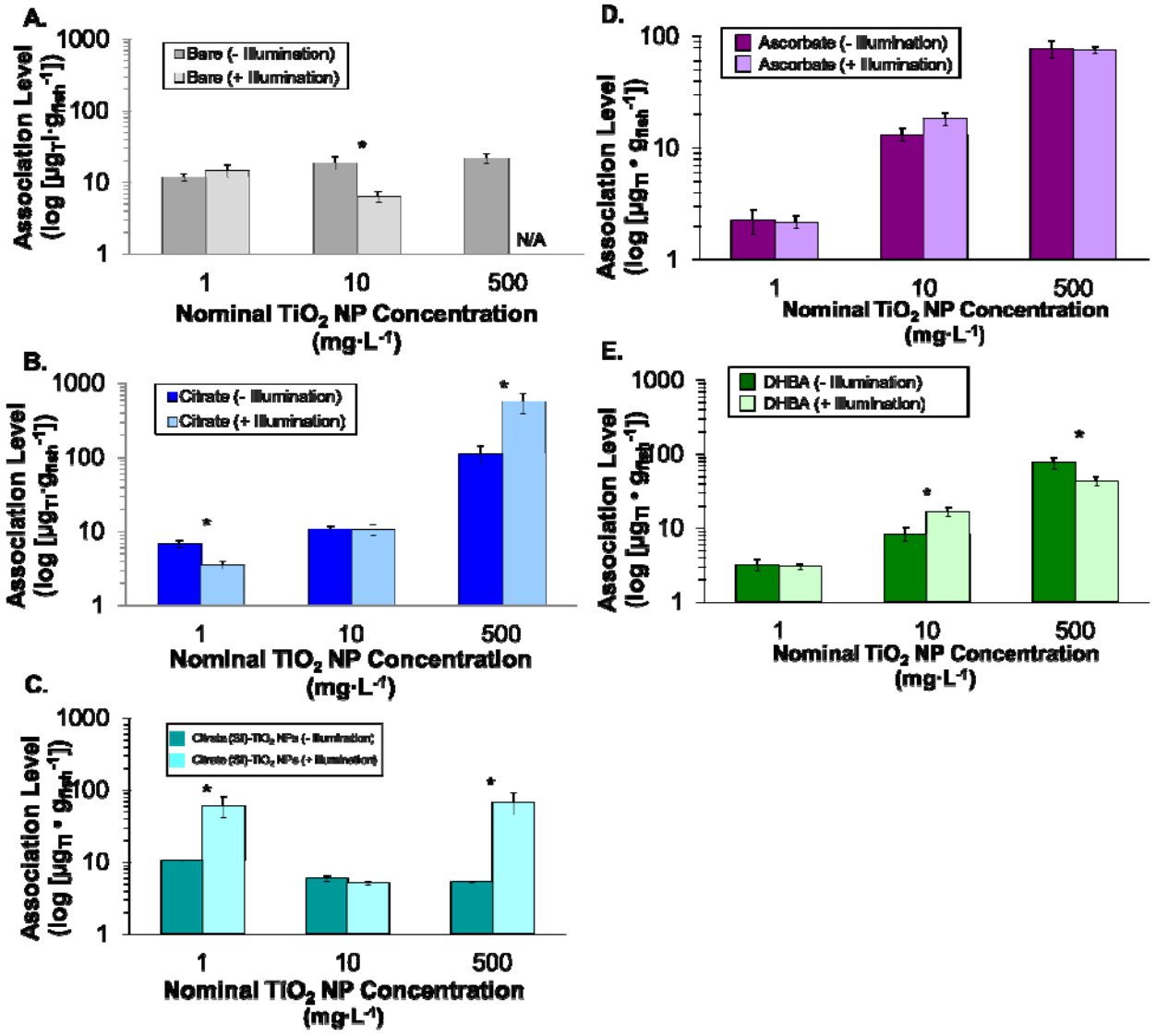

Figure 3.7. Effect of illumination on TiO_2 NP association level in developing zebrafish. Titanium levels (log) associated with zebrafish at 5 dpf after exposure in the absence and presence of simulated sunlight illumination to bare (A), citrate (B), citrate (SI) (D), ascorbate (D), and DHBA (E)-TiO_2 NPs (1, 100, and 500 mg·L^{-1}) (n = 2-6 replicates, 4 measurements per replicate). Measurements at 500 mg·L^{-1} bare TiO_2 NPs under illumination were not available (N/A) due to extensive mortality. Bars correspond to mean values and error bars represent SEM. The * indicates significant difference in association levels in fish between exposed to TiO_2 NPs in the absence and presence of simulated sunlight illumination. All differences assessed at p = 0.05 level of significance.

Table 3.2. Influence of functionalization and illumination on the incidence (%) of failed yolk sac absorption and edema in fish exposed to control or bare, and functionalized-TiO_2 NPs (250 mg L^{-1} at 5 dpf)[a-b]

	Edema		Failed Yolk Sac Absorption	
Illumination:	**-**	**+**	**-**	**+**
Fish Water	0.0	5.0 ± 2.2	0.0	10 ± 4.5
Bare TiO_2 NPs	0.0	15 ± 1.6	0.0	5.0 ± 1.6
Citrate-TiO_2 NPs	20 ± 0	15 ± 2.2	5.0 ± 2.2	10 ± 0
Citrate (SI)-TiO_2 NPs	5.0 ± 1.6	0.0	0.0	0.0
Ascrobate-TiO_2 NPs	0.0	0.0	0.0	0.0
DHBA-TiO_2 NPs	5.0 ± 1.6	0.0	10 ± 2.2	0.0

[a] n = 2 replicates with 10 fish per replicate. [b] All values presented as mean ± SEM.

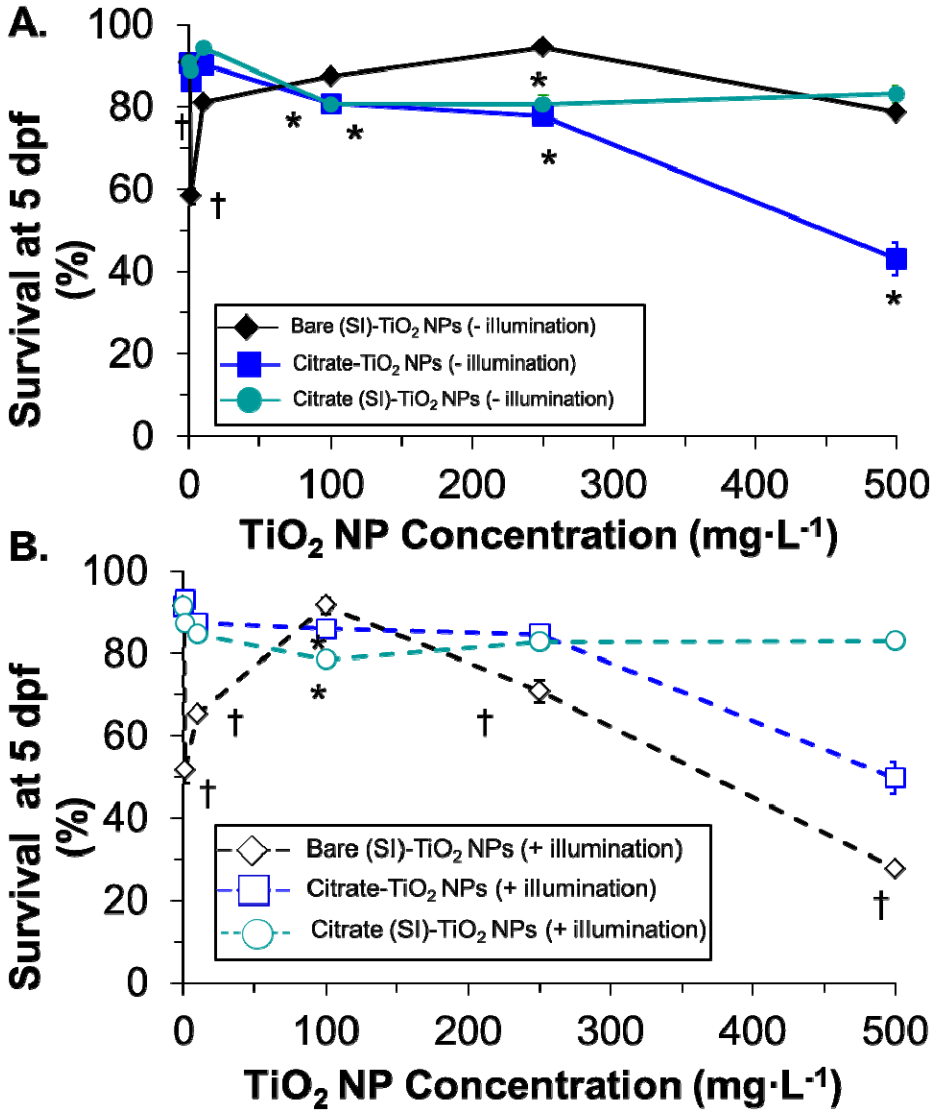

Figure 3.8. Influence of citrate functionalization on the toxicity of TiO_2 NPs. Dose-response curves at 5 dpf for fish exposed to bare, citrate, and citrate (SI)-TiO_2 NPs (0-500 mg·L^{-1}) in the absence (A) and presence (B) of simulated sunlight illumination (n = 3 replicates; 12 fish/replicate; each experiment conducted two times). Data points correspond to mean values, and error bars represent SEM. Lines are provided to guide the eye. The * indicates significant decrease in survival for the functionalized TiO_2 NPs relative to the bare TiO_2 NPs and the † indicates significant decrease in survival for the bare TiO_2 NPs relative to the functionalized TiO_2 NPs. All differences assessed at p = 0.05 level of significance.

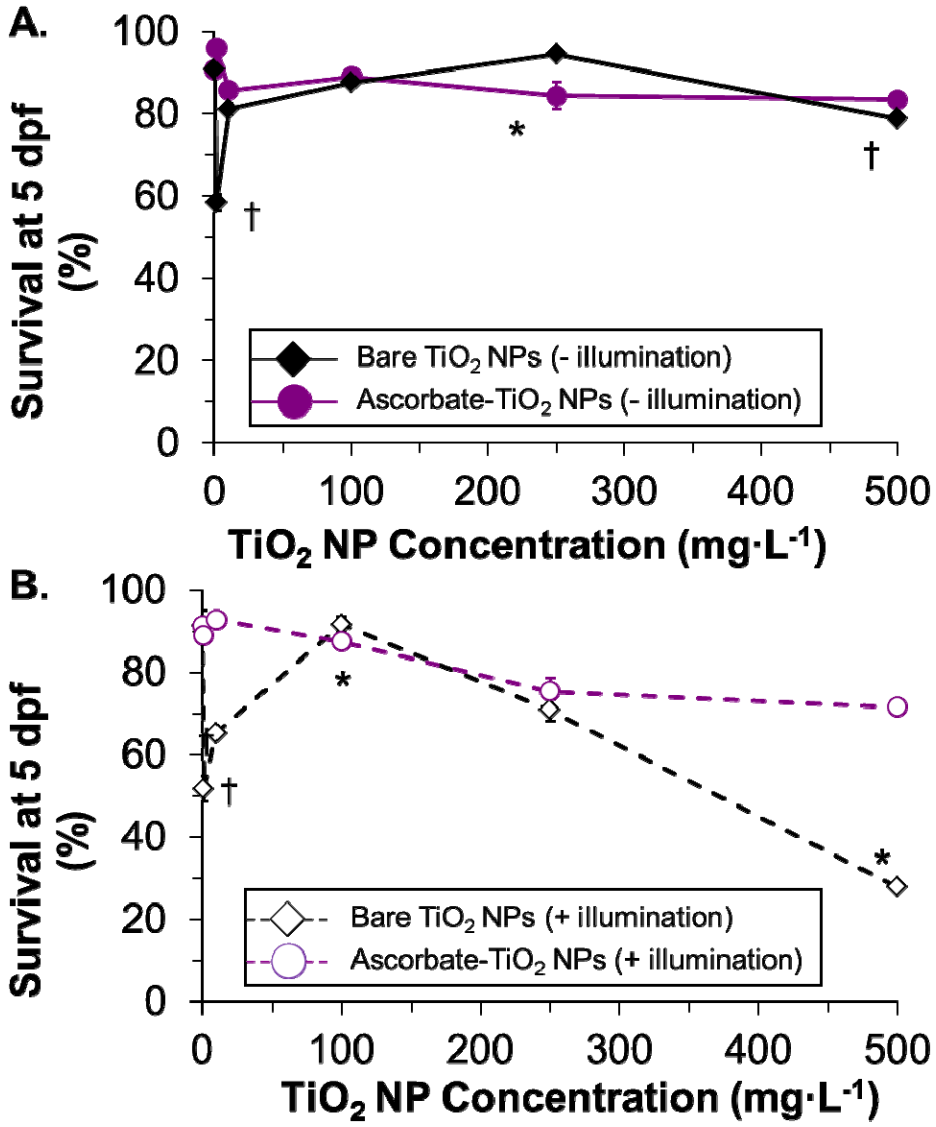

Figure 3.9. Influence of ascorbate functionalization on the toxicity of TiO_2 NPs. Dose-response curves at 5 dpf for fish exposed to bare and ascorbate-TiO_2 NPs (0-500 mg·L^{-1}) in the absence (A) and presence (B) of simulated sunlight illumination (n = 3 replicates; 12 fish/replicate; each experiment conducted two times). Data points correspond to mean values, and error bars represent SEM. Lines are provided to guide the eye. The * indicates significant decrease in survival for the functionalized TiO_2 NPs relative to the bare TiO_2 NPs and the † indicates significant decrease in survival for the bare TiO_2 NPs relative to the functionalized TiO_2 NPs. All differences assessed at p = 0.05 level of significance.

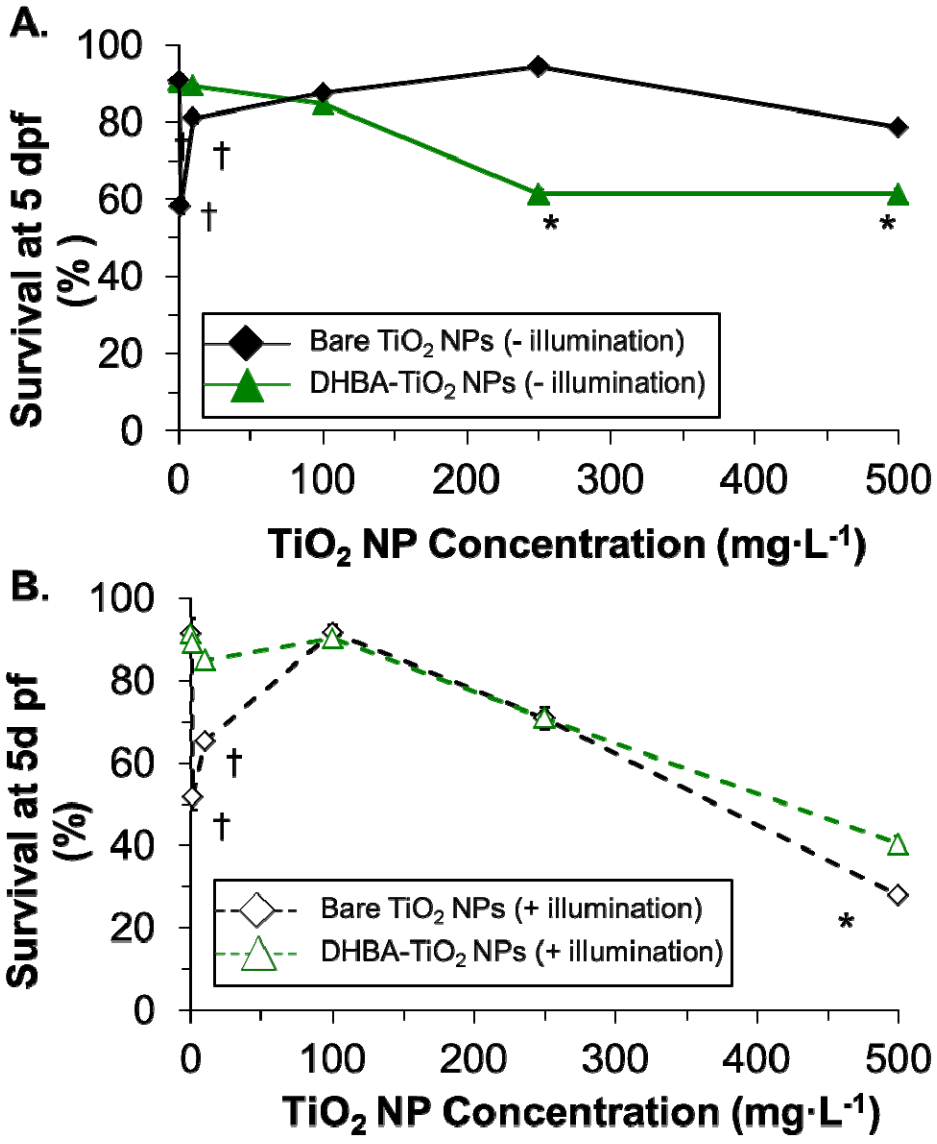

Figure 3.10. Influence of DHBA functionalization on the toxicity of TiO_2 NPs. Dose-response curves at 5 dpf for fish exposed to bare and DHBA-TiO_2 NPs (0-500 mg·L^{-1}) in the absence (A) and presence (B) of simulated sunlight illumination (n = 3 replicates; 12 fish/replicate; each experiment conducted two times). Data points correspond to mean values, and error bars represent SEM. Lines are provided to guide the eye. The * indicates significant decrease in survival for the functionalized TiO_2 NPs relative to the bare TiO_2 NPs and the † indicates significant decrease in survival for the bare TiO_2 NPs relative to the functionalized TiO_2 NPs. All differences assessed at p = 0.05 level of significance.

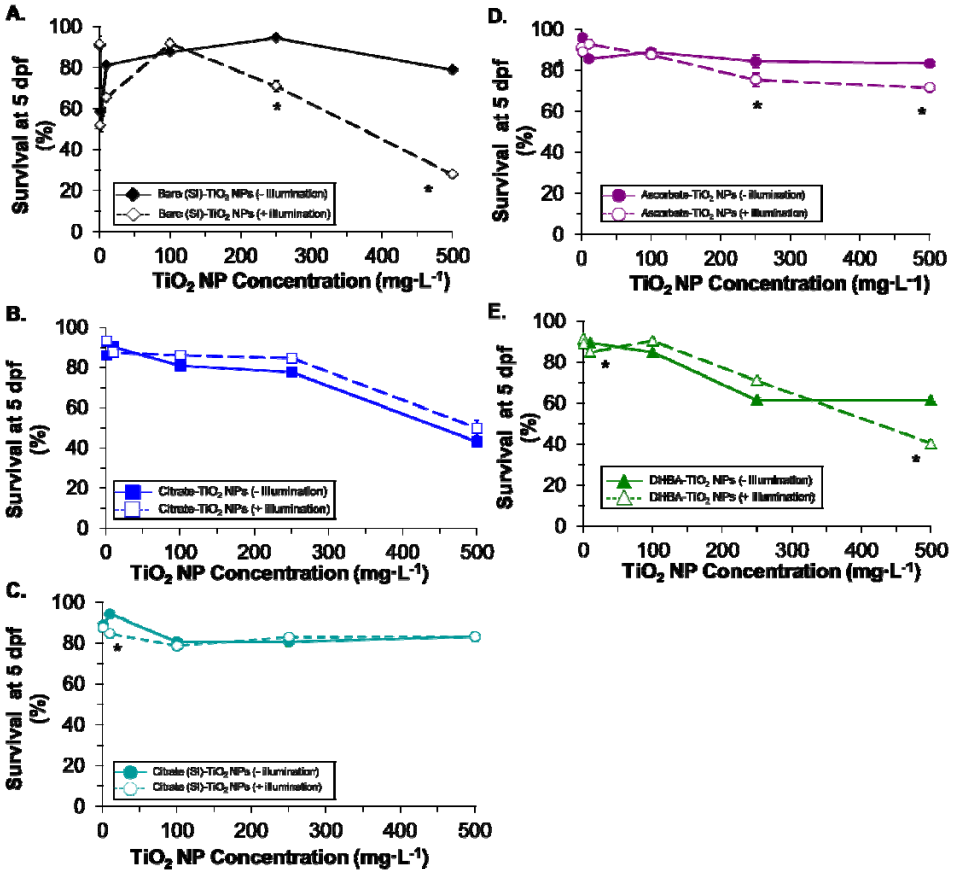

Figure 3.11. Influence of illumination on the toxicity of TiO_2 NPs. Dose-response curves at 5 dpf for fish exposed to bare (A), citrate (B), and citrate (SI) (C), ascorbate (D), and DHBA (E)-TiO_2 NPs (0-500 mg·L^{-1}) in the absence and presence of simulated sunlight illumination (n = 3 replicates; 12 fish/replicate; each experiment conducted 2 times). Data points correspond to mean values and error bars represent SEM. Lines are provided to guide the eye. The * indicates significant decrease in survival in fish exposed to TiO_2 NP suspensions under illumination relative to the absence of illumination. All differences assessed at p = 0.05 level of significance.

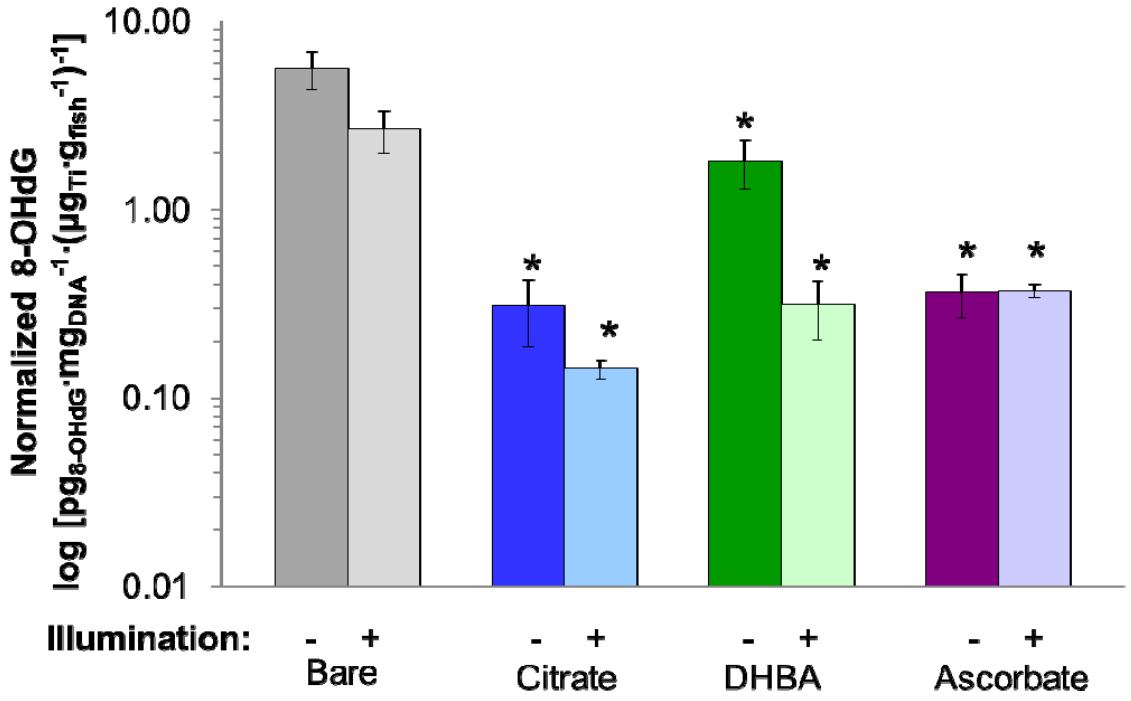

Figure 3.12. Influence of functionalization and illumination on TiO_2 NPs induced oxidative DNA damage. Amount of 8-OHdG normalized to the amount of Ti associated with fish exposed to bare, citrate, DHBA, and ascorbate-functionalized TiO_2 NPs (500 mg·L^{-1} until 3 dpf) in the presence and absence of illumination (n = 2 replicates; 40 fish/replicate; each experiment conducted 2 times). Oxidative DNA damage expressed as mass of 8-OHdG normalized to mass of DNA ($pg_{8\text{-}OHdG}$·mg_{DNA}^{-1}), and association levels expressed as mass of Ti normalized to wet weight of fish (μg_{Ti}·μg_{fish}^{-1}). Bars represent means, and error bars are SEM. The * indicates significant increase in normalized 8-OHdG level in fish exposed to bare TiO_2 NPs relative to those exposed to functionalized-TiO_2 NPs. All differences assessed at p = 0.05 level of significance.

References

1. Grassian, V. H.; Meyer, G.; Abruna, H.; Coates, G. W.; Achenie, L. E.; Allison, T.; Brunschwig, B.; Ferry, J.; Garcia-Garibay, M.; Gardea-Torresdey, J.; Grey, C. P.; Hutchison, J.; Li, C. J.; Liotta, C.; Ragauskas, A.; Minteer, S.; Mueller, K.; Roberts, J.; Sadik, O.; Schmehl, R.; Schneider, W.; Selloni, A.; Stair, P.; Stewart, J.; Thorn, D.; Tyson, J.; Voelker, B.; White, J. M.; Wood-Black, F. Chemistry for a sustainable future. *Environ. Sci. Technol.* **2007,** *41*, 4840-4846.
2. Nel, A.; Xia, T.; Madler, L.; Li, N. Toxic potential of materials at the nanolevel. *Science* **2006,** *311*, 6[15]-627.
3. Heinlaan, M.; Ivask, A.; Blinova, I.; Dubourguier, H. C.; Kahru, A. Toxicity of nanosized and bulk ZnO, CuO and TiO_2 to bacteria *Vibrio fischeri* and crustaceans *Daphnia magna* and *Thamnocephalus platyurus*. *Chemosphere* **2008,** *71*, 1308-1316.
4. Zhu, X. S.; Zhu, L.; Duan, Z. H.; Qi, R. Q.; Li, Y.; Lang, Y. P. Comparative toxicity of several metal oxide nanoparticle aqueous suspensions to Zebrafish (*Danio rerio*) early developmental stage. *J. Environ. Sci. Health A* **2008,** *43*, 278-284.
5. Blinova, I.; Ivask, A.; Heinlaan, M.; Mortimer, M.; Kahru, A. Ecotoxicity of nanoparticles of CuO and ZnO in natural water. *Environ. Pollut.* **2010,** *158*, 41-47.
6. Scown, T. M.; van Aerle, R.; Tyler, C. R. Review: Do engineered nanoparticles pose a significant threat to the aquatic environment? *Crit. Rev. Toxicol.* **2010,** *40*, 653-670.
7. Yu, L. P.; Fang, T.; Xiong, D. W.; Zhu, W. T.; Sima, X. F. Comparative toxicity of nano-ZnO and bulk ZnO suspensions to zebrafish and the effects of sedimentation, (center dot)OH production and particle dissolution in distilled water. *J. Environ. Monit.* **2011**, *13*, 1975-1982.
8. Xiong, D. W.; Fang, T.; Yu, L. P.; Sima, X. F.; Zhu, W. T. Effects of nano-scale TiO_2, ZnO and their bulk counterparts on zebrafish: Acute toxicity, oxidative stress and oxidative damage. *Sci. Total Environ.* **2011,** *409*, 1444-1452.
9. Hoffmann, M. R.; Martin, S. T.; Choi, W. Y.; Bahnemann, D. W. Environmental applications of semiconductor photocatalysis. *Chem. Rev.* **1995,** *95*, 69-96.
10. Armstrong, D. *Oxidative stress biomarkers and antioxidant protocols*; Humana Press Inc.: Totowa, New Jersey, 2002; Vol. 186.
11. Bar-Ilan, O.; Louis, K. M.; Yang, S. P.; Pedersen, J. A.; Hamers, R. J.; Peterson, R. E.; Heideman, W., Titanium dioxide nanoparticles produce phototoxicity in the developing zebrafish. *Nanotoxicol.* **2012,** *6*, 670-679.

12. Bar-Ilan, O.; Chuang, C.C.; Schwahn, D.J.; Yang, S.P.; Joshi, S.; Pedersen, J.A.; Hamers, R.J.; Peterson, R.E.; Heideman, W. TiO_2 nanoparticle exposure and illumination during zebrafish development: Mortality at parts per billion concentrations. . *Environ. Sci. Technol.*, **2013**, 47, 4726-4733
13. King-Heiden, T. C.; Wiecinski, P. N.; Mangham, A. N.; Metz, K. M.; Nesbit, D.; Pedersen, J. A.; Hamers, R. J.; Heideman, W.; Peterson, R. E. Quantum dot nanotoxicity assessment using the zebrafish embryo. *Environ. Sci.Technol.* **2009,** *43*, 1605-1611.
14. Lin, S.; Zhao, Y.; Nel, A.; Lin, S. Zebrafish: An *in vivo* model for nano EHS studies. *Small* **2012**, *9*, 1608-1618.
15. Yang, S.P.; Bar-Ilan, O.; Peterson, R.E.; Heideman, W.; Hamers, R.J.; Pedersen, J.A. Influence of humic acid on titanium dioxide nanoparticle toxicity to developing zebrafish. *Environ. Sci. Technol.* **2013**, 47, 4718-4725.
16. Kotsokechagia, T.; Cellesi, F.; Thomas, A.; Niederberger, M.; Tirelli, N. Preparation of ligand-free TiO_2 (anatase) nanoparticles through a nonaqueous process and their surface functionalization. *Langmuir* **2008,** *24*, 6988-6997.
17. Mudunkotuwa, I. A.; Grassian, V. H. Citric acid adsorption on TiO_2 nanoparticles in aqueous suspensions at acidic and circumneutral pH: Surface coverage, surface speciation, and its impact on nanoparticle-nanoparticle interactions. *JACS* **2010,** *132*, 14986-14994.
18. Tejamaya, M.; Roemer, I.; Merrifield, R. C.; Lead, J. R. Stability of Citrate, PVP, and PEG coated silver nanoparticles in ecotoxicology media. *Environ. Sci. Technol.* **2012,** *46*, 7011-7017.
19. Packer, L.; Jürgen, F. *Vitamin C in Health and Disease.* M. Dekker: New York: New York, 1997.
20. Smith, M.; March, J. *March's Advanced Organic Chemistry: Reactions, Mechanisms, and Structure.* 5, Wiley: New York, New York, 2001.
21. Louis, K. M. Surface functionalization of TiO_2 nanoparticles: Photo-stability and reactive oxygen species (ROS) generation. PhD Dissertation. University of Wisconsin, Madison, WI, 2012.
22. Gomes, A.; Fernandes, E.; Lima, J. Fluorescence probes used for detection of reactive oxygen species. *J. Biochem. Biophys. Meth.* **2005,** *65*, 45-80.
23. Pal, A. K.; Bello, D.; Budhlall, B.; Rogers, E.; Milton, D. K., Screening for oxidative stress elicited by engineered nanomaterials: Evaluation of acellular DCHF assay. *Dose-Response* **2012,** *10*, 308-330.
24. Jassby, D.; Budarz, J. F.; Wiesner, M. Impact of aggregate size and structure on the photocatalytic properties of TiO_2 and ZnO nanoparticles. *Environ. Sci. Technol.* **2012**, *46*, 6934-6941.

25. Kelly, K. A.; Havrilla, C. M.; Brady, T. C.; Abramo, K. H.; Levin, E. D. Oxidative stress in toxicology: established mammalian and emerging piscine model systems. *Environ. Health Perspect.* **1998,** *106*, 375-384.
26. Petersen, E. J.; Nelson, B. C. Mechanisms and measurements of nanomaterial-induced oxidative damage to DNA. *Anal. Bioanal. Chem.* **2010,** *398*, 613-650.
27. Hamilton, M. A.; Russo, R. C.; Thurston, R. V. Trimmed Spearman-Karber method for estimating median lethal concentration in toxicity bioassays. *Environ. Sci. Technol.* **1977**, *11*, 714-719.
28. Wachs, I. E.; Deo, G.; Jehng, J. M.; Kim, D. S.; Hu, H. The activity and selectivity properties of supported metal oxide catalysts during oxidation reactions. *Hetero. Hydrocarb. Oxid.* **1996,** *638*, 292-299.
29. Zhang, W. F.; He, Y. L.; Zhang, M. S.; Yin, Z.; Chen, Q. Raman scattering study on anatase TiO_2 nanocrystals. *J.Phys. D* **2000,** *33*, 912-916.
30. Balachandran, U.; Eror, N. G. Raman spectra of titanium dioxide. *J. Solid State Chem.* **1982**, *42*, 276-282.
31. Bichara, L. C.; Lanus, H. E.; Nieto, C. G.; Brandan, S. A. Density functional theory calculations of the molecular force field of L-ascorbic acid, vitamin C. *J. Phys. Chem. A* **2010,** *114*, 4997-5004.
32. Velcheva, E. A.; Juchnovski, I. N.; Binev, I. G. IR studies in the substituted benzaldehyde series provide a new definition of sigma-plus constants of ionic substituents. *Spectrochim. Acta, Part A* **2003,** *59*, 1745-1749.
33. Gulley-Stahl, H.; Hogan, P. A., II; Schmidt, W. L.; Wall, S. J.; Buhrlage, A.; Bullen, H. A. Surface Complexation of Catechol to Metal Oxides: An ATR-FTIR, adsorption, and dissolution study. *Environ. Sci. Technol.* **2010**, *44*, 4116-4121.
34. Araujo, P. Z.; Mendive, C. B.; Rodenas, L. A. G.; Morando, P. J.; Regazzoni, A. E.; Blesa, M. A.; Bahnemann, D. FT-IR-ATR as a tool to probe photocatalytic interfaces. *Colloid.Surf. A* **2005**, *265*, 73-80.
35. Elimelech, M.; Jia, X.; Gregory, J.; Williams, R. *Particle Deposition & Aggregation: Measurement, Modelling and Simulation*. 1; Butterworth-Heinemann: Oxford, England, 1998.
36. Liufu, S. C.; Mao, H. N.; Li, Y. P. Adsorption of poly(acrylic acid) onto the surface of titanium dioxide and the colloidal stability of aqueous suspension. *J. Colloid Interf. Sci.* **2005**, *281*, 155-163.
37. Kwon, S.; Fan, M.; Cooper, A. T.; Yang, H. Q. Photocatalytic applications of micro- and nano-TiO_2 in environmental engineering. *Crit. Rev. Environ. Sci. Technol.* **2008**, *38*, 197-156.
38. Gaya, U. I.; Abdullah, A. H. Heterogeneous photocatalytic degradation of organic contaminants over titanium dioxide: A review of fundamentals, progress and problems. *J. Photochem. Photobio. C*, **2008**, *9*, 1-12

39. Almroth, B. C.; Sturve, J.; Berglund, A.; Forlin, L. Oxidative damage in eelpout (*Zoarces viviparus*), measured as protein carbonyls and TBARS, as biomarkers. *Aquat. Toxicol.* **2005**, *73*, 171-180.
40. Federici, G.; Shaw, B. J.; Handy, R. D. Toxicity of titanium dioxide nanoparticles to rainbow trout (*Oncorhynchus mykiss*): Gill injury, oxidative stress, and other physiological effects. *Aquat. Toxicol.* **2007,** *84*, 415-430.
41. Sharma, V. K. Aggregation and toxicity of titanium dioxide nanoparticles in aquatic environment-A review. *J. Environ. Sci. Health A* **2009**, *44*, 1485-1495.
42. Iavicoli, I.; Leso, V.; Fontana, L.; Bergamaschi, A. Toxicological effects of titanium dioxide nanoparticles: a review of in vitro mammalian studies. *Eur. Rev. Med. Pharmacol. Sci.* **2011**, *15*, 481-508.
43. Hao, L. H.; Wang, Z. Y.; Xing, B. S. Effect of sub-acute exposure to TiO_2 nanoparticles on oxidative stress and histopathological changes in Juvenile Carp (*Cyprinus carpio*). *J. Environ. Sci. China* **2009,** *21*, 1459-1466.
44. Ma, H. B.; Brennan, A.; Diamond, S. A. Photocatalytic reactive oxygen species production and phototoxicity of titanium dioxide nanoparticles are dependent on the solar ultraviolet radiation spectrum. *Environ. Toxicol. Chem.* **2012**, *31*, 2099-2107.
45. Ma, H. B.; Brennan, A.; Diamond, S. A. Phototoxicity of TiO_2 nanoparticles under solar radiation to two aquatic species: Daphnia magna and Japanese medaka. *Environ. Toxicol. Chem.* **2012**, *31*, 1621-1629.
46. Ma, H. B.; Diamond, S. A. Phototoxicity of TiO_2 nanoparticles to zebrafish (*Danio rerio*) is dependent on life stage. *Environ. Toxicol. Chem.* **2013**, *32*, 2139-2143.

Chapter 4: Conclusions and Future Directions

Conclusions

In this dissertation, the influence of organic coatings on the toxicity of TiO_2 NPs was examined using zebrafish as a model aquatic vertebrate. As the applications of TiO_2 NPs continues to increase, so does the likelihood that these materials will be released into the environment. Organic coatings can impact the fate and bioavailability of nanomaterials in the environment. Nanomaterials can acquire organic coatings unintentionally (i.e., adsorption of organic ligands in the environment) or intentionally (i.e., functionalization during synthesis). The collections of works described in this thesis have shown that (1) dissolved organic matter can impact the suspension stability and uptake and toxicity of uncoated TiO_2 NPs to developing zebrafish; and (2) functionalization can impact the inherent and photo-enhanced toxicity of TiO_2 NPs to developing zebrafish.

The experiments within this dissertation have highlighted the importance of thoroughly investigating the impact of organic coating on TiO_2 NP suspension stability and uptake. Although differences in suspension stability may result in differences in uptake, these changes do not necessarily correspond with differences in toxicity. In fact, in both studies in this work, organic coatings increased the toxicity of TiO_2 NPs while reducing uptake. Both studies found evidence that the organic coatings increased toxicity by increasing oxidative stress. However, further studies need to be preformed in order to ascertain the mechanism behind this increase. Such future directions are briefly discussed below. The research in this thesis will help in the development of safe, sustainable nanotechnologies for future use.

Future Directions

Further evaluation of the influence of organic coating on TiO_2 NP-induced oxidative stress

We have shown that organic coating can increase oxidative DNA damage and lipid peroxidation and that these increases are present even upon normalization to TiO_2 NP exposure levels. These findings warrant further investigation into the mechanism behind the increase.

Under normal conditions, antioxidant enzymes (e.g., catalase, glutathione peroxidase, superoxide dismutase) detoxify ROS. However, if the levels of ROS are too great for the antioxidant enzymes to handle and/or there is a decrease in the amount/reactivity of the antioxidant enzymes, oxidative stress occurs and can result in cell damage, disease, and death.

The pathways involved in antioxidant enzyme response are complex. Antioxidant enzyme transcription is regulated by antioxidant response elements (AREs). In order for transcription to occur, transcription factors (e.g., Nrf2) must bind to the ARE and activate the gene. Transcription factors activation requires translocation of the transcription factor from the cytosol into the nucleus in response to numerous signaling pathways.

Further steps to determine exactly how organic coatings increase TiO_2 NP induced oxidative stress should examine the antioxidant response pathway in detail. This may involve (1) determining if differences in antioxidant enzyme levels and/or activity are responsible for the observed differences; (2) examining alterations in antioxidant response element (ARE) using a transgenic zebrafish reporter line Tg(are:eGFP); and (3)

investigating transcription factor pathway by assessing the expression of key factors (e.g., Nf-κB, interleukins, TNF-α) using microarray technology as the use of transgenic fish lines.[1]

Development of surface coating designed to reduce TiO_2 NP toxicity

The research in this thesis has shown that surface coating can alter TiO_2 NP toxicity. Recently, our collaborators have been working to engineer a surface functionalization that reduces ROS generation.[2] In this work, they have generated an amphiphilic ligand by first attaching a hydrophobic ligand (i.e., undecanoic acid) to the nanoparticle core.[2] A hydrophobic ligand (i.e., polyethylene glycol) is then attached the hydrophobic ligand using "click" chemistry.[1] More specifically, a Cu (I) catalyzed azide alkyne cycloaddition reaction was used in which a terminal azide is coupled with an alkyne resulting in a 1,4-disubstituted 1,2,3-triazole linkage.[2] For these particles, the hydrophobic ligand prevents water from reaching the surface of the molecule reducing hydroxyl radical formation while the hydrophilic ligand allows the particle to be stable in aqueous solutions.[2] By comparing the toxicity of this amphiphilic ligand to that of the hydrophilic ligand, further investigations into the role of ROS generation in the toxicity of TiO_2 NP are possible.

Influence of organic coating on the toxicity of TiO_2 NPs to developing zebrafish at environmentally relevant exposure levels

The work in this thesis was conducted using an acute zebrafish toxicity assay utilizing lethality and gross malformations as endpoints for toxicity. Furthermore, the concentrations utilized were drastically greater than those predicted in environmental matrices. However, we recently found that subchronic exposure (i.e., 23d) to low levels of uncoated TiO_2 NPs (1 $\mu g \cdot L^{-1}$) resulted in photo-enhanced toxicity in developing zebrafish due to increased oxidative stress upon simulated sunlight exposure.[3] The results from this

study and the work in this thesis necessitate further studies examining the influence of organic coatings on the toxicity of TiO_2 NPs to developing zebrafish at environmentally relevant concentrations.

References

1. Udvadia, A. J.; Linney, E. Windows into development: Historic, current, and future perspectives on transgenic zebrafish. *Develop. Biol.* 2003, *256*, 1-17.
2. Louis, K. M. Surface functionalization of TiO_2 nanoparticles: Photo-stability and reactive oxygen species (ROS) generation. PhD Dissertation. University of Wisconsin, Madison, WI, 2012.
3. Bar-Ilan, O. Toxicity of metal and metal oxide nanoparticles in developing zebrafish. PhD Dissertation. University of Wisconsin, Madison, WI, 2011.